Report No.: NIH/TR/2024-25/C4S/**
Final Report

CLIMATE CHANGE SCENARIOS FOR ANDHRA PRADESH AND ITS IMPACT ON STREAMFLOW AND GROUNDWATER LEVELS IN PENNAR RIVER BASIN

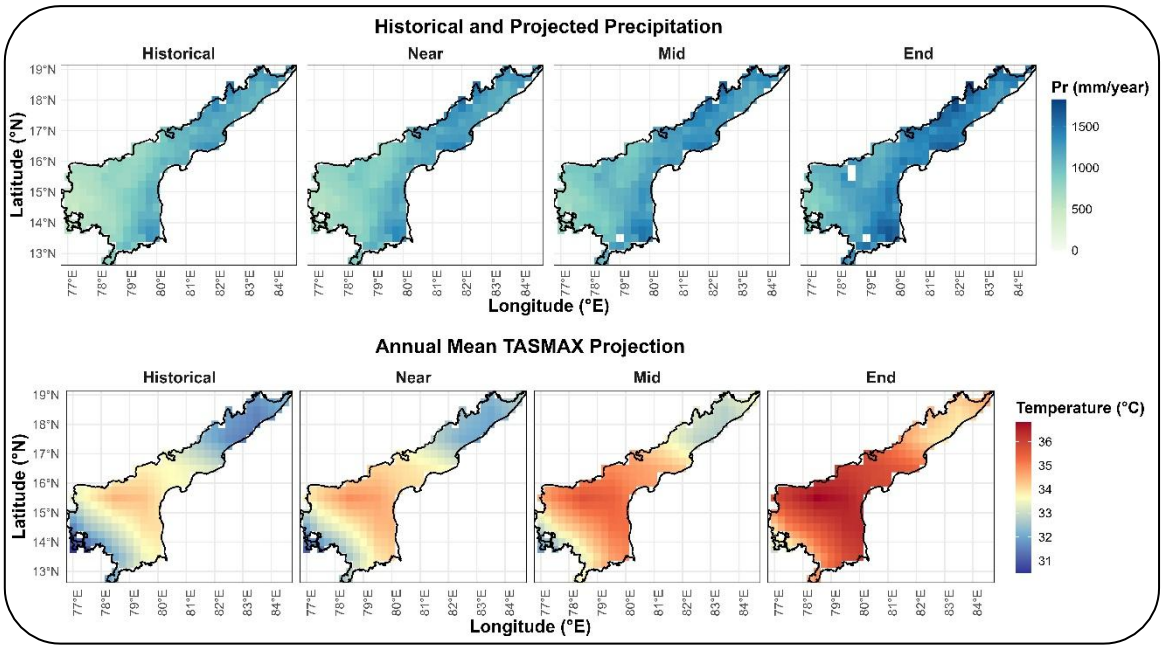

आपो हि ष्ठा मयोभुवः

National Institute of Hydrology
Department of WR, RD & GR,
Ministry of Jal Shakti, Govt. of India
Jal Vigyan Bhawan, Roorkee - 247667 (Uttarakhand), INDIA

March 2026

Blank Page

Report No.: NIH/TR/2024-25/C4S/**

Final Report

CLIMATE CHANGE SCENARIOS FOR ANDHRA PRADESH AND ITS IMPACT ON STREAMFLOW AND GROUNDWATER LEVELS IN PENNAR RIVER BASIN

National Institute of Hydrology

Department of WR, RD & GR

Ministry of Jal Shakti, Govt. of India

Jal Vigyan Bhawan, Roorkee – 247667 (Uttarakhand), India

March 2026

Citation:
Gurrapu S, Rao YRS, Ramana R V, Patidar N, Kumar TVNAR. 2026. Climate Change Scenarios for Andhra Pradesh and its Impact on Streamflow and Groundwater Levels in Pennar River Basin. National Institute of Hydrology, Roorkee, Technical Report No. NIH/TR/2024-25/C4S/**, 112 pp.

Published By:
National Institute of Hydrology, Roorkee
Jal Vigyan Bhawan, Roorkee – 247667 (Uttarakhand), INDIA

DIRECTOR: Dr. Y R S Rao

Division: Centre for Cryosphere and Climate Change Studies (C4S)

Head: Dr. Surjeet Singh, Scientist ‘G’

Principal Investigator: Dr. Sunil Gurrapu, Scientist ‘D’

Co-Principal Investigator: Dr. Y R S Rao, Scientist ‘G’

STUDY TEAM:

Mr. R Venkata Ramana, Scientist ‘F’

Dr. Nitesh Patidar, Scientist ‘C’

Mr. T V N A R Kumar, Chief Engineer, WRD, Govt. of Andhra Pradesh

PREFACE

Recent changes in global and regional climate increasingly influence hydrological processes and shift the frequency, magnitude, and variability of extreme events. Changes in land use and land cover, along with modifications to river flow regimes driven by human activities, further alter basin-scale hydrological dynamics. Together, these factors create growing imbalance in hydrological systems, particularly in vulnerable semi-arid regions. These changes already appear in parts of Andhra Pradesh. For instance, the state experienced above-normal rainfall and higher temperatures in 2021 compared with long-term averages. During the same period, the Pennar River Basin experienced extreme hydrological events that damaged water resources infrastructure. These developments highlight the need to understand the complex interactions between climate variability and hydrological response and support effective water resource management.

This study evaluates how future climate change may affect hydrology in Andhra Pradesh, with a detailed focus on the Pennar River Basin. The study uses projections from selected CMIP6 General Circulation Models and develops multi-model scenarios of rainfall and temperature. The analysis applies these projections to a calibrated Variable Infiltration Capacity (VIC) model and simulates streamflow at selected gauging sites. In parallel, the study develops a Random Forest–based model and estimates groundwater levels at selected locations across the basin. Together, these approaches provide a comprehensive framework and assess future hydrological scenarios across both surface and subsurface systems. The findings of this study support water managers, irrigation planners, and engineers and help them develop climate-resilient strategies for water allocation, infrastructure planning, and mitigation of hydrological risks.

Dr. Sunil Gurrapu (PI), Scientist ‘D’, Centre for Cryosphere and Climate Change Studies (C4S), prepared this report and carried out most of the analysis. Dr. Y R S Rao (Co-PI), Scientist ‘G’ and Director, NIH provided technical guidance. Mr. R Venkata Ramana, Scientist ‘F’, and Dr. Nitesh Patidar, Scientist ‘C’, provided domain support for the analysis. Mr. T V N A R. Kumar, Chief Engineer, AP WRD, provided domain support and inputs. NIH, Roorkee funded this internal research project.

EXECUTIVE SUMMARY

Climate change and anthropogenic activities increasingly influence hydro-climatic and hydrological systems, leading to significant alterations in the frequency, magnitude, and variability of hydrological extremes. Changes in land use and land cover, along with modifications to river flow regimes, further affect basin-scale hydrological processes. Together, these factors contribute to growing imbalances in hydrological systems, particularly in semi-arid regions. In Andhra Pradesh, recent events highlight these emerging risks. For instance, parts of the state experienced above-normal rainfall and elevated temperatures in 2021, while the Pennar River Basin witnessed extreme hydrological events that caused substantial damage to water infrastructure. These observations underscore the need to understand the complex interactions between climate variability and basin hydrology to support sustainable water resource management.

This study evaluates how future climate change may affect hydrology in Andhra Pradesh and the Pennar River Basin using an integrated modelling framework. We used projections from CMIP6 General Circulation Models to develop multi-model scenarios of precipitation and temperature. We then applied these projections to a calibrated Variable Infiltration Capacity (VIC) model to simulate streamflow. In parallel, we developed a Random Forest–based model to estimate groundwater levels at selected locations across the basin. The results indicate a consistent warming trend and increasing rainfall variability across the region. Hydrological simulations reveal a redistribution of water availability rather than a uniform change, characterized by increasing peak flows, enhanced inter-annual variability, and persistence of low-flow conditions during dry periods. Groundwater projections show a general tendency toward increasing groundwater depth across most wells, indicating reduced recharge efficiency and growing groundwater stress, although responses vary spatially due to local hydrogeological conditions.

These findings highlight that even moderate changes in climate can produce amplified hydrological responses in semi-arid basins. The increasing variability in both surface and subsurface water systems poses significant challenges for water resource management, including flood risk, seasonal water scarcity, and uncertainty in water availability. The outcomes of this study provide valuable insights for water managers,

irrigation planners, and infrastructure developers. The projected changes emphasize the need for climate-resilient water management strategies, including improved flood preparedness, adaptive reservoir operation, enhanced groundwater recharge, and efficient water allocation. Integrating climate-informed hydrological projections into planning and policy will be essential to reduce the adverse impacts of hydrological extremes and ensure long-term water security in the Pennar River Basin.

Keywords: CMIP6, Climate Change, Streamflwo Simulation, Groundwater Modelling, VIC Model, Random Forest, Hydrological Variability, Pennar River Basin

CONTENTS

LIST OF FIGURES

LIST OF TABLES

1.0. INTRODUCTION

Climate change has emerged as a dominant driver of alterations in hydroclimatic and hydrological systems across the globe. Numerous studies confirm that rising temperatures, shifting precipitation patterns, and increasing climate variability have already modified the frequency, magnitude, and timing of hydrological extremes (Liu et al., 2021; Tabari, 2020; Manfreda et al., 2018; Wang et al., 2016; Gossain et al., 2006). The special issue on “Impacts of Climate on Hydrological Extremes” emphasized the growing evidence linking historically observed hydrological extremes with ongoing climatic changes across diverse watersheds worldwide (Manfreda et al., 2018). These findings underscore the need to understand the complex interactions between climate dynamics and basin-scale hydrological processes in order to assess future water risks. Alongside climatic shifts, anthropogenic changes in land use, land cover, and river regulation further modify catchment responses, thereby compounding hydrological variability and amplifying extreme events.

Semi-arid river basins face particularly acute risks under changing climate conditions. The Intergovernmental Panel on Climate Change (IPCC) highlights significant regional variations in temperature and precipitation across South Asia and projects substantial implications for streamflow regimes and groundwater recharge (IPCC, 2021). Peninsular Indian rivers, which depend heavily on monsoon rainfall and exhibit predominantly non-perennial flow regimes, remain highly sensitive to intra-seasonal rainfall variability and temperature-induced evapotranspiration increases. In such systems, even moderate shifts in rainfall timing or intensity can trigger disproportionate hydrological responses. Therefore, any comprehensive basin-level assessment must integrate projected climatic changes with basin characteristics to evaluate evolving water availability and hydrological extremes.

Recent observations indicate that these changes are not merely theoretical projections but ongoing realities. Studies suggest that hydrological extremes may become more frequent and spatially widespread under intensified climate variability (ICHARM 2009; Vogel et al., 2011). For instance, the state of Andhra Pradesh recorded a spatially averaged temperature anomaly of +0.1 °C above the long period average (1981–2010) in 2021, while minimum temperatures showed a +0.3 °C anomaly (IMD, 2022), Figure 1.1. During the same period, several districts received

excess rainfall relative to the long period average (1961–2010), Figure 1.2. Extreme precipitation events during the 2021 monsoon generated unusually high inflows across the Pennar River Basin, leading to severe reservoir stress and infrastructure failures. The partial breach of the Annamayya Dam on the Cheyyeru River and exceptionally high inflows, reported to be nearly four times the usual volume at the Mylavaram Dam illustrate the basin's vulnerability to intensified hydrological extremes, Figure 1.3. These recent events reinforce the urgency of conducting basin-specific climate impact assessments to inform resilient water resources planning.

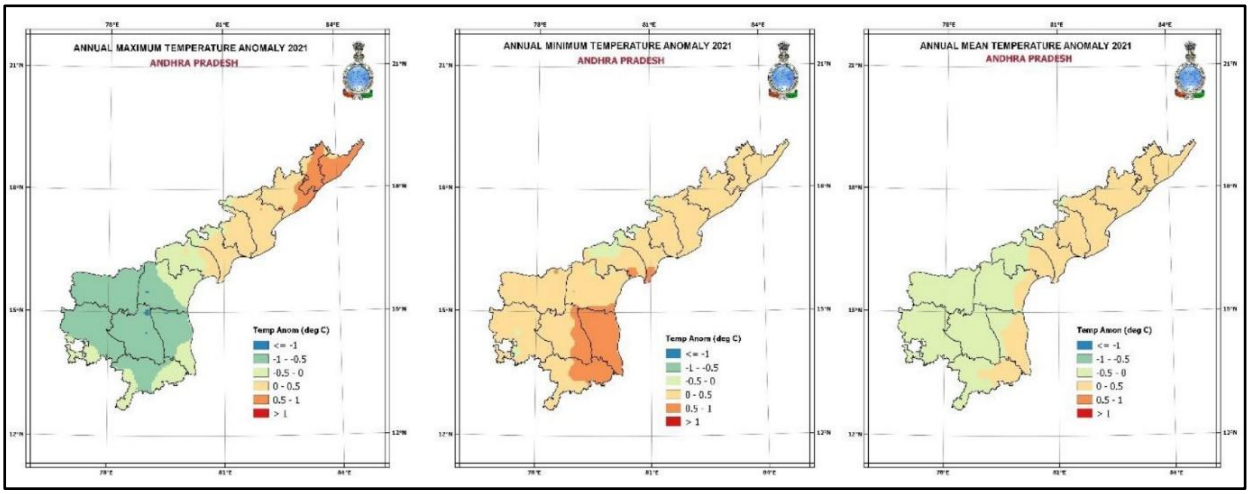

Figure 1.1. Spatial patterns of annual maximum, minimum and mean temperature anomalies over Andhra Pradesh during 2021. Anomalies represent deviations from the long-period average for the 1981–2010 base period. (*Ref: Figure 2 from "Statement on Climate for the State of Andhra Pradesh: 2021", July 2022, Climate Monitoring and Prediction Group, Indian Meteorological Department*), IMD (2022).

Several investigations have applied regional climate models (RCMs) and statistically or dynamically downscaled GCM outputs to assess future climate conditions over Andhra Pradesh. Under different Representative Concentration Pathways (RCPs) and Shared Socioeconomic Pathways (SSPs), projections consistently indicate a rise in average annual temperature of approximately 1.5–2.5 °C by the mid-21st century. These studies also project increasing irregularity and intensification of monsoonal precipitation (Raju et al., 2020; Srinivas et al., 2019). Dynamic downscaling experiments conducted under the CORDEX-South Asia framework further highlight enhanced inter-annual rainfall variability and a greater frequency of extreme rainfall events (Ghosh et al., 2018). Such projected shifts in

temperature and precipitation patterns carry direct implications for hydrological processes in semi-arid river basins.

Jacob et al. (2014) demonstrate that climate-induced changes in temperature and precipitation can substantially alter water availability in semi-arid basins such as the Pennar River Basin. The Pennar River system shows high sensitivity to monsoon variability (Kumar et al., 2013), and therefore any seasonal redistribution of rainfall under warming scenarios can modify runoff generation mechanisms. Increased rainfall concentration within shorter durations may produce higher peak flows, while prolonged dry spells and elevated evapotranspiration may reduce baseflows and lean-season water availability (Mishra & Lilhare, 2016). These hydro-climatic sensitivities underscore the need for basin-specific modelling approaches that translate projected climate signals into streamflow responses.

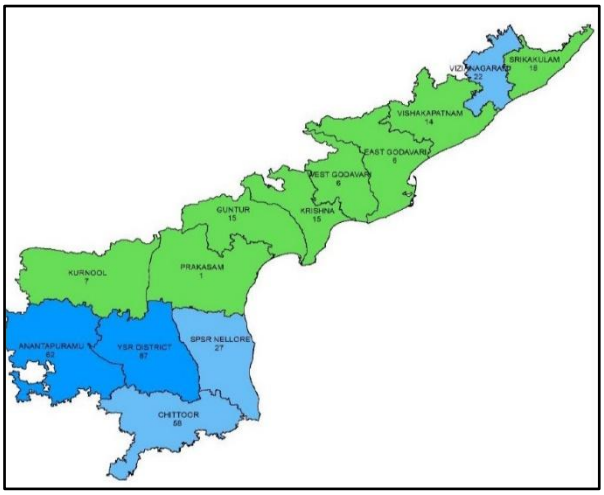

Figure 1.2. District annual rainfall departure map for Andhra Pradesh for the year 2021. Dark blue indicates Large Excess (60% or more), light blue indicates Excess (20% to 59%), and green indicates Normal (-19% to 91%). (*Ref: Figure 2 from "Statement on Climate for the State of Andhra Pradesh: 2021", July 2022, Climate Monitoring and Prediction Group, Indian Meteorological Department*), IMD (2022).

Groundwater dynamics in the Pennar basin also respond strongly to rainfall characteristics and land-use patterns. The Central Ground Water Board (CGWB, 2022) reports that recharge conditions depend heavily on rainfall intensity, duration, and spatial distribution, along with anthropogenic alterations in land cover. Shah et al. (2019) show that shifts in rainfall timing reduce effective infiltration opportunities, while

rising temperatures increase evapotranspiration losses and lower recharge efficiency (Acharjee et al., 2017). Together, these findings establish a clear linkage between projected climatic changes and both surface and subsurface water resources in the Pennar basin, thereby reinforcing the importance of integrated climate–hydrology impact assessment.

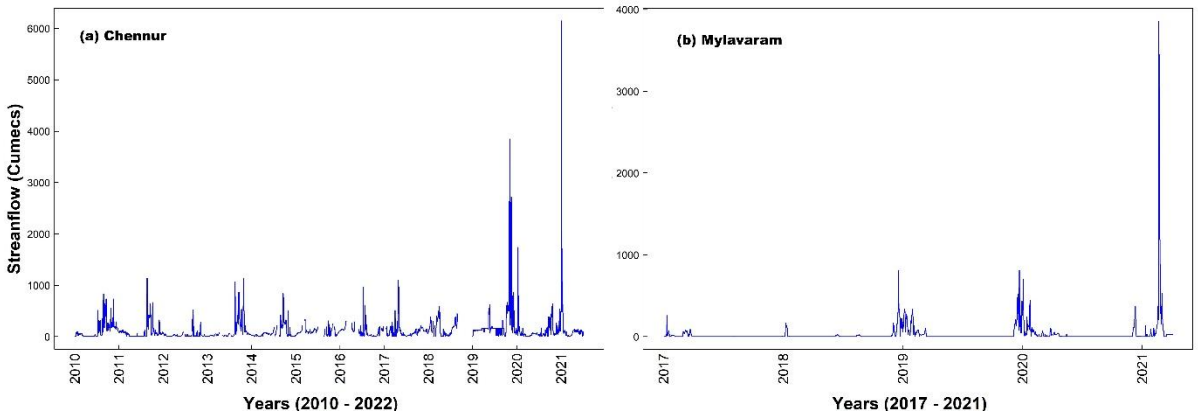

Figure 1.3. Observed daily streamflow (cumecs) at (a) Chennur (2010–2021) and (b) Mylavaram (2017–2021) gauging stations in the Pennar River Basin, illustrating pronounced inter-annual variability and extreme peak flow events during recent monsoon years.

Although several studies have analysed projected climate scenarios over Andhra Pradesh using regional climate models and downscaled CMIP simulations, fewer investigations translate these projections into integrated surface water and groundwater responses at the river basin scale. Climate projections alone do not provide actionable information for water allocation, irrigation planning, reservoir operation, or groundwater management. Decision-makers require hydrological projections that quantify changes in streamflow seasonality, variability, and recharge dynamics under different emission pathways. This study addresses that need by integrating multi-model CMIP6 climate projections with a physically based hydrological modelling framework and data-driven groundwater simulation. By combining climate analysis, process-based modelling, and machine learning techniques, the research develops a comprehensive assessment of future hydrological conditions in the Pennar River Basin. The findings aim to support climate-resilient water resource planning and adaptive management strategies in semi-arid river systems.

The remainder of this report follows the structure as follows:

- **Chapter 2** presents a detailed review of relevant literature on climate change impacts, hydrological modelling, and groundwater assessment.
- **Chapter 3** defines the objectives and scope of the study.
- **Chapter 4** describes the study area and the datasets used, including climate projections and hydrometeorological observations.
- **Chapter 5** outlines the methodological framework, including climate scenario development, hydrological modelling using VIC, and groundwater simulation using machine learning approaches.
- **Chapter 6** presents the results and discusses projected changes in climate, streamflow, and groundwater levels.
- **Chapter 7** summarizes the key findings and provides overall conclusions.
- **Chapter 8** outlines the way forward and recommendations for future research and policy integration.

2.0. LITERATURE REVIEW

The Intergovernmental Panel on Climate Change (IPCC) has consistently highlighted that anthropogenic greenhouse gas emissions are altering the global hydrological cycle (Mondal & Lakshmi, 2021). For the Indian subcontinent, recent studies utilizing the Coupled Model Intercomparison Project Phase 6 (CMIP6) indicate a warmer and potentially wetter future, though with high spatial variability (Chuphal & Mishra, 2023). Andhra Pradesh (AP) has a tropical, semi-arid climate. IMD data show AP's long-term annual rainfall is ~880–890 mm, mostly from the southwest monsoon (≈55–56%) and the post-monsoon northeast monsoon (≈33%) (Nageswararao et al., 2023). Recent trends (1991–2018) indicate a ~10% rise in both monsoon and post-monsoon rainfall across most AP districts (Nageswararao et al., 2023), suggesting a wetting tendency in recent decades. Over India as a whole, CMIP6 model ensembles project substantial warming by mid-21st century. For example, Dhara et al. (2025) report ~0.9°C historical warming (2015–24 vs. 1901–30) and project an additional +1.2–1.3°C by mid-century (SSP2-4.5). Average Indian monsoon rainfall is also projected to increase modestly: roughly +6–8% by ~2050 relative to recent decades (Dhara et al., 2025), though with strong regional variability. Climate change is expected to increase the intensity of extreme rainfall in Coastal Andhra (including the Pennar Basin), even if annual total change little, due to higher atmospheric moisture under warming.

In Andhra Pradesh, high-resolution climate modeling based on the PRECIS system projects an annual mean surface temperature rise ranging from 3°C to 4°C by the end of the 21st century (Majra & Gur, 2009). Earlier studies used Hadley-CM3 or PRECIS RCM outputs under IPCC SRES scenarios: e.g. Gummadi & Rao (2010) applied PRECIS-A2/B2 delta scenarios for Pennar. They found mean annual rainfall rising from ~660 mm historically to ~709 mm (A2) or 683 mm (B2) – roughly +8% (A2) or +4% (B2). Pechlivanidis et al. (2016) forced the India-HYPE hydrological model with bias-corrected CORDEX RCP runs; their results indicate the Pennar basin "becomes less water-scarce" by late century under high-emission scenarios. Near-future projections (2015–2030) under the SSP2-4.5 scenario suggest a significant increase in Potential Evapotranspiration (PET) by approximately 37.5% compared to baseline levels (Rentachintala et al., 2024). While some models suggest a general rise in summer monsoon rainfall for India, winter precipitation in regions like Andhra Pradesh

may see reductions of 5% to 25%, increasing the risk of seasonal droughts (Rentachintala et al., 2024). In summary, climate scenarios for Andhra Pradesh and Pennar River Basin point to clear warming (1 – 2 °C by mid-century) and uncertain rainfall changes: modest increases in annual totals but likely seasonal shifts and extremes that are more frequent. For example, Gummadi & Rao (2015) identified a ~+4 - 8% increase in mean rainfall and +10 - 15% rise in streamflows, whereas other studies suggest possible localized drying in dry seasons. These projections serve as inputs to hydrological models of the Pennar River Basin.

Hydrological modeling studies have examined how these climate scenarios affect Pennar flows. SWAT modeling (Pennar basin), which simulates rainfall-runoff processes – has been widely used. Gummadi & Rao (2015) calibrated SWAT over the basin and ran A2/B2 scenarios. They found that the slight rain increase (4 - 8%) yields a disproportionately larger flow increase: mean annual runoff rises ~8% (A2) or 4% (B2) compared to baseline. In their results, a 4 - 8% rainfall rise led to 10 - 15% higher flows, because evapotranspiration decreased under the scenarios (ET down ~10 - 12%). They cautioned, however, that flows became much more variable, so dry-year shortages could worsen despite the higher average flow. Multi-model hydrology studies offer a contrasting view. In another study, Pechlivanidis et al. (2016) used an ensemble of CORDEX-SSP projections in a large-scale HYPE model and found that Pennar's water availability actually improves under climate change (basin no longer "water-scarce" by 2100). This optimistic result runs counter to earlier work: Gosain et al. (2011) had projected reduced water yields in Pennar under 21st century warming. Pechlivanidis et al. (2016) note their result – increased flows – "is in contrast" to Gosain et al. (2011) for this basin.

In summary, streamflow projections for Pennar vary widely by model and scenario. The latest CORDEX-based results generally show slight increases in runoff, whereas some older models (particularly A2/B2) suggested similar modest increases or even declines. Notably, Gummadi & Rao (2015) found that a +4 – 8% rainfall increase produced +10–15% runoff gain. These divergent results reflect scenario uncertainty. In practice, flows will respond to both rainfall and evapotranspiration changes; SWAT and other models generally show warming-driven evapotranspiration increases, which reduces net runoff fraction (the A2 simulation had runoff =19% of rainfall vs. 15% in B2), highlighting the delicate balance. The consensus is that Pennar

is likely to warm by mid-century; monsoon rainfall may rise modestly but with higher inter-annual variability. High-flow season (monsoon) may intensify, while low flows (dry season) could shrink – a pattern seen in other peninsular basins.

While studies have modelled streamflow, fewer studies examine climate impacts on groundwater in the Pennar Basin. Groundwater serves as the primary source for irrigation and domestic use and supports a significant share of the region's water security. Changes in precipitation and infiltration directly control recharge and influence groundwater systems (Bhanja et al., 2020). Unlike some South Indian basins that show positive trends in Terrestrial Water Storage (TWS) due to localized conservation, the Pennar remains under "water stress" conditions due to over-exploitation and climate-induced recharge variability (Mondal & Lakshmi, 2021). Long-term droughts (2 years or more) have lasting implications. Persistent drought leads to increased groundwater pumping for irrigation, which further depletes the aquifers and lowers the water table (Mondal & Lakshmi, 2021). Nonetheless, emerging studies highlight vulnerability. Climate change affects groundwater mainly through altered recharge (precipitation minus evapotranspiration) and demand. In semi-arid peninsular India, higher temperatures tend to increase evapotranspiration and soil moisture loss, reducing recharge even if rainfall rises slightly (Bera et al., 2025). One recent case study in the Chitravathi sub-basin (in Rayalaseema, a tributary of upper Pennar) used CMIP6 projections and SWAT+MODFLOW. Chandra & Sahoo (2023) found dramatic groundwater declines by 2060: water table drops of ~54 m under SSP2-4.5 and ~62 m under SSP5-8.5 relative to today. This corresponds to an average drawdown rate of ~1.2–1.3 m/year under climate change. They attributed most of this decline to reduced recharge under warmer, more variable climate and expanding land use. Importantly, they conclude Pennar-tributary groundwater resiliency will be “poor” under future scenarios.

These findings are alarming but plausible given baseline stress. The Pennar basin is already heavily groundwater-dependent, with many areas experiencing annual recharge shortfalls. The Central Groundwater Board (CGWB) reports large unsustainable pumping in Pennar districts (especially in Kurnool, Kadapa, Nellore), leading to falling water levels. Climate change will likely exacerbate this: higher temperatures reduce rainfall efficiency, while any drying trend in pre- and post-

monsoon periods reduces recharge. As one hydrogeology review notes, “climate change is likely to reduce groundwater recharge and worsen depletion” in many parts of India (notably Andhra Pradesh and peninsular regions) (Bera et al. 2025). Although data for Pennar specifically are sparse, the Chitravathi study suggests groundwater will decline substantially unless mitigated. In addition, stream–aquifer interactions may weaken lower base flows (from reduced dry-season runoff) mean less natural seepage into groundwater. Conversely, higher monsoon floods might raise recharge in some years. The net effect is uncertain, but models point to a decline in baseflow contributions and recharge. The overall picture is that climate change will strain Pennar groundwater – pumping may remain the dominant driver in the short term, but reduced recharge means water tables will fall faster and recover less after monsoons.

In summary, recent literature indicates that climate change will warm Andhra Pradesh substantially by mid-century, with complex hydrologic responses in the Pennar basin. Key points include:

- **Warming**: All studies agree on significant warming (+1–2°C) for AP and Pennar this century. Higher temperatures increase evapotranspiration, raising irrigation demand and reducing soil moisture.

- **Rainfall changes**: Models project only modest average increases in monsoon rainfall for the region, but with large uncertainty. Some RCM scenarios (e.g. PRECIS-A2) found +4–8% annual rain in Pennar, while others show near-neutral changes. Observations show AP rainfall rose ~10% recently, but future variability is high, with some dry years becoming drier.

- **Streamflow impacts**: Hydrological models yield mixed outcomes. Gummadi & Rao found climate change under A2/B2 yields *higher* flows (+8% A2, +4% B2) due to increased rain and reduced ET. Similarly, Sharma *et al.* found Pennar flows increasing by late century (basin less water-scarce). In contrast, Gosain *et al.* and others predicted reduced flows under climate change. These differences largely stem from the balance of rainfall vs. ET changes. Notably, Gummadi showed that even a 4–8% rain increase could translate to a 10–15% flow increase, illustrating nonlinear effects.

- **Seasonality**: Nearly all studies emphasize seasonal effects. There is consensus that monsoon (wet-season) flows may rise or shift slightly, whereas pre- and post-monsoon (dry-season) flows are likely to fall. For example, Palanisamy *et al.* reported a ~20% December rain decline, portending much lower winter flows. The increased variability noted by Gummadi suggests more frequent low-flow years.

- **Groundwater**: Fewer studies exist, but those available warn of severe groundwater depletion. The Chitravathi case predicts tens of meters of water-table decline by 2060 under projected climate and land-use trends. This is consistent with the notion that AP (unlike some northern basins) may see *reduced* recharge under warming (since evaporation rises more than rain). Declining baseflow and recharge will likely lead to a decline in groundwater levels.

Overall, the literature underscores uncertainty in quantifying Pennar's hydrologic response. Climate–hydrology models differ in inputs (A2/B2 vs RCP/SSP), resolution, and hydrological structure. Results vary by scenario: e.g. under a high-warming SSP5-8.5, most models project greater stress (larger flow changes and deeper water-level drops) than under moderate scenarios. A clear takeaway is that small percentage changes in rainfall can yield large impacts on river flows and aquifer replenishment. The literature consistently shows that climate change will significantly warm Andhra Pradesh and modify its rainfall patterns, with profound implications for the Pennar River basin. While some models suggest modest increases in overall streamflow, all models indicate that evapotranspiration will rise and that dry-season water availability will decrease. Groundwater resources, which users already exploit intensively, will likely decline further under projected climate scenarios. Overall, published literature over the past few centuries indicate potentially higher wet-season flows but lower dry-season flows and declining groundwater, yet the magnitude and even sign of changes remain uncertain.

3.0 OBJECTIVES AND SCOPE OF STUDY

Several key gaps emerge from this review. First, projections for the Pennar basin use different models and scenarios, yielding contradictory results. No consensus exists on how much dry-season runoff or baseflow will change. Second, there are very few studies of Pennar groundwater; impacts on recharge and aquifers are poorly quantified. Third, many studies rely on single models or older scenarios; uncertainties from climate model choice, downscaling method, and land-use change are large. In particular, studies note that climate scenario and model selection introduce major uncertainty in hydrologic projections. Finally, most analyses focus on mean changes, with less attention to seasonal timing, extreme events, or integrated surface-subsurface interactions. These gaps suggest targeted research is needed. We therefore propose specific objectives that directly address the identified uncertainties and data needs.

1. Analyse CMIP6 projected rainfall and temperature for Andhra Pradesh and generate multi-model climate change scenarios.
2. Develop, calibrate, and validate a hydrological model to simulate surface water and groundwater dynamics in the Pennar River Basin.
3. Generate future hydrological scenarios (streamflow and groundwater levels) using CMIP6 climate projections.

4.0. STUDY AREA & DATA USED

Andhra Pradesh (AP) is a state in the Peninsular India lying between 12° 41´ to 19° 7´ N latitude and 77° to 84° 40´ E Longitudes, Figure 4.1. It has the second largest coastline (≈ 974 km) among the Indian states. The major geographical divisions of the state include Eastern Ghats, Coastal plains and Pene Plains and the major rivers flowing through the state include Godavari, Krishna and Pennar, delta regions of which constitute the coastal plains. Depending the on the geographical region, the climate varies considerably, summer temperature ranges between 20° and 41° C and the winter temperature ranges between 12° and 30° C. The annual average rainfall is spatially variable ranging between 700 mm (Rayalaseema) and 1100 mm (Coastal Andhra). Majority of the rainfall is received during the southwest monsoon during July to September, however low pressure systems and cyclones formed in the Bay of Bengal and the northeast monsoon contribute substantial amount of rainfall in southern part of the state and along the coastal regions during October to December. The weather in the state is monitored by the Indian Meteorological Department (IMD) through various meteorological stations spread across the state. To analyse the historical climate of the state and to make necessary bias corrections, historically observed climate datasets (station data and/or gridded datasets) are obtained from IMD (https://dsp.imdpune.gov.in/).

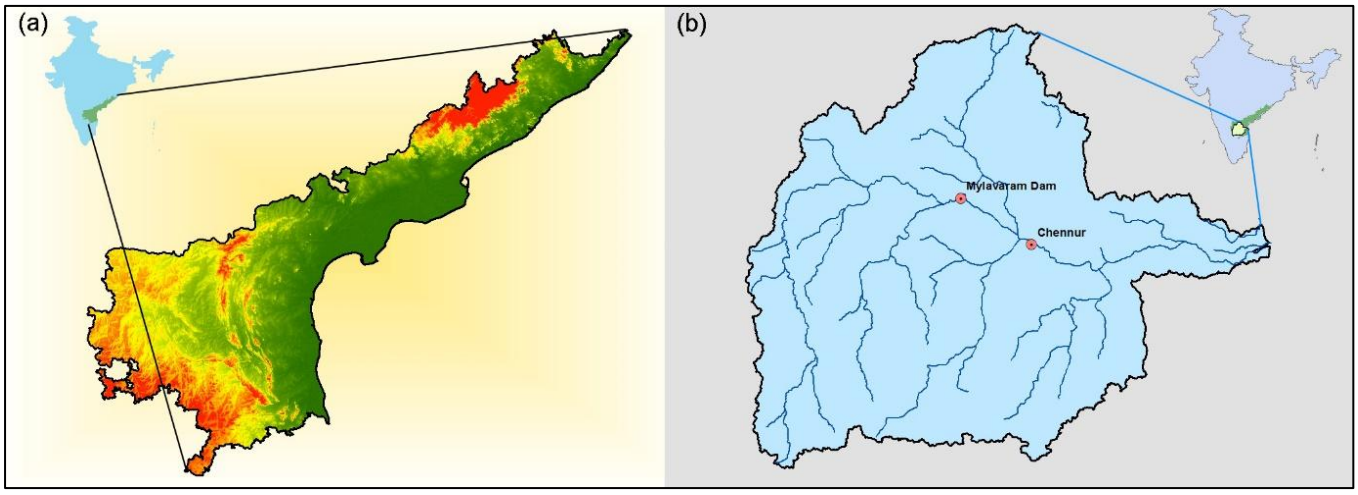

Figure 4.1. Location of the study area, (a) the state of Andhra Pradesh, and (b) drainage basin area of the Pennar River Basin (PRB). The red dots in (b) indicates the streamflow gauging station located near Mylavaram Dam and Chennur.

To evaluate the projected climate in the state of Andhra Pradesh, 10 Global Climate Models (GCM) are chosen from a set of 36 models from Coupled Model Intercomparison Project Phase 6 (CMIP6). These GCMs are developed by various research institutes/centers from across the world and they are built at varying spatial resolution and are run by different initial and boundary conditions. A few details of these 10 GCMs are listed in the Table 1 and more may be obtained from literature review. Raw output from these 10 GCMs are bias corrected and downscaled to a common grid of 0.25° resolution by NASA Center for Climate Simulation. NASA Earth Exchange Global Daily Downscaled Projections (NEX-GDDP-CMIP6) data set is comprised of global downscaled climate scenarios derived from the GCM runs conducted under the CMIP6 and across two of the four "Tier 1" greenhouse gas emissions scenarios known as Shared Socioeconomic Pathways (SSP). The purpose of this dataset is to provide a set of global, high resolution, bias-corrected climate change projections that can be used to evaluate climate change impacts on processes that are sensitive to finer-scale climate gradients and the effects of local topography on climate conditions. A statistical downscaling algorithm, Bias-Correction Spatial Disaggregation (BCSD) method is adopted by NASA for bias correcting the CMIP6 GCM output. The climatic variables used of this study are mean (*tas*), maximum (*tasmax*), and minimum (*tasmin*) temperature in °K and mean daily precipitation rate (*pr*) in kg/m^2/sec. In addition, to generate hydrological scenarios wind speed data is required, so daily mean near surface wind speed (*sfcWind*) provided in m/sec is used. Figure 4.2. presents the selected grid points of NEX-GDDP-CMIP6 datasets covering the state of Andhra Pradesh, a total of 221 grid points fall within the state of Andhra Pradesh.

Table 4.1: List of selected global climate models (GCMs) from the Coupled Modeled Inter-comparison Project 6 (CMIP6) used in the study

CMIP6 GCM	Institute
ACCESS-CM2	Commonwealth Scientific and Industrial Research (CSIRO)
ACCESS-ESM1-5	CSIRO
BCC-CSM2-MR	Beijing Climate Centre
CanESM5	Canadian Center for Climate Modeling and Analysis

CNRM-CM6-1	National Center of Meteorological Research (Centre National de Recherches Météorologiques), France
EC-Earth3	EC-EARTH Consortium, The Netherlands/Ireland
EC-Earth3-Veg-LR	EC-EARTH Consortium, The Netherlands/Ireland
INM-ESM1-2-LR	Institute for Numerical Mathematics (INM), Russia
MPI-ESM1-2-LR	Max Planck Institute for Meteorology, Germany
MPI-ESM1-2-HR	Max Planck Institute for Meteorology, Germany

Pennar River basin located in the Peninsular India extends over the states of Andhra Pradesh (≈ 48,276 km^2) and Karnataka (≈ 6,937 km^2) with a total basin area of approximately 55,213 km^2. The basin lies between 13° 18´ to 15° 49´ N latitudes and 77° 1´ to 80° 10´ E longitudes. The river rises from the Chenna Kesava hills of the Nandi Ranges in Karnataka and flows about 597 km before draining in to the Bay of Bengal. The basin lies mostly in the rain shadow region of the Eastern Ghats, the zone of poor rainfall, and hence is frequently hit by drought. The annual mean rainfall received in the basin ranges between 400 mm (near Rayalaseema region) and 1200 mm (near coastal plains). Groundwater is one of the important sources of water in the basin and the fluctuations in the groundwater is monitored through groundwater observation wells, there are approximately 426 observation wells maintained and operated by the Central Ground Water Board (CGWB) and the AP Groundwater Board (APGWB). The streamflow in the Pennar River is monitored by the Central Water Commission (CWC) and the state's Water Resources Department (WRD) through various gauging stations spread across the basin. In addition, the climatic conditions are monitored through various meteorological stations operated and maintained by IMD. For this study, the historical climate is represented by the IMD gridded datasets (precipitation at 0.25° resolution and temperature at 1° resolution). For VIC model calibration, we obtained daily averaged streamflow at Chennur gauging station from India-WRIS database (India Water Resources Information Systems; https://indiawris.gov.in/wris/).

We obtained observed groundwater level data from the Central Groundwater Board (CGWB) to develop AI/ML model for groundwater level prediction. We selected 60 observation wells for the analysis, Figure 4.3. We used the seasonal data collected from these observation wells to develop Random Forest (RF) model to simulate

groundwater level variations and evaluate the potential impacts of climate change on groundwater level variability.

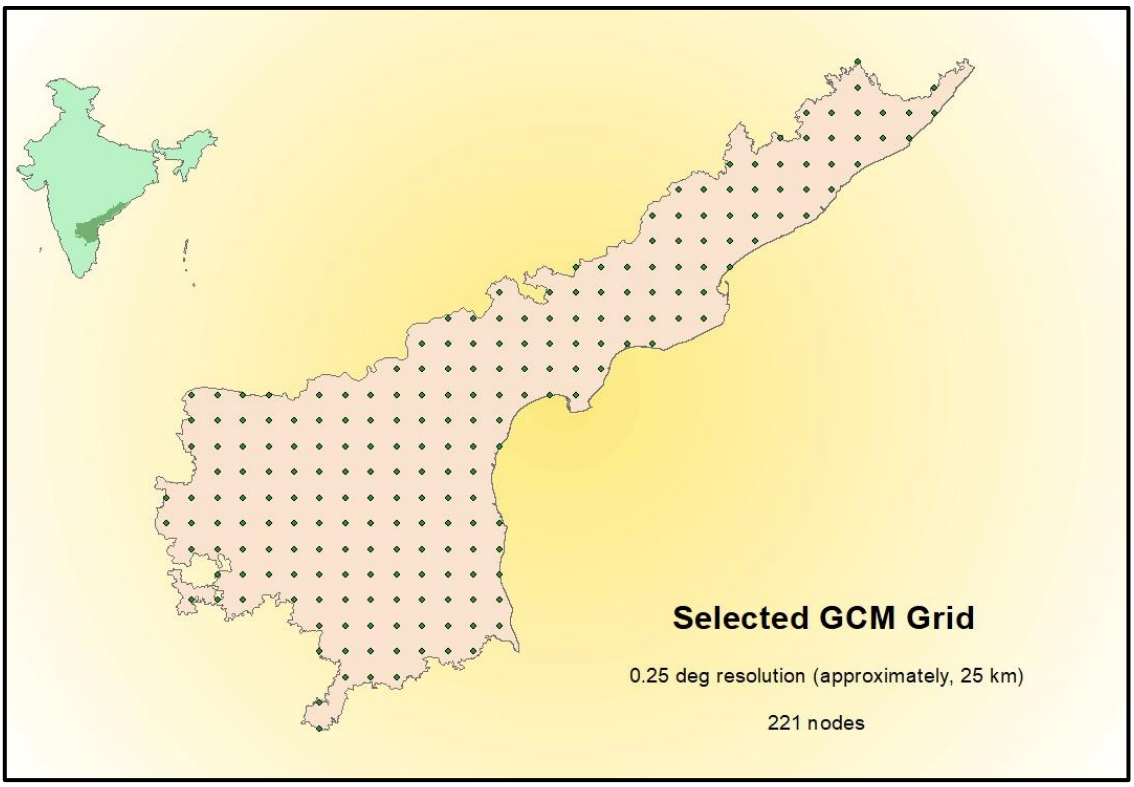

Figure 4.2. Selected grid points of NEX-GDDP-CMIP6 datasets covering the state of Andhra Pradesh.

The other important data required for building a hydrological model include basin elevation data, soil characteristics of the basin and land use-land cover (LULC) information. Elevation data of the basin obtained from Digital Elevation Model (DEM), which is provided by various institute/centers from across the globe including ISRO, NASA, etc. In this study, DEM provided by the Shuttle Radar Topography Mission (SRTM), a mission launched by NASA. The spatial resolution of this dataset is 30m and is available for download from https://dwtkns.com/srtm30m/. In addition, the soil characteristics dataset is obtained from the Digital Soil Map of the World (DSMW) in the ESRI shapefile format provided by FAO of the United Nations soil mapping of Indian region has been done by FAO and UNESO in 1961. Some of the associated properties such as soil types, texture and classes were derived from it (https://www.fao.org/soils-portal/data-hub/soil-maps-and-databases/faounesco-soil-map-of-the-world/en/). The LULC map used in this study is Copernicus Global Land Cover Layers at 100 m spatial resolution and is obtained from

https://developers.google.com/earth-engine/datasets/catalog/COPERNICUS_Landcover_100m_Proba-V-C3_Global, (Buchhorn et al., 2020). In addition, wind speed data is required for the computation of evapotranspiration in the VIC model. In this study, we obtained wind speed from the ERA5 reanalysis dataset developed by the European Centre for Medium-Range Weather Forecasts (ECMWF) under the Copernicus Climate Change Service (https://cds.climate.copernicus.eu/). ERA5 provides hourly atmospheric variables at a spatial resolution of 0.25° × 0.25° (approximately 25 km), which offers improved spatial representation compared to coarser global datasets.

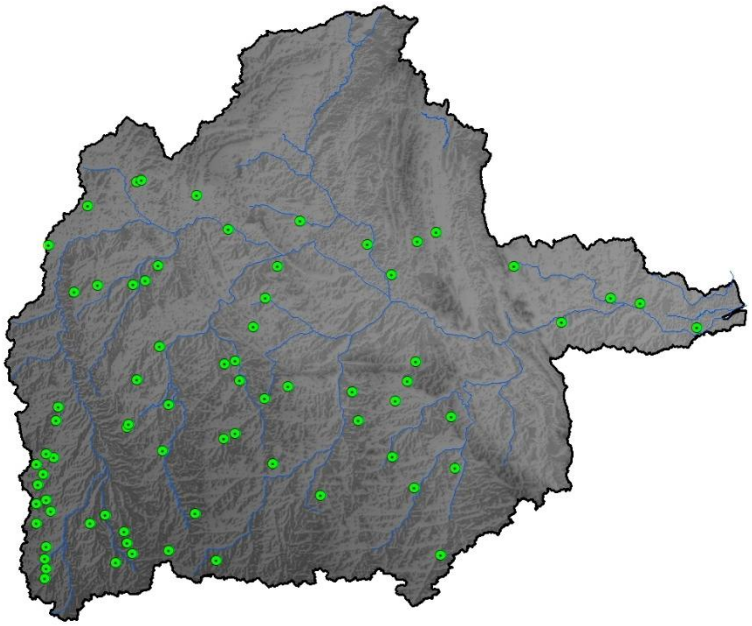

Figure 4.3. Locations of CGWB observations wells used for groundwater level analysis in the study area.

5.0. METHODOLOGY

5.1. Climate Change Assessment

The climate change assessment for Andhra Pradesh follows a systematic workflow from data acquisition to analysis of projected changes. The key steps include gathering observational and model data, preprocessing (regridding and bias-adjustment), computing climate statistics (means and extremes), and synthesizing results across multiple models. A flowchart, Figure 5.1. summarizes the procedure.

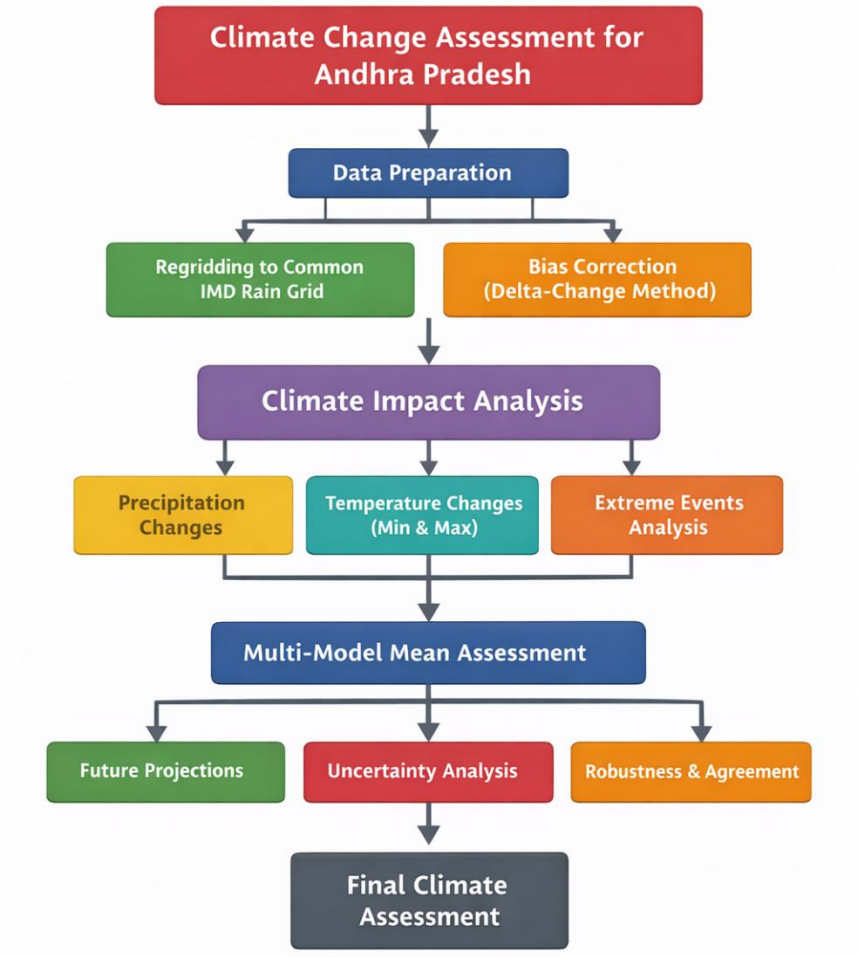

Figure 5.1. Methodology adopted for climate change impact assessment for the state of Andhra Pradesh.

5.1.1. Data Sources. We use high-quality observational climate data and outputs from global climate models. Observational inputs include gridded temperature (minimum and maximum) and precipitation data for India from the India Meteorological Department (IMD). In particular, IMD provides a long-term gridded daily rainfall dataset

at 0.25°×0.25° resolution covering 1901–2024 (https://www.imdpune.gov.in/cmpg/Griddata/Rainfall_25_Bin.html), and similarly gridded daily temperature data (built from station observations). These IMD datasets (and extensions by Pai et al. (2014) serve as our historical baseline. For future projections, we select multiple General Circulation Models (GCMs) from CMIP6 under the relevant emission scenario (SSP2-4.5 & SSP3-7.0). To address uncertainty, we focus on a subset of leading models (for example, the top 5 GCMs selected by performance) that have the required daily temperature and precipitation outputs for the historical (baseline) period and the future horizons of interest (e.g. 2021–2040, 2041–2070, 2071–2100). The precipitation data in the GCM output is stored as a flux term (unit = kg/m^2/sec) which is to be converted to depth units (mm/day). So, the magnitude of daily precipitation per day was computed using a conversion factor, 86,400 mm/day. Similarly, the temperature data which is stored as degree K is also converted to degree C using an additive faction of -273.9.

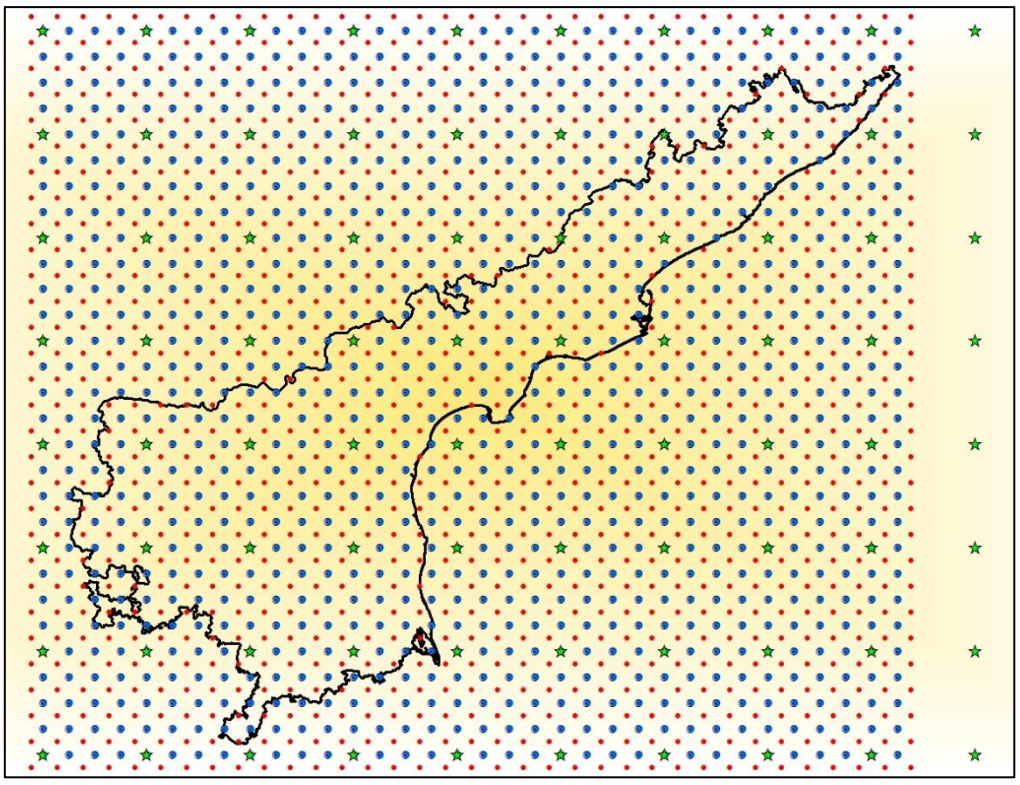

Figure 5.2. Overlay of GCM (Red Dots), IMD Rainfall (Blue Dots), and IMD Temperature (Green Stars) Grids Covering the State of Andhra Pradesh

5.1.2. Pre-processing: Regridding to a Common Grid: Because model outputs and observational data often come on different spatial grids, Figure 5.2., all data are interpolated to a single reference grid before analysis. We adopt the IMD rainfall grid (0.25°×0.25°) as the common grid. First, the IMD temperature fields are interpolated to this grid (maintaining consistency between variables). Although the spatial resolution of IMD precipitation is similar to that of the GCM grid, their alignments differ. So, each GCM's outputs are regridded from their native resolution to the IMD grid. We use bilinear interpolation, a widely used method for climate data regridding (https://climatedataguide.ucar.edu/climate-tools/regridding-overview), to regrid temperature and wind speed datasets. For example, prior studies emphasize that bilinear interpolation is appropriate for smoothly varying atmospheric variables when remapping between rectilinear grids. For precipitation, the study uses the nearest-neighbour interpolation method. This approach preserves the original rainfall magnitudes and avoids artificial smoothing of precipitation fields. The effect of regridding is checked by ensuring that large-scale means (e.g. area-averaged monsoon precipitation) are preserved. Indeed, in Mishra et al. (2020) the authors regridded CMIP6 data to 1° using bilinear interpolation and found negligible change in all-India mean temperature. Similarly, our regridding preserves the state-averaged climatology by construction.

5.1.3. Preprocessing: Bias Correction (Delta Adjustment): Raw GCM outputs typically exhibit systematic biases relative to observations, due to coarse model resolution and incomplete physics (Christensen et al., 2008; Mishra et al., 2020). For example, precipitation and temperature projections from GCMs often have spatially-varying biases that make them unreliable for regional impacts unless corrected. To address this, we apply a simple statistical bias-correction using the *delta change* (change-factor) approach. Specifically, for each model and grid cell, we compute the difference (or ratio) between the GCM's future climatology and its historical baseline climatology. We then *add* (for temperature) or *multiply* (for precipitation) this model-projected change onto the observed baseline climatology. In practice, this aligns the model's baseline mean with the observed mean, while preserving the projected anomaly. This delta method provides a first-order adjustment that ensures consistency with the observed historical climate. It is a transparent approach commonly used in climate change impact studies. Although more sophisticated bias-correction methods

(e.g. quantile mapping) exist, the delta approach is straightforward and preserves relative changes well when only mean shifts are of interest.

5.1.4. Integrated GCM Skill Score (IGSS): We computed the Integrated GCM Skill Score (IGSS) to evaluate how well the selected ten General Circulation Models (GCMs) reproduce the historical climate of the study region. We compared model simulations with observed data and assessed their performance using mean bias, variability ratio, Pearson correlation coefficient, and root mean square error (RMSE). We calculated these metrics for mean and extreme precipitation, along with minimum and maximum temperature. This approach considers errors in magnitude, the ability to capture variability, and agreement with observed temporal patterns. By combining these measures, the IGSS reflects how closely each GCM represents both average climate conditions and extremes and supports the ranking and selection of suitable models for hydrological impact assessment of changing climate.

5.1.5. Computation of Climate Statistics: With the bias-adjusted data on a common grid, we compute climate metrics for Andhra Pradesh. First, we define the baseline (historical) and future periods of interest. For example, a baseline might be 1981–2014, and future periods 2021–2040, 2041–2070, 2071–2100 (following standard multi-decadal horizons). For each grid cell, we calculate the long-term (mean) climatology of precipitation (annual and seasonal totals) and temperature (annual mean, seasonal mean, and extremes) for both baseline and future. Seasonal means typically include the summer monsoon (JJAS) and post-monsoon/winter (OND) seasons, as these have distinct climate signals. Next, we quantify changes by taking the difference (future minus historical) for temperature and the absolute or percentage change for precipitation. We also examine extremes: for example, we compute changes in percentile-based indices (such as the 95^{th} percentile of daily rainfall, or the number of hot days above a threshold). These indices capture shifts in climate extremes, which are critical for impact assessment.

5.1.6. Multi-Model Ensemble Analysis: To account for model uncertainty, we analyze each selected GCM separately and then aggregate results across models. Specifically, for each climate metric (e.g. monsoon rainfall change, extreme temperature change), we compile the projections from all models and compute the ensemble mean (multi-model average) and spread (e.g. one standard deviation or

model range). The ensemble mean gives a robust central estimate of the climate signal, while the spread indicates the level of agreement or uncertainty among models. Where appropriate, we also identify the number or fraction of models that agree on the sign of change. This multi-model approach follows best practices in climate assessments, as used in IPCC reports and regional studies.

5.1.7. Visualization and Documentation: The computed changes are visualized through maps, charts, and tables. Spatial maps show the geographic pattern of change (e.g. maps of °C temperature change or % precipitation change). Time series plots and boxplots may be used to summarize changes in state-average values. Extreme indices (percentiles, return levels) are plotted to illustrate shifts in variability and extremes. Finally, all results are compiled into the report. The methodological steps are depicted in the flowchart below (Figure 5.1.), and supporting information (e.g. model lists, scenario descriptions) is provided as needed.

The flowchart, Figure 5.1 presents the workflow used in this study. First, observed IMD climate grids and selected CMIP6 GCM outputs are collected. Second, all datasets are regridded or interpolated to the common IMD rainfall grid of 0.25° resolution. Third, delta-change bias correction is applied. Next, the study computes baseline and future climatologies for precipitation and temperature. These include mean values and extreme indices. It then combines results from multiple models to obtain ensemble mean changes and associated uncertainties. Finally, the study generates maps and plots to visualize the projected changes. This systematic workflow ensures a transparent and reproducible assessment and follows established climate impact assessment practices.

5.2. VIC Hydrological Model for Impact Assessment

The hydrological impact assessment for the Pennar River basin employs the Variable Infiltration Capacity (VIC) model version 4.2d. The VIC model (Liang et al., 1994) is a large-scale, semi-distributed hydrological model developed by the University of Washington (http://www.hydro.washington.edu). It is used to represent surface energy fluxes as well as hydrological fluxes at ranges ranging from vast river basins to the entire plant. This semi-distributed hydrological model is grid-based and quantifies the main hydro-meteorological processes occurring at the interface between the

atmosphere and the ground. VIC model consists of two primary components, the rainfall runoff and routing models, which allows the simulation of a number of processes including the infiltration of water, soil moisture retention, evapotranspiration, and runoff. Here, the evapotranspiration is estimated using the Penman-Monteith equation (Shuttleworth, 1991) for the three items, namely canopy evaporation, vegetation transpiration, and soil evaporation. The rainfall-runoff model simulates the physical exchange of water and energy among the soil, vegetation and atmosphere that govern the terrestrial hydrological cycle (Liang et al., 1994). In each computational cell, the model utilizes one vegetation layer and three soil layers: the upper soil layer controls evaporation, infiltration, and runoff while the lowest layer manages the baseflow simulation. The cell-based simulations are then transferred to the large-scale routing model (Lohmann et al., 1998), which generates basin discharge through a river-channel network using the St. Venant equation (Litrico and Fromion, 2003). We refer the readers to (Gao et al., 2010) to obtain more theoretical details. The schematic of the VIC 4.2.d model is shown in the Figure 5.3. One gauging station, Chennur operated and maintained by the Water Resources Department, Andhra Pradesh were chosen to calibrate and validate the VIC model of Pennar River Basin.

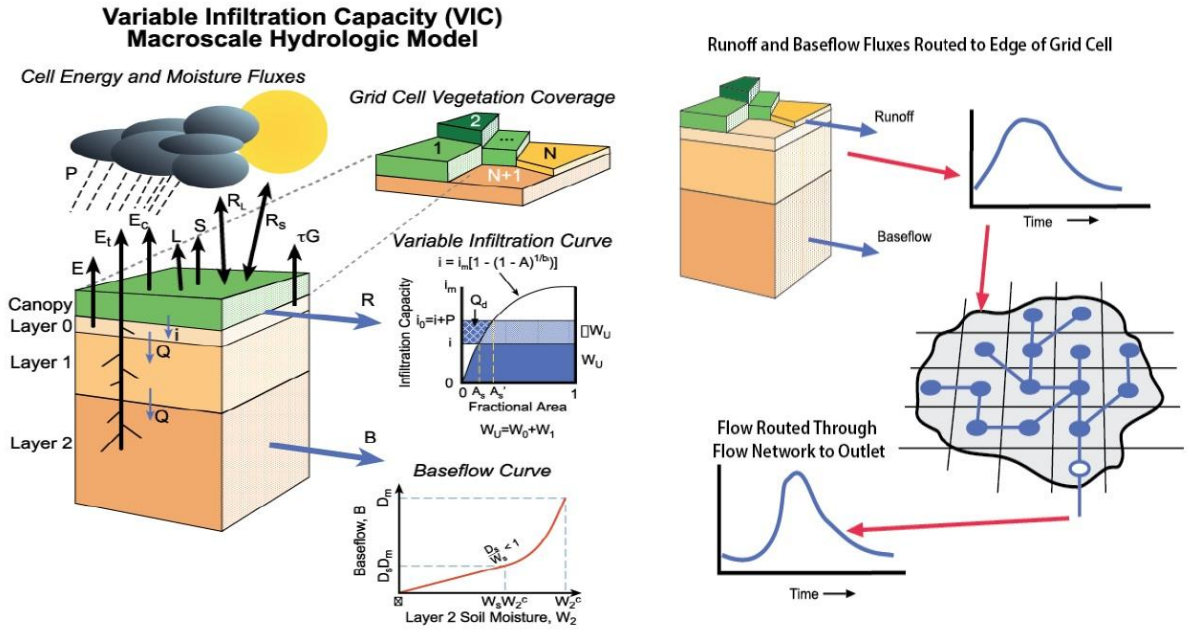

Figure 5.3.: Schematic of the Variable Infiltration Capacity (VIC) 4.2.d model. *Source: https://vic.readthedocs.io/en/vic.4.2.d/Overview/ModelOverview/*

Some key assumptions made in VIC model include (i) equation derived for a small uniform case are applied to a very large heterogenous areas and sub-grid heterogeneity is handled via statistical distributions, viz. elevation, soil class, land cover, etc. (ii) water can enter a grid cell only via the atmosphere (i.e. through precipitation), non-channel flow between grids is ignored, most runoff reached local channel network before reaching the grid cell boundary, and once the water reaches the channel network, it is assumed to stay in the channel and can't flow back into the soil. Grid cells are simulated independently of each other and routing of streamflow is performed separately from the land-surface simulation, using a separate model (Lohmann et al., 1996; 1998). The VIC model can be run in two modes, names water balance mode and energy balance mode. In water balance mode, air temperature and land surface temperature are assumed to be equal. In full energy balance mode, a repeated strategy that seeks to determine a surface temperature that modifies the surface energy fluxes (outgoing long waves, sensible heat, ground heat, ground heat storage, and indirect latent heat) is used to close the surface energy balance. The energy balance mode replicates surface energy fluxes which are crucial for comprehending the hydrological cycle and interactions between the land surface and the atmosphere in a basin. Moisture fluxes by both energy balance and water balance modes have been shown to be identical, if there is no frozen soil in the basin. Both moisture and energy flows are affected by the frozen soil. Frozen soil algorithm used in the VIC model has been found to boost springtime peak flows and decrease wintertime base flows. However, the Pennar River basin is located in Peninsular India and has no influence of snow or frozen soil, so VIC 4.2.d hydrological model is developed for the basin and is run in water-balance mode only.

5.2.1. Basin and Data Preperation: Developing a VIC hydrological model using VIC4.2d involves several sequential steps: preparing basin and forcing data, setting up the VIC model, calibrating/validating the model against observed flows, and performing scenario simulations for impact analysis. First the Pennar basin was delineated using ~30 m spatial resolution DEM from Shuttle Radar Topography Mission (SRTM) and Hydrology toolbox in ArcGIS. On the ArcGIS platform, a 5 km resolution VIC grid was created and overlaid on the Pennar River basin to identify which VIC grid cells lie within Pennar catchment. Input datasets for all these VIC grid cells are then compiled. All input files follow VIC's required formats. A global parameter

(control) file specifies model options (start/end date, time step, snow bands, output options) and lists the locations of all the input files.

Meteorological forcing: Daily time series of precipitation, maximum and minimum temperature, and wind speed. Historical forcing comes from observed or gridded data. For future scenarios, NEX-GDDP CMIP6 projections are prepared as time series. **Soil parameters**: For each grid cell, the soil layer depths, porosity, field capacity, wilting point, and texture (sand/clay fraction) are specified in the VIC soil parameter file. The soil properties were obtained from global soil map prepared and provided FAO.
Vegetation parameters: A vegetation library describes plant functional types (PFTs). A vegetation parameter file then gives each cell's fractional area of PFTs, rooting depths, maximum leaf area index, and other vegetation attributes. These parameters are derived from Copernicus Global Land Cover Layers at 100 m spatial resolution.

5.2.2. Model Setup and Execution: The VIC model was executed via the Cygwin interface on a windows based system. The model was compiled from the source, to generate a VIC executable (vicNl) executable and then executed with the global control file. VIC is inherently a spatial water–energy balance model: at each time step and for each grid cell, it computes infiltration, evapotranspiration, runoff (surface and baseflow), and snow dynamics (not computed in this study). The runoff and baseflow outputs for each cell are routed to the basin outlet via a routing algorithm to generate streamflow. By default, VIC writes standard output files unless specified otherwise, (runoff, baseflow and actual ET, were simulated in this study. Model log output (warnings/errors) should be captured to ensure the run is successful.

5.2.3. Calibration and Validation: Before applying VIC for prediction, it was be calibrated to the observed streamflow data at Chennur, obtained from WRD, Govt. of Andhra Pradesh. Calibration adjusts certain model parameters so that simulated discharge matches observed hydrographs. Since some VIC parameters (such as infiltration and baseflow parameters) represent effective basin-scale values, they often require tuning. The following steps are commonly followed for an effective calibration of VIC hydrological model.

1. Route the VIC runoff through the stream network to simulate discharge at the basin outlet.

2. Compare simulated discharge to gauged streamflow. Calculate performance metrics (e.g. Nash-Sutcliffe Efficiency (NSE), percent bias) to quantify fit.
3. Adjust key parameters (most often the infiltration curve exponent *infilt*, baseflow parameters *Ds*, *Ws*, *Dsmax*, and effective soil layer depth) to improve the fit. Although VIC model calibration allows both manual and automated optimization approaches, we conducted manual calibration in this study.
4. It is important to hold out part of the record for independent validation. Only about half the observed period is used for calibration; the remainder is reserved for validation to ensure the model generalizes well.

During calibration, the parameters must remain within physically realistic ranges, Table 5.1. lists the ranges of some of the calibration parameters. Iterations continue until the simulated hydrograph reasonably matches the timing and magnitude of observed flows (e.g. a high NSE and low bias). A successful calibration yields a set of parameter values that provides a good statistical fit. We subsequently ran the model for the validation period while retaining calibrated parameter values to evaluate model performance using independent data.

Table 5.1. Recommended ranges and general guidelines for the use of selected soil parameters for calibration of VIC hydrological model

Soil Parameter	Recommended Range	General guidelines
infilt (n/a)	0.00001 to 0.4	This parameter defines the shape of the VIC curve. It describes the amount of available infiltration capacity as a function of relative saturated grid cell area. Higher value of *infilt* gives lower infiltration and yields higher surface runoff.
Ds (fraction)	0.001 to <1	This is the fraction of *Dsmax* where non-linear (rapidly increasing) baseflow begins. With a higher value of *Ds*, the baseflow will be higher at lower water content in the lowest soil layer
Dsmax (mm/day)	>0 to 30	Depends on hydraulic conductivity. This is the maximum baseflow that can occur from the lowest soil layer (in mm/day).
Ws (fraction)	>0.5 to 0.9	The fraction of maximum soil moisture (lowest soil layer) where non-linear baseflow occurs. This is analogous to *Ds*. A higher value of *Ws* will raise water content required for rapidly increasing, non-linear baseflow, which will tend to delay runoff peak

5.2.4. Scenario simulation and Impact Analysis: With a calibrated and validated VIC model, we simulate future scenarios. For climate change impact analysis, the meteorological forcings are replaced by projected climate data from NEX-GDDP-CMIP6, regridded and bias-corrected as described section 5.2.1. Each scenario run uses the same calibrated VIC parameters and produces a simulated streamflow time series under that scenario. We compared VIC-simulated hydrological responses under each climate scenario against baseline (historical) conditions to quantify hydrological changes, including variations in mean annual and seasonal runoff, shifts in peak and low flows, and changes in major water balance components such as evapotranspiration and runoff. We generated spatial maps to illustrate projected changes in basin-scale hydrology, particularly streamflow, and aggregated the results to obtain multi-model ensemble means and associated ranges. These analyses quantify projected changes in streamflow and related hydrological variables and help assess potential alterations in the hydrological regime of the Pennar River Basin under the selected climate change scenarios.

5.3. Machine Learning Model for Groundwater Levels

Machine learning (ML) comprises a set of computational algorithms that allow computers to learn patterns from data and make predictions or decisions without explicit rule-based programming. Researchers have developed several categories of machine learning approaches to address different types of data structures and modelling problems, including supervised learning, unsupervised learning, reinforcement learning, semi-supervised learning, transfer learning, and deep learning algorithms. Recent studies increasingly apply machine-learning techniques in groundwater modelling because these methods effectively analyse complex and nonlinear hydroclimatic datasets and identify underlying relationships among multiple controlling variables. Different ML approaches address specific modelling objectives depending on data availability and problem characteristics. Commonly applied ML frameworks include supervised learning, unsupervised learning, reinforcement learning, semi-supervised learning, transfer learning, and deep learning approaches (Gurrapu, 2025).

5.3.1. Data Collection and Pre-processing: In this study, we developed and calibrated a Random Forest (RF) machine-learning model at selected CGWB

groundwater observation wells across the Pennar River Basin (PRB). Numerous groundwater-forecasting studies report strong predictive performance of the Random Forest algorithm and recognize it as one of the most widely applied machine-learning approaches in this field (e.g. Gilbert et al., 2025). It is particularly suited to our problem because it naturally handles nonlinear relationships and interactions among predictors (e.g. how temperature and precipitation together affect groundwater), without requiring explicit specification of those relationships. Random Forest represents a supervised learning technique suitable for both regression and classification applications. The RF algorithm constructs an ensemble of decision trees using multiple subsets of the training dataset and combines predictions from individual trees to produce more accurate, stable, and robust model outputs. Predictor variables used in the model include precipitation, temperature (daily minimum and maximum), soil moisture flux, baseflow, and the Standardized Precipitation-Evapotranspiration Index (SPEI). The target variable is the seasonal groundwater level, separately for the pre-monsoon (summer) and monsoon seasons. The study aligns all datasets to a common time grid (e.g., monthly resolution) and aggregates them into seasonal values. For example, pre-monsoon season variables can be averaged (or summed for precipitation and SPEI) over March–May, and monsoon season over June–September. We normalized selected predictors to maintain comparable scales, although Random Forest models do not strictly require normalization. We also computed additional predictors, including lagged groundwater levels (e.g., groundwater levels from the previous season), which improved forecasting skill. By incorporating historical groundwater levels and meteorological indices such as SPEI, the model accounted for antecedent hydrological conditions influencing groundwater variability.

After assembling the dataset, we divided it into training, validation, and test subsets. Considering the time-series nature of groundwater observations, we performed temporal splitting instead of random sampling by allocating approximately 70–80% of the earliest records for model training and cross-validation, while reserving the most recent 20–30% of records as an independent test dataset. This approach enabled us to evaluate model performance using unseen data and thereby replicate realistic forecasting conditions. We ensured the inclusion of both pre-monsoon and monsoon observations for each year to capture seasonal variability adequately. We

conducted hyper-parameter tuning exclusively within the training and validation subsets while preserving the test dataset for final model evaluation.

5.3.2. Seasonal Predictor Development and Variable Selection: To represent seasonal hydroclimatic variability, we derived predictor variables at the seasonal timescale. For each year and season, we computed total seasonal precipitation, seasonal average, maximum, and minimum temperature, and cumulative soil moisture flux obtained from land surface model outputs or soil moisture observations, total baseflow contribution derived from hydrological simulations or gauged flow records, and seasonal SPEI values. We also incorporated antecedent groundwater conditions, including groundwater levels observed during the preceding season or year, because groundwater systems exhibit strong temporal persistence. These predictors collectively constituted the input feature matrix, while the observed groundwater level at the end of each season represented the target variable (y).

We selected predictor variables based on hydrological relevance and process understanding. The selected predictors included precipitation, maximum and minimum temperature, soil moisture flux, baseflow, SPEI, and antecedent groundwater levels. We evaluated inter-variable collinearity and removed highly redundant predictors where necessary to improve model parsimony, although Random Forest algorithms generally handle correlated inputs effectively. When required, we derived additional variables such as temperature anomalies or interaction terms and evaluated dimensionality reduction techniques, including principal component analysis, only when they improved model performance. Throughout model development, we strictly avoided data leakage by ensuring that future information did not influence predictor construction or model training.

5.3.3. Model Development: Random Forest Training: We developed the RF model within the R statistical computing environment using established machine learning packages, primarily the *randomForest* package. The model configuration included key hyper-parameters such as the number of trees (*ntree*), number of predictor variables randomly selected at each split (*mtry*), maximum tree depth, and minimum node size. We optimized these hyper-parameters through systematic cross-validation procedures. We conducted hyper-parameter tuning using grid-search optimization implemented through the *caret* package across predefined parameter ranges,

including the number of trees (100–1000), *mtry* values representing different subsets of predictor variables, and minimum node sizes controlling tree complexity. We evaluated model performance using k-fold cross-validation (k = 5 or 10) applied to the training dataset and selected optimal parameter combinations based on performance metrics such as Root Mean Square Error (RMSE) and coefficient of determination (R^2). This procedure reduced the risk of model overfitting to specific data partitions. For datasets with limited temporal records, we additionally adopted a leave-one-year-out cross-validation strategy, in which each hydrological year served sequentially as a validation subset.

During model training, the RF algorithm generated individual decision trees using bootstrap samples drawn from the training dataset and determined optimal split conditions by minimizing prediction error. We employed a sufficiently large ensemble size (500–1000 trees) to ensure model stability and convergence. We controlled model complexity by specifying minimum node sizes and optimizing predictor selection at each split. We monitored the out-of-bag (OOB) error throughout model calibration to obtain an internal estimate of predictive performance. Because bootstrap sampling excluded approximately one-third of observations during individual tree construction, the algorithm used these excluded samples to compute independent prediction errors without requiring an additional validation dataset. We derived variable importance measures from the calibrated RF model to evaluate the relative contribution of predictor variables and to confirm the dominant influence of hydroclimatic drivers such as precipitation and antecedent groundwater conditions on seasonal groundwater variability.

5.3.4. Model Validation and Uncertainty Analysis: After completing hyper-parameter tuning, we evaluated the final Random Forest model using an independent test dataset consisting of the most recent years excluded from model training and validation. We assessed model performance using statistical metrics including the coefficient of determination (R^2), Root Mean Square Error (RMSE), Kling-Gupta Efficiency (KGE), and Mean Absolute Error (MAE) for both pre-monsoon and monsoon seasons. We examined scatterplots of observed and predicted groundwater levels to assess prediction bias and heteroscedasticity. We further conducted residual analysis

by analysing residuals against fitted values and temporal sequences to identify systematic patterns not captured by the model.

To quantify predictive uncertainty, we adopted two complementary approaches. First, we estimated model uncertainty using the inherent variability among predictions generated by individual decision trees within the Random Forest ensemble. We derived prediction intervals by calculating the standard deviation of tree-based predictions for each observation. Second, we implemented an ensemble modelling approach by training multiple RF models using different random data subsets and alternative hyper-parameter configurations and subsequently evaluated the spread of simulated groundwater levels. This analysis enabled assessment of model sensitivity to sampling variability and parameter selection. We additionally compared RF model performance with baseline approaches, including multiple linear regression and persistence-based models that relied solely on antecedent groundwater levels, to justify the adoption of a machine-learning framework. We applied k-fold cross-validation on the training dataset to estimate average model performance and associated variability, thereby providing a robust evaluation of predictive skill. We documented all validation procedures and performance metrics systematically to ensure transparency and reproducibility.

6.0. RESULTS AND DISCUSSION

This chapter presents and discusses how projected climate change influences the hydrology of the Pennar River Basin. The analysis begins with an evaluation of future changes in temperature and precipitation over Andhra Pradesh derived from selected high-skill General Circulation Models under different emission scenarios. These projections form the basis for simulating basin-scale hydrological responses using the calibrated Variable Infiltration Capacity (VIC) model. The simulated streamflow responses highlight how changing climatic conditions alter surface water availability across the basin. In parallel, a Random Forest–based groundwater modelling framework uses hydro-climatic and land surface variables to estimate groundwater level variations under future climate conditions. By integrating climate projections with both physically based and data-driven modelling approaches, this study evaluates the combined response of surface and subsurface water systems and provides insights into the future hydrological sustainability of the Pennar River Basin.

6.1. Historical Climate Normal

Figure 6.1 depicts the spatial variation of long-term climate conditions across Andhra Pradesh using IMD gridded climate datasets for the period 1981–2014. Mean annual precipitation increases from the southwestern interior toward the coastal and northeastern regions, indicating strong spatial contrasts in water availability across the state. In contrast, both maximum and minimum temperatures rise toward the inland southern regions, reflecting warmer semi-arid conditions away from the coast. These climatic gradients strongly influence runoff generation, evapotranspiration demand, and groundwater recharge processes within the Pennar River Basin. Lower rainfall combined with higher temperatures over interior regions suggests greater hydrological stress and higher sensitivity of basin water resources to future climate change. The observed historical patterns therefore provide an essential reference for interpreting projected changes in streamflow and groundwater levels under future climate scenarios.

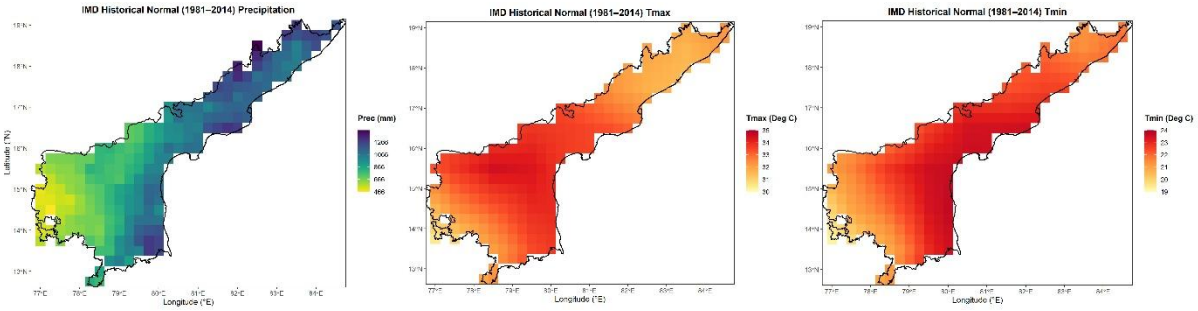

Figure 6.1. Spatial distribution of IMD Historical Climate Normals (1981 – 2014) over Andhra Pradesh: (i) Precipitation, (ii) Maximum Temperature, and (iii) Minimum Temperature.

Figure S1 shows the spatial distribution of historical precipitation, maximum temperature, and minimum temperature simulated by the selected ten (10) GCMs over Andhra Pradesh for the period 1981–2014. A comparison with the observed IMD climatology presented in Figure 6.1 indicates that the GCMs generally reproduce the large-scale spatial gradients across the state, including higher precipitation along the coastal and northeastern regions and warmer conditions over the inland southern areas. However, the models differ in the magnitude and spatial smoothness of these patterns, and several GCMs introduce systematic wet or dry biases along with slightly higher temperature estimates over interior regions. Although the models represent the overall climatic structure reasonably well, they fail to capture the localized variability evident in the IMD observations, which points to limitations in resolving regional-scale processes and coastal influences. These differences justify the application of bias correction prior to hydrological simulations and guide the selection of high-skill GCMs for assessing future climate impacts on streamflow and groundwater dynamics in the Pennar River Basin.

Table 6.1. Ranking of Selected GCMs over Andhra Pradesh Based on Integrated GCM Skill Score (IGSS)

GCM	Skill Score (IGSS)	Rank
BCC-CSM2-MR	0.30	1
ACCESS-ESM1-5	0.37	2
INM-CM4-8	0.41	3
CanESM5	0.43	4
EC-Earth3	0.45	5

Figure 6.2 presents the historical climate normals of the five best-performing GCMs selected using the Integrated GCM Skill Score (IGSS) for Andhra Pradesh, Table 6.1. The figure shows the spatial distribution of mean precipitation, maximum temperature, and minimum temperature simulated by BCC-CSM2-MR, ACCESS-ESM1-5, INM-CM4-8, CanESM5, and EC-Earth3 for the period 1981–2014. In comparison with the IMD historical normals, all selected GCMs successfully reproduce the dominant spatial gradients across the state, including higher precipitation toward the coastal and northeastern regions and relatively lower rainfall over the southwestern interior. The temperature fields also follow patterns consistent with IMD observations, with warmer conditions over inland southern regions and comparatively cooler zones along coastal and northern areas. Although minor differences remain in magnitude and spatial smoothness, the selected models show an improved agreement with observed climatology relative to the full GCM ensemble, particularly in capturing regional rainfall distribution and temperature gradients. This close correspondence confirms the robustness of the IGSS-based model selection and supports the use of these GCMs for bias correction and subsequent assessment of climate change impacts on streamflow and groundwater dynamics in the Pennar Basin.

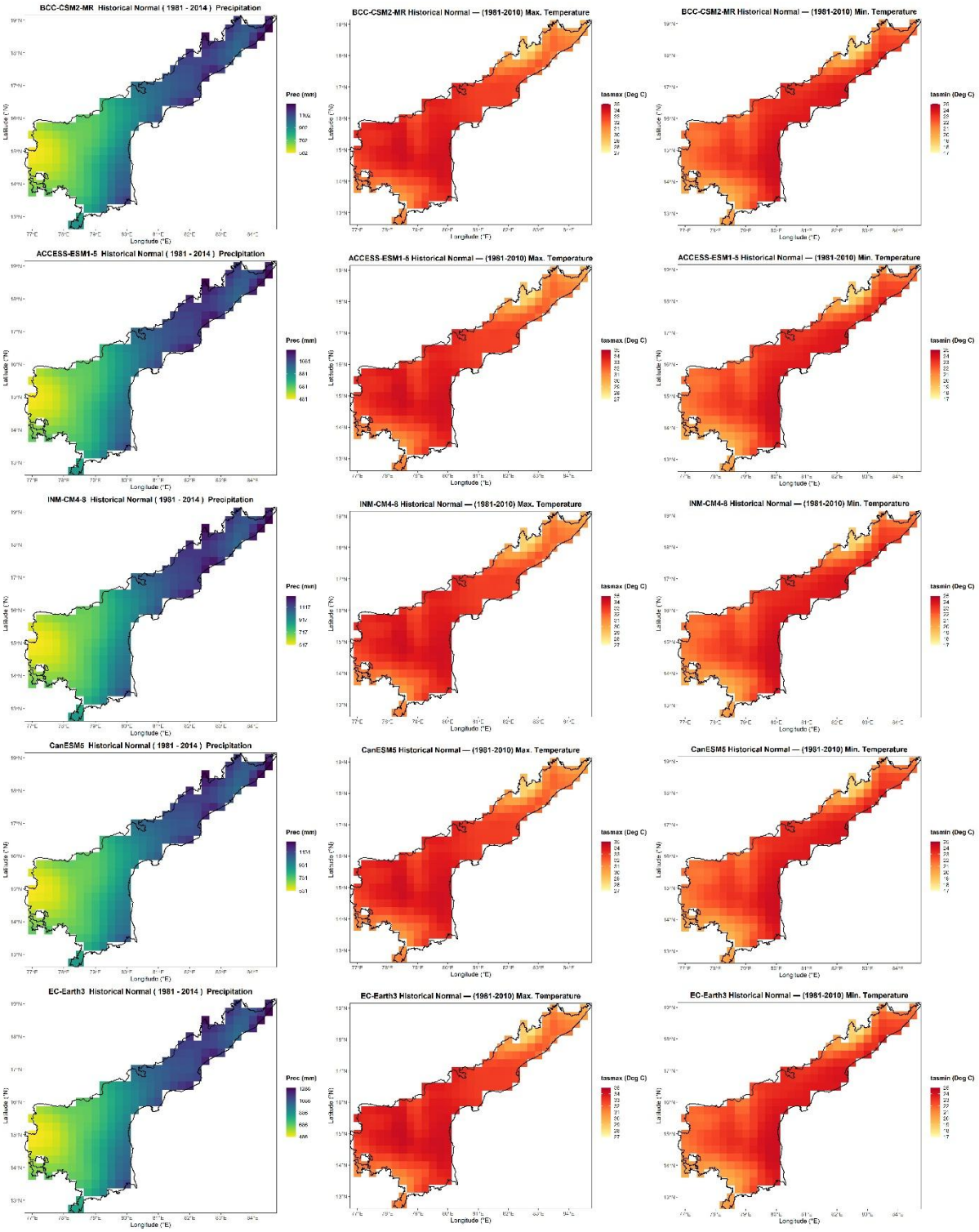

Figure 6.2. Spatial distribution of historical climate normals (1981–2014) simulated by the top five GCMs selected based on the Integrated GCM Skill Score (IGSS) over Andhra Pradesh, showing precipitation, maximum temperature, and minimum temperature.

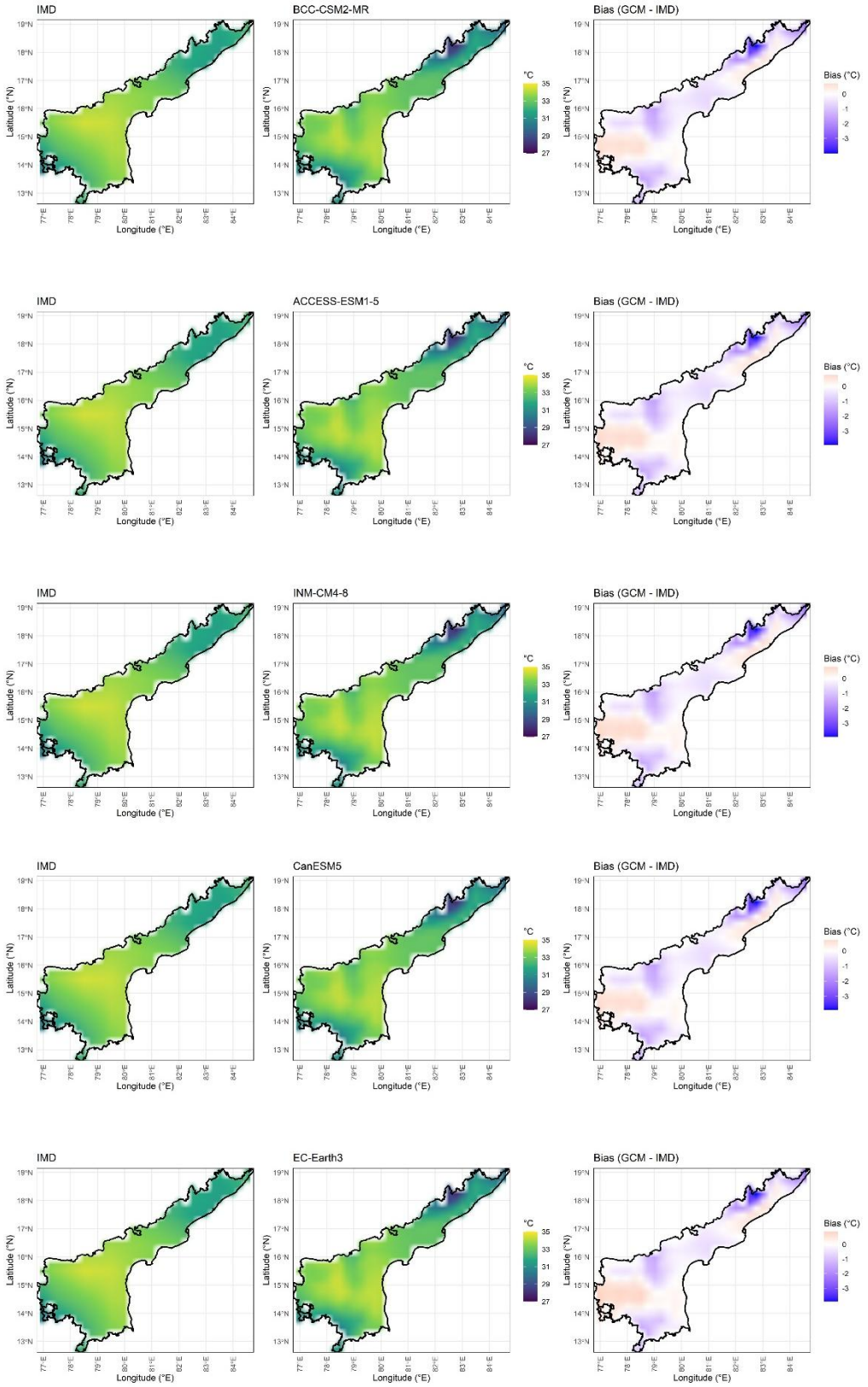

Figure 6.3. Spatial Evaluation of Historical Maximum Temperature (T_{max}) Simulated by Selected GCMs and Associated Bias (GCM − IMD) over Andhra Pradesh (1981–2014)

Figure 6.3 compares the spatial distribution of historical maximum temperature simulated by the five IGSS-selected GCMs with IMD observations and illustrates the corresponding model bias across Andhra Pradesh for the period 1981–2014. All selected models reproduce the major temperature gradient identified in the IMD historical normals, with relatively cooler conditions along coastal and northeastern regions and higher temperatures over inland southern areas. Despite this agreement in spatial patterns, the bias maps indicate systematic differences in temperature magnitude across the state. Most models underestimate maximum temperature over northern and coastal regions while generating localized warm biases over parts of the interior domain. These results confirm the reliability of the IGSS-based model selection while also highlighting the need for bias correction before using climate projections to drive VIC-based streamflow simulations and Random Forest–based groundwater assessments in the Pennar River Basin.

6.2. Future Climate Projections

6.2.1. Precipitation: Figure 6.4 illustrates the spatial distribution of annual precipitation projected by the five top-ranked CMIP6 models selected using the Integrated GCM Skill Score (IGSS), namely BCC-CSM2-MR, ACCESS-ESM1-5, INM-CM4-8, CanESM5, and EC-Earth3, after applying the Delta (factor) change bias correction method. The figure compares historical simulations with future projections for the near future (2021–2040), mid-century (2041–2070), and end-century (2071–2100) periods. The bias correction preserves the observed spatial rainfall gradients derived from IMD climatology while adjusting model magnitude, thereby enabling consistent assessment of projected hydro-climatic change.

All models maintain the characteristic spatial pattern observed in earlier historical figures, with relatively higher precipitation along the coastal and northeastern regions and lower rainfall over the southwestern interior parts of Andhra Pradesh. However, future projections indicate a gradual intensification of annual precipitation across most regions of the state, although the magnitude and spatial extent of change vary among models and time horizons. During the near-future period, models project modest increases in rainfall, primarily along coastal and central regions, while interior zones show comparatively smaller changes. By mid-century, several models, particularly INM-CM4-8, CanESM5, and EC-Earth3, indicate a noticeable expansion

of higher precipitation zones toward inland areas, suggesting strengthening monsoonal influence and enhanced moisture availability.

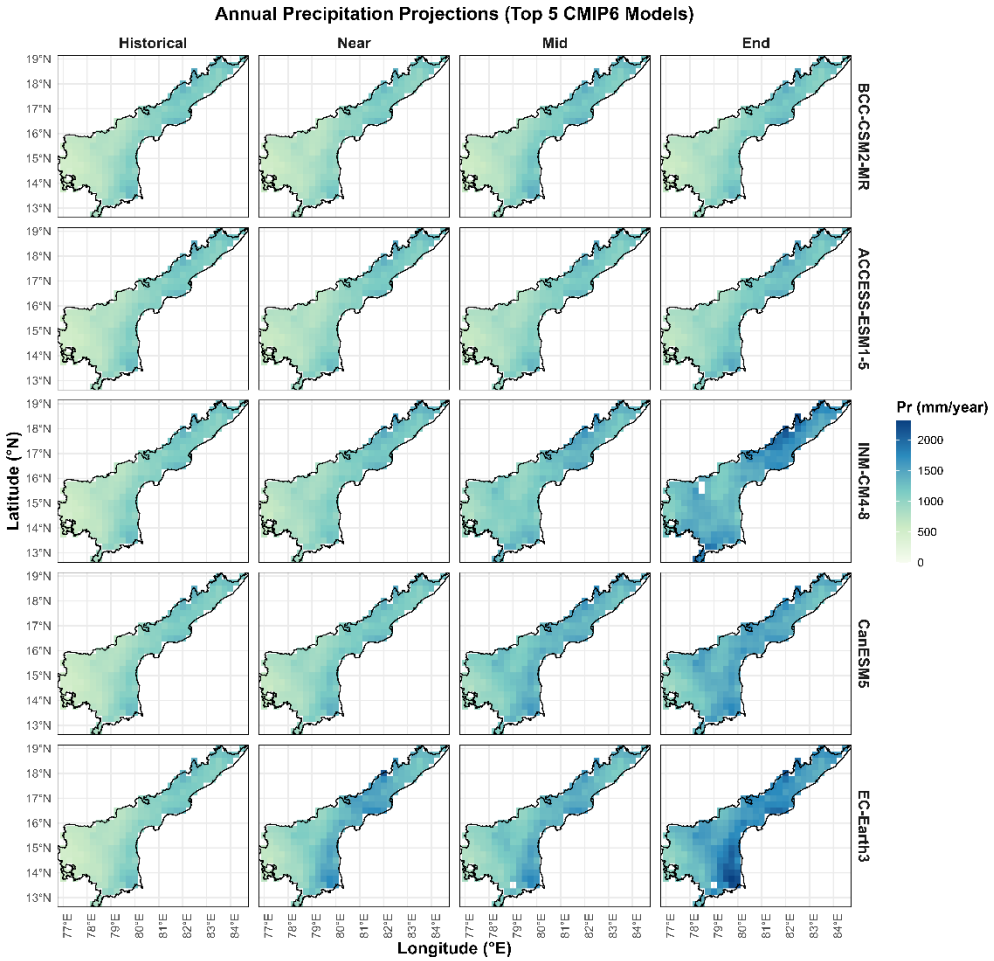

Figure 6.4. Spatial distribution of annual precipitation projected by the top five IGSS-selected CMIP6 GCMs under the SSP3–7.0 scenario after Delta change bias correction for historical, near future (2021–2040), mid-century (2041–2070), and end-century (2071–2100) periods over Andhra Pradesh.

End-century projections show the strongest precipitation response, with most models simulating widespread rainfall increases across Andhra Pradesh. EC-Earth3 and INM-CM4-8 project pronounced wetting over southern and central regions, whereas BCC-CSM2-MR and ACCESS-ESM1-5 indicate relatively moderate increases while preserving existing spatial gradients. Despite inter-model variability, all selected GCMs consistently suggest an overall shift toward wetter future conditions compared with the historical baseline. The persistence of spatial agreement among independently selected high-skill models increases confidence in the projected

precipitation signal. These projected increases in precipitation have important implications for basin hydrology. Enhanced rainfall may increase surface runoff generation and seasonal streamflow in the Pennar River Basin, while spatial redistribution of rainfall could alter groundwater recharge patterns and hydrological extremes.

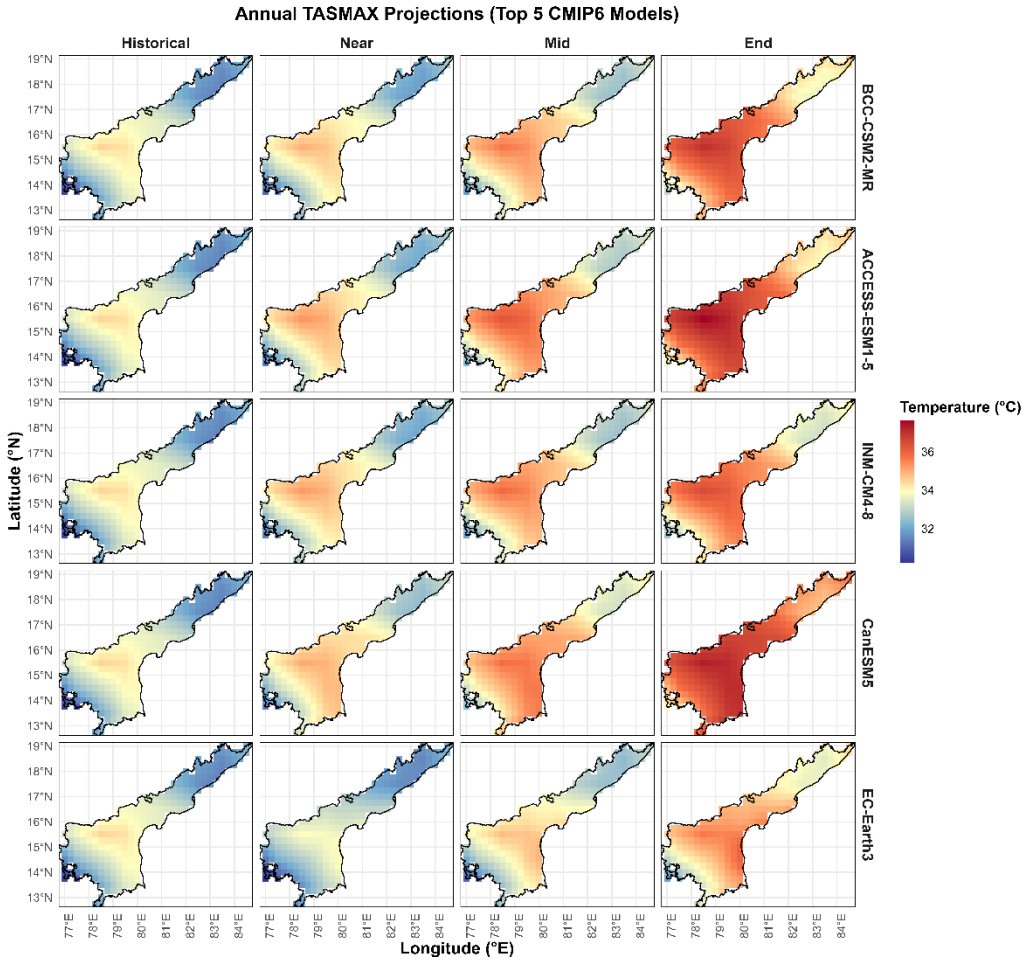

Figure 6.5. Spatial distribution of bias-corrected annual maximum temperature projected by the top five IGSS-selected CMIP6 GCMs under the SSP3–7.0 scenario for historical, near future (2021–2040), mid-century (2041–2070), and end-century (2071–2100) periods over Andhra Pradesh.

6.2.2. Maximum Temperature: Figure 6.5 shows the spatial distribution of annual maximum temperature (T_{max}) projected by the five IGSS-selected CMIP6 models after applying the Delta (factor) change bias correction method for Andhra Pradesh. The figure compares historical simulations with projections for the near future (2021–2040), mid-century (2041–2070), and end-century (2071–2100) periods. The bias correction

preserves the observed spatial temperature gradients derived from IMD climatology while adjusting model magnitude, which allows consistent evaluation of future warming trends. All models maintain the historical spatial pattern identified in earlier IMD and GCM climatology figures, where coastal and northeastern regions remain relatively cooler and inland southern regions experience higher temperatures. Future projections indicate a clear and progressive warming signal across the state throughout the twenty-first century. During the near-future period, all models project moderate temperature increases, with warming emerging more strongly over interior regions of Andhra Pradesh. By mid-century, the warming intensifies and expands spatially, producing widespread increases in T_{max} across both coastal and inland areas. End-century projections show the strongest warming response, with all models indicating substantial temperature rise across the entire state, particularly over the southwestern and central interior regions.

Although the magnitude of warming varies among models, CanESM5 and ACCESS-ESM1-5 project relatively higher temperature increases, while INM-CM4-8 and EC-Earth3 indicate comparatively moderate warming. Despite these differences, all selected GCMs consistently project a robust warming trend from historical to end-century conditions, which strengthens confidence in the projected temperature signal. Increasing T_{max} directly influences evapotranspiration demand, soil moisture depletion, and surface water losses within the Pennar River Basin. Consequently, rising temperature conditions may offset projected precipitation gains and intensify hydrological stress, thereby affecting future streamflow generation and groundwater recharge processes simulated using the VIC and Random Forest modelling frameworks.

6.2.3. Minimum Temperature: Figure 6.6 presents the spatial distribution of annual minimum temperature (T_{min}) projected by the five IGSS-selected CMIP6 models following application of the Delta (factor) change bias correction method over Andhra Pradesh. The figure compares historical conditions with projections for the near future (2021–2040), mid-century (2041–2070), and end-century (2071–2100) periods. The bias correction retains the observed spatial temperature gradients derived from IMD climatology while adjusting model magnitude, which enables consistent evaluation of future night-time warming trends.

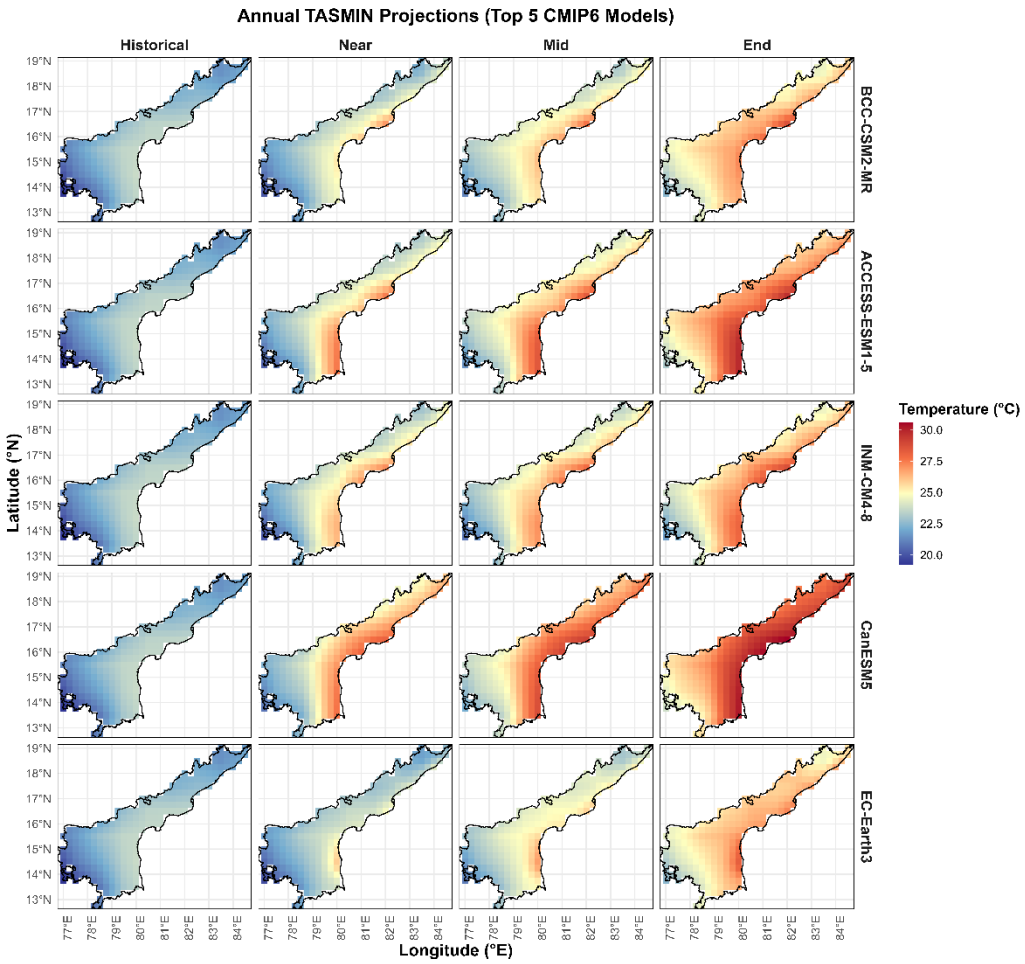

Figure 6.6. Spatial distribution of bias-corrected annual minimum temperature projected by the top five IGSS-selected CMIP6 GCMs under the SSP3–7.0 scenario for historical, near future (2021–2040), mid-century (2041–2070), and end-century (2071–2100) periods over Andhra Pradesh.

All models preserve the historical T_{min} pattern identified in earlier climatological analyses, where lower minimum temperatures occur over southwestern interior regions and relatively higher T_{min} values appear along coastal and northeastern areas. Future projections indicate a steady and spatially coherent rise in minimum temperature across the state throughout the century. During the near-future period, warming emerges primarily along coastal and central regions, while interior areas begin to experience noticeable increases in nighttime temperature. By mid-century, T_{min} increases expand across most parts of Andhra Pradesh, reducing the spatial contrast between coastal and inland regions. End-century projections show

pronounced and widespread warming, with all models indicating substantial increases in minimum temperature across the entire domain.

Among the selected models, CanESM5 and ACCESS-ESM1-5 project relatively stronger T_{min} increases, whereas INM-CM4-8 and EC-Earth3 simulate comparatively moderate warming. Despite differences in magnitude, all models consistently indicate intensified nighttime warming from historical to end-century periods. Rising minimum temperature reduces nocturnal cooling, increases atmospheric moisture retention, and enhances evapotranspiration losses, which may accelerate soil moisture depletion and influence groundwater recharge processes in the Pennar River Basin. When considered together with projected increases in T_{max}, the T_{min} projections confirm a robust warming signal that has important implications for future hydrological response simulated using the VIC and Random Forest modelling frameworks.

6.3. Climate Change Scenarios

6.3.1. Percentage Shift in Precipitation: Figure 6.7 illustrates the projected shift in annual precipitation over Andhra Pradesh under the SSP3–7.0 emission scenario based on the five top-performing CMIP6 models selected using the Integrated GCM Skill Score (IGSS). The left panel presents the historical precipitation distribution simulated by each model, while the right panels show the relative percentage change in precipitation for the near future (2021–2040), mid-century (2041–2070), and end-century (2071–2100) periods with respect to the historical baseline. All models maintain the historical rainfall gradient characterized by higher precipitation along the northeastern and coastal regions and comparatively lower rainfall across the southwestern interior. The projected change signal indicates a gradual intensification of precipitation across most parts of the state as the century progresses. During the near-future period, models project relatively small and spatially heterogeneous changes, with localized increases appearing mainly over southern and central regions. By mid-century, the wetting signal strengthens and expands spatially, particularly over inland areas, indicating an increase in monsoon-driven rainfall contribution. End-century projections show the most pronounced precipitation increase, with several models, including INM-CM4-8, CanESM5, and EC-Earth3, projecting widespread positive precipitation anomalies across large parts of Andhra Pradesh.

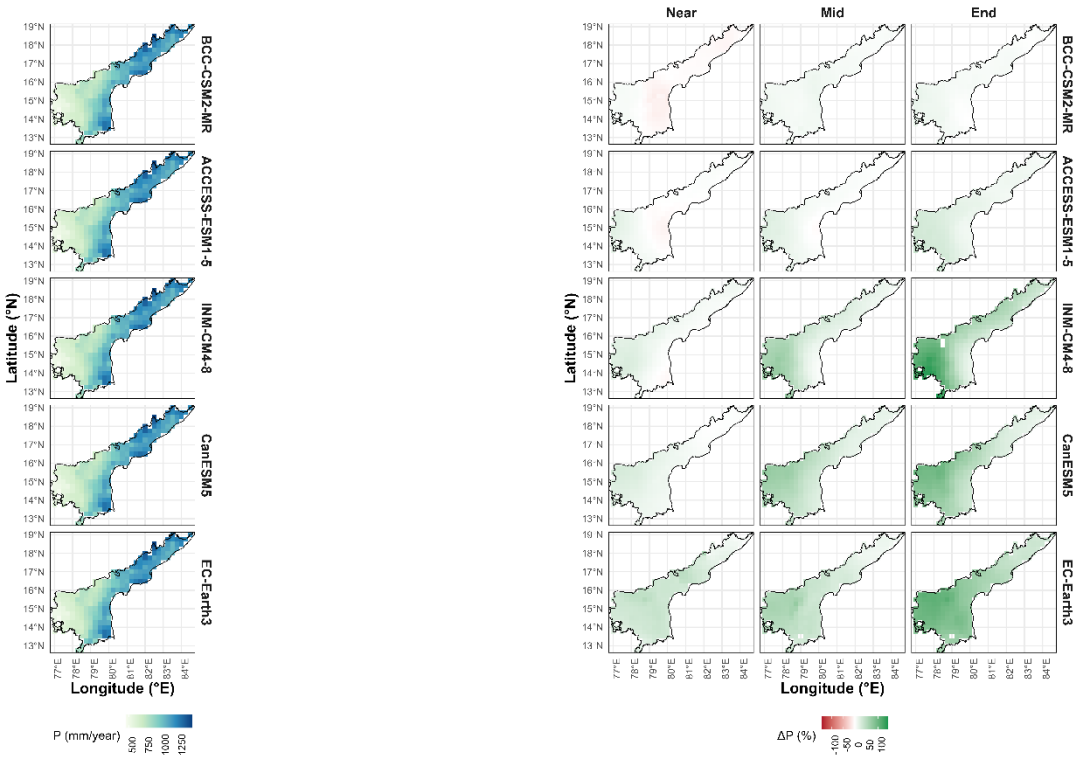

Figure 6.7. Spatial distribution of historical precipitation and projected percentage change in annual precipitation under the SSP3–7.0 scenario for near future (2021–2040), mid-century (2041–2070), and end-century (2071–2100) periods derived from the top five IGSS-selected CMIP6 models

Although the magnitude of change varies among models, all selected GCMs consistently indicate a dominant wetting tendency under the SSP3–7.0 scenario. The strengthening precipitation signal toward the end of the century suggests potential increases in runoff generation and seasonal water availability within the Pennar River Basin. However, spatially uneven rainfall enhancement may also increase the likelihood of hydrological extremes, including localized flooding and variability in groundwater recharge. The agreement among independently selected high-skill models enhances confidence in the robustness of the projected precipitation change signal used for subsequent hydrological impact assessment.

6.3.2. Shift in Maximum Temperature: Figure 6.8 illustrates the projected shift in annual maximum temperature (T_{max}) over Andhra Pradesh under the SSP3–7.0 emission scenario based on the five IGSS-selected CMIP6 models. The left panel presents the historical T_{max} distribution simulated by each model, while the right panels show the projected temperature change relative to the historical baseline for the near

future (2021–2040), mid-century (2041–2070), and end-century (2071–2100) periods. All models reproduce the historical spatial temperature gradient characterized by relatively lower maximum temperatures along coastal and northeastern regions and higher temperatures across inland southern areas. The projected change signal indicates a consistent and spatially coherent warming trend across the entire state throughout the twenty-first century. During the near-future period, models project modest increases in T_{max}, generally ranging from slight warming across coastal regions to stronger warming over interior zones. By mid-century, the warming signal intensifies and expands spatially, with most regions experiencing substantial temperature increases. End-century projections show the strongest warming response, with all models indicating widespread temperature rise across Andhra Pradesh, particularly over the southwestern and central interior regions.

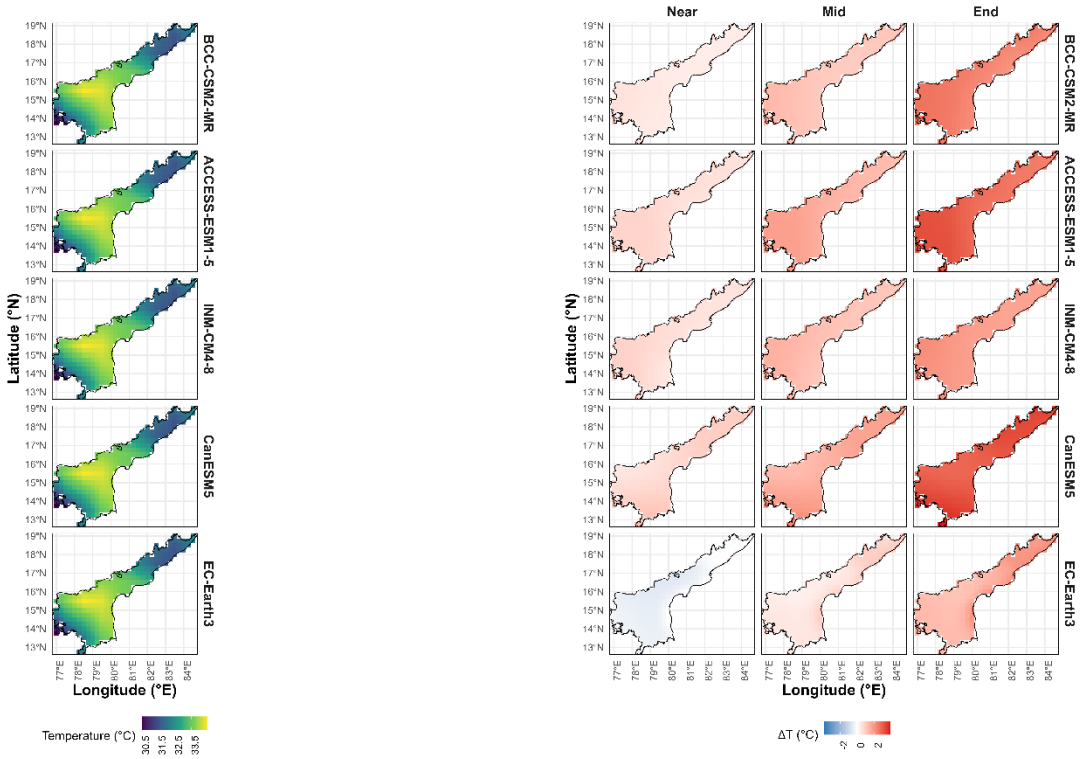

Figure 6.8. Spatial distribution of historical maximum temperature and projected change in annual T_{max} under the SSP3–7.0 scenario for near future (2021–2040), mid-century (2041–2070), and end-century (2071–2100) periods derived from the top five IGSS-selected CMIP6 models.

Although the magnitude of warming varies among models, CanESM5 and ACCESS-ESM1-5 project relatively higher increases in T_{max}, whereas INM-CM4-8 and

EC-Earth3 indicate comparatively moderate warming. Despite these differences, all selected GCMs consistently project positive temperature anomalies under the SSP3–7.0 scenario, demonstrating strong inter-model agreement in future warming trends. Increasing maximum temperature directly enhances evapotranspiration demand and accelerates soil moisture loss, which may reduce effective water availability even under projected precipitation increases. The projected T_{max} shift therefore represents a critical climatic driver influencing future streamflow response and groundwater recharge dynamics within the Pennar River Basin.

6.3.3. Shift in Minimum Temperature: Figure 6.9 illustrates the projected shift in annual minimum temperature (T_{min}) across Andhra Pradesh under the SSP3–7.0 emission scenario based on the five IGSS-selected CMIP6 models. The left panel shows the historical T_{min} distribution simulated by each model, while the right panels present projected temperature changes relative to the historical baseline for the near future (2021–2040), mid-century (2041–2070), and end-century (2071–2100) periods. All models reproduce the historical spatial T_{min} gradient characterized by relatively lower minimum temperatures over southwestern interior regions and higher T_{min} values along coastal and northeastern areas. The projected change signal indicates a consistent rise in minimum temperature across the state throughout the century. During the near-future period, models project moderate nighttime warming across most regions, with slightly stronger increases emerging over inland areas. By mid-century, T_{min} increases become spatially widespread and reduce the contrast between coastal and interior regions. End-century projections show pronounced warming across the entire state, with all models indicating strong positive temperature anomalies, particularly over central and southern inland regions.

Although the magnitude of warming varies among models, CanESM5 and ACCESS-ESM1-5 project relatively higher T_{min} increases, whereas INM-CM4-8 and EC-Earth3 indicate comparatively moderate warming. Despite inter-model differences, all selected GCMs consistently indicate intensified nighttime warming under the SSP3–7.0 scenario. Rising minimum temperature limits nocturnal cooling, increases atmospheric moisture retention, and sustains higher evapotranspiration demand, which may influence soil moisture persistence and groundwater recharge processes in the Pennar River Basin. Together with projected T_{max} increases, the T_{min} shift

confirms a robust warming signal that plays a critical role in shaping future hydrological response under changing climate conditions.

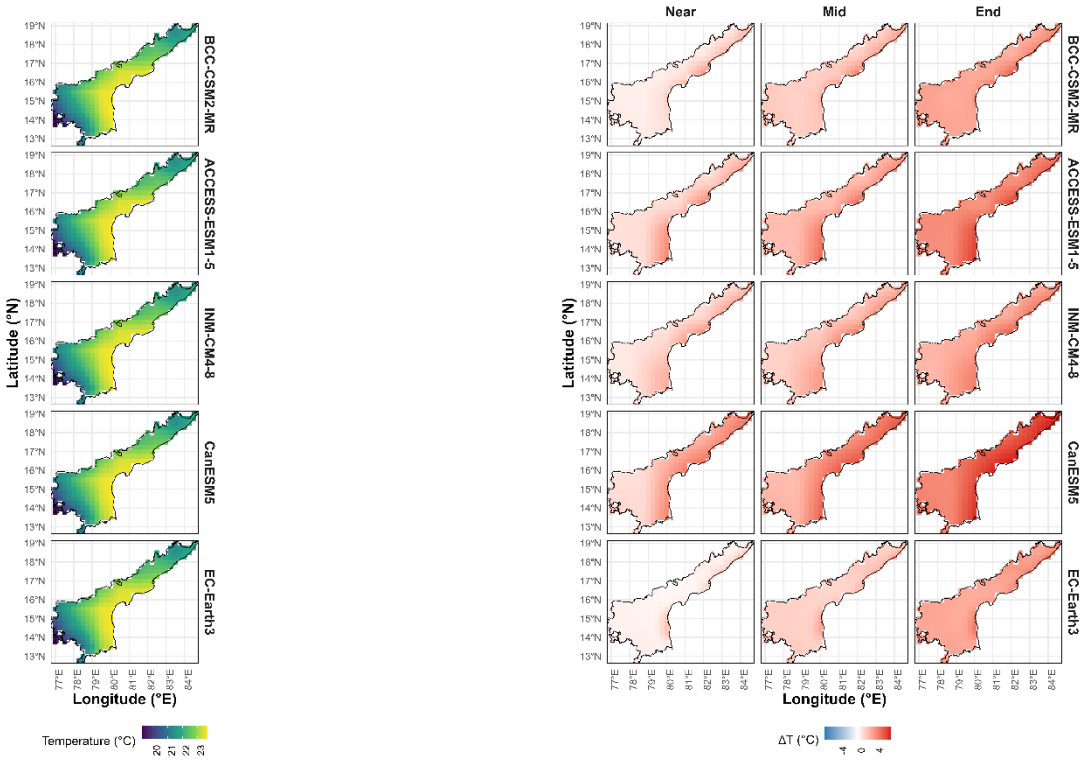

Figure 6.9. Spatial distribution of historical minimum temperature and projected change in annual T_{min} under the SSP3–7.0 scenario for near future (2021–2040), mid-century (2041–2070), and end-century (2071–2100) periods derived from the top five IGSS-selected CMIP6 models.

6.3.4. Changes in Seasonal Monsoon (DJAS) Rainfall: Figure 6.10 illustrates the projected shift in monsoon seasonal rainfall during the JJAS period over Andhra Pradesh under the SSP3–7.0 emission scenario using the five IGSS-selected CMIP6 models. The left panel shows the historical distribution of JJAS rainfall simulated by each model, while the right panels present projected percentage changes relative to the historical baseline for the near future (2021–2040), mid-century (2041–2070), and end-century (2071–2100) periods. All models reproduce the historical monsoon rainfall gradient characterized by higher seasonal rainfall along the northeastern and coastal regions and comparatively lower rainfall over the southwestern interior parts of the state. The projected change signal indicates a gradual strengthening of monsoon rainfall as the century progresses, although the magnitude and spatial extent of change vary across models. During the near-future period, models project relatively

small and spatially heterogeneous changes, with localized increases emerging mainly over southern and central regions. By mid-century, positive rainfall anomalies expand across inland regions, indicating enhanced monsoon moisture transport and increased seasonal rainfall contribution.

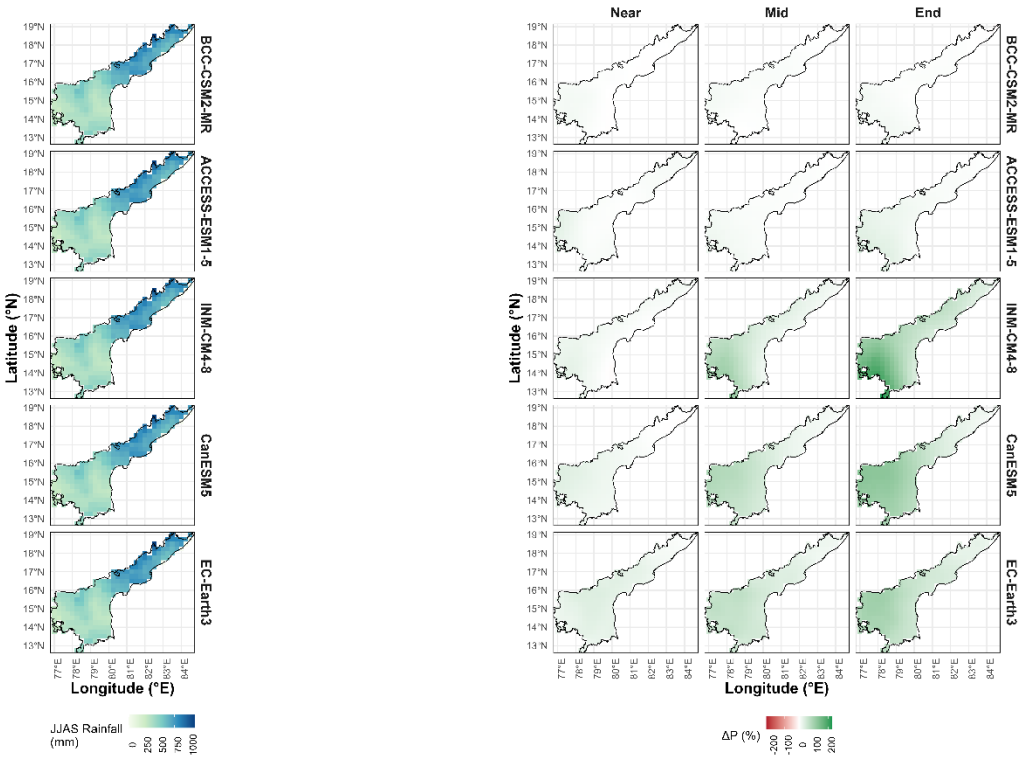

Figure 6.10. Spatial distribution of historical monsoon (JJAS) rainfall and projected percentage change under the SSP3–7.0 scenario for near future (2021–2040), mid-century (2041–2070), and end-century (2071–2100) periods derived from the top five IGSS-selected CMIP6 models

End-century projections show the strongest monsoon response, with INM-CM4-8, CanESM5, and EC-Earth3 projecting substantial increases in JJAS rainfall across large parts of Andhra Pradesh, particularly over southern and central areas. BCC-CSM2-MR and ACCESS-ESM1-5 indicate comparatively moderate increases while maintaining existing spatial rainfall gradients. Despite inter-model variability, all selected GCMs consistently suggest an overall intensification of monsoon rainfall under the SSP3–7.0 scenario. Changes in JJAS rainfall directly influence runoff generation, reservoir inflows, and groundwater recharge within the Pennar River Basin, as monsoon precipitation accounts for the dominant share of annual water availability. Increasing seasonal rainfall may enhance streamflow during monsoon

months; however, uneven spatial distribution and intensified rainfall events may also increase hydrological variability and flood risk. The projected monsoon rainfall shift therefore represents a key climatic driver governing future surface and subsurface hydrological response in the basin.

6.3.5. Changes in Northeast Season Monsoon (OND) Rainfall: Figure 6.11 illustrates the projected shift in northeast monsoon (OND) seasonal rainfall over Andhra Pradesh under the SSP3–7.0 emission scenario using the five IGSS-selected CMIP6 models. The left panel shows the historical OND rainfall distribution simulated by each model, while the right panels present projected percentage changes relative to the historical baseline for the near future (2021–2040), mid-century (2041–2070), and end-century (2071–2100) periods.

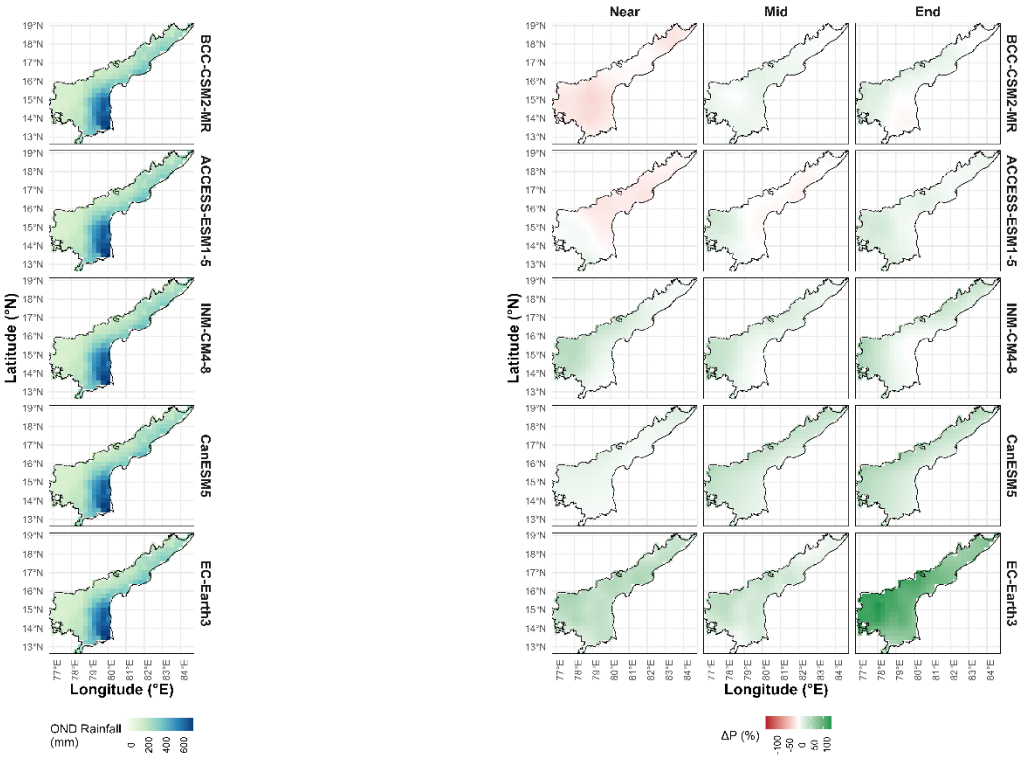

Figure 6.11. Spatial distribution of historical northeast monsoon (OND) rainfall and projected percentage change under the SSP3–7.0 scenario for near future (2021–2040), mid-century (2041–2070), and end-century (2071–2100) periods derived from the top five IGSS-selected CMIP6 models

All models reproduce the historical northeast monsoon rainfall pattern characterized by higher rainfall over southern coastal and south-central regions and

comparatively lower rainfall toward northern parts of the state. The projected change signal indicates noticeable temporal evolution in OND rainfall response across the century. During the near-future period, models project relatively small and spatially mixed changes, with localized decreases appearing in some regions alongside moderate increases elsewhere. By mid-century, positive rainfall anomalies begin to dominate across southern and central Andhra Pradesh, indicating strengthening northeast monsoon contribution in several models.

End-century projections show a clearer wetting tendency, particularly in simulations from INM-CM4-8, CanESM5, and EC-Earth3, which project substantial increases in OND rainfall across southern and coastal regions. BCC-CSM2-MR and ACCESS-ESM1-5 indicate comparatively moderate increases while maintaining existing spatial rainfall gradients. Despite inter-model differences, most models suggest an overall enhancement of northeast monsoon rainfall under the SSP3–7.0 scenario. Changes in OND rainfall carry significant hydrological implications for the Pennar River Basin, where post-monsoon precipitation contributes to reservoir inflows, soil moisture recovery, and groundwater recharge following the southwest monsoon season. Increasing OND rainfall may improve late-season water availability; however, spatial variability in projected changes may also influence seasonal runoff timing and recharge efficiency. The projected northeast monsoon rainfall shift therefore represents an important component of future hydro-climatic variability in the basin under changing climate conditions.

6.4. Multi-model Ensembles

6.4.1. Precipitation: Figure 6.12 presents the multi-model ensemble mean projection of annual precipitation over Andhra Pradesh derived from the five highest-ranking CMIP6 models selected using the Integrated GCM Skill Score (IGSS) under the SSP3–7.0 scenario. The ensemble mean reduces individual model uncertainty and highlights the robust climate signal shared among the selected GCMs. The historical panel reproduces the established precipitation gradient across the state, with higher rainfall concentrated along the northeastern and coastal regions and comparatively lower precipitation over the southwestern interior areas. Future projections indicate gradual but spatially uneven changes in precipitation rather than abrupt basin-wide shifts. During the near-future period (2021–2040), the ensemble shows only marginal

increases in annual rainfall across most regions. Coastal and northeastern zones exhibit slight enhancement in precipitation, while interior regions experience minimal change relative to historical conditions. These subtle differences suggest that short-term climate response primarily manifests as redistribution of rainfall intensity rather than large increases in total annual precipitation.

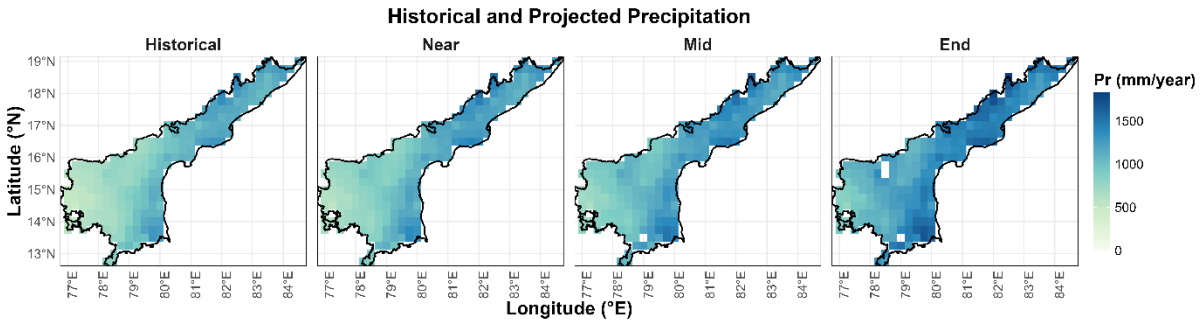

Figure 6.12. Historical and projected annual precipitation derived from the multi-model ensemble mean of the top five IGSS-selected CMIP6 models for near future (2021–2040), mid-century (2041–2070), and end-century (2071–2100) periods under the SSP3–7.0 scenario

By mid-century (2041–2070), the precipitation signal strengthens moderately across central and southern parts of Andhra Pradesh. The ensemble indicates a noticeable inland expansion of higher rainfall zones, particularly along the central belt adjoining the Pennar Basin. Although the overall increase remains moderate, the spatial continuity of wetter conditions becomes more evident compared with the near-future period. This transition reflects gradual intensification of monsoonal moisture transport and enhanced atmospheric water-holding capacity under warming conditions. End-century projections (2071–2100) show the clearest precipitation response. The ensemble mean indicates widespread increases across much of the state, with stronger enhancement over southern and central regions while maintaining relatively high rainfall along the northeastern coastal belt. Importantly, the spatial gradient observed under historical conditions persists, indicating that climate change amplifies existing hydro-climatic patterns rather than fundamentally altering them. The projected increase therefore appears as an intensification of current wet regions accompanied by moderate improvement in rainfall over semi-arid interior zones.

Despite the overall wetting tendency, the changes remain spatially subtle, which highlights the importance of examining hydrological response rather than relying solely on precipitation magnitude. Even modest increases in annual rainfall, when combined with rising temperature and evapotranspiration demand, may produce complex impacts on runoff generation, soil moisture dynamics, and groundwater recharge within the Pennar River Basin. The ensemble projection thus provides a robust climatic forcing framework for evaluating future streamflow and groundwater variability using the VIC and Random Forest modelling systems.

6.4.2. Maximum Temperature: Figure 6.13 presents the multi-model ensemble mean projection of annual maximum temperature (T_{max}) over Andhra Pradesh derived from the five top-performing CMIP6 models selected using the Integrated GCM Skill Score (IGSS) under the SSP3–7.0 scenario. The ensemble mean highlights the common warming signal across models while minimizing individual model variability. The historical panel captures the established spatial temperature gradient across the state, with relatively cooler conditions along the northeastern coastal belt and higher temperatures across the inland southern and central regions.

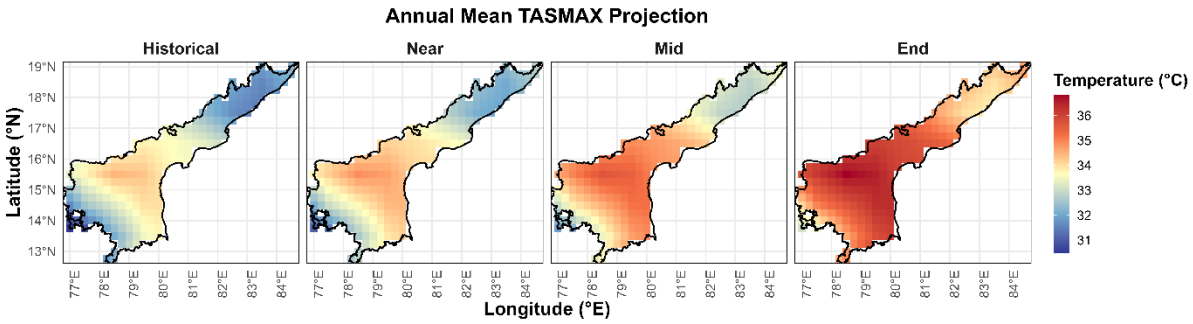

Figure 6.13. Historical and projected annual maximum temperature derived from the multi-model ensemble mean of the top five IGSS-selected CMIP6 models for near future (2021–2040), mid-century (2041–2070), and end-century (2071–2100) periods under the SSP3–7.0 scenario

Future projections reveal a gradual yet spatially coherent increase in maximum temperature throughout the twenty-first century. During the near-future period (2021–2040), the ensemble indicates modest warming across most parts of Andhra Pradesh, generally on the order of about 0.5–1.0°C relative to historical conditions. The warming appears slightly stronger over interior regions, whereas coastal and northeastern

areas retain comparatively lower temperatures due to maritime influence. These early changes remain subtle and primarily reflect incremental intensification of existing thermal conditions rather than major spatial restructuring. By mid-century (2041–2070), the warming signal strengthens considerably and expands across the entire state. Interior regions experience more pronounced temperature increases, and the contrast between coastal and inland zones begins to reduce as elevated temperatures spread toward northern and coastal areas. The ensemble suggests a transition toward persistently warmer surface conditions, indicating enhanced land–atmosphere feedback and increased sensible heat flux across semi-arid regions.

End-century projections (2071–2100) show the strongest and most spatially uniform warming pattern. Maximum temperature increases become widespread across Andhra Pradesh, with large portions of the state experiencing temperatures exceeding historical averages by approximately 2–3°C. The persistence of the historical spatial gradient indicates that climate change amplifies existing warm regions rather than shifting their location. Consequently, already warm inland regions of the Pennar River Basin emerge as future thermal hotspots. Although precipitation projections indicate moderate wetting tendencies, the sustained rise in T_{max} significantly increases evapotranspiration demand and atmospheric moisture capacity. Even subtle temperature increases during earlier projection periods may offset gains in rainfall by accelerating soil moisture loss and reducing effective water availability. The ensemble T_{max} projection therefore represents a dominant climatic driver governing future hydrological response, influencing streamflow generation, reservoir inflows, and groundwater recharge dynamics simulated within the VIC and Random Forest modelling frameworks.

6.4.3. Minimum Temperature: Figure 6.14 presents the multi-model ensemble mean projection of annual minimum temperature (T_{min}) over Andhra Pradesh derived from the five IGSS-selected CMIP6 models under the SSP3–7.0 scenario. The ensemble mean highlights the consistent nighttime warming signal shared across models while reducing individual model uncertainty. The historical panel shows the established T_{min} gradient across the state, with relatively lower minimum temperatures over the southwestern interior regions and comparatively higher nighttime temperatures along coastal and northeastern areas.

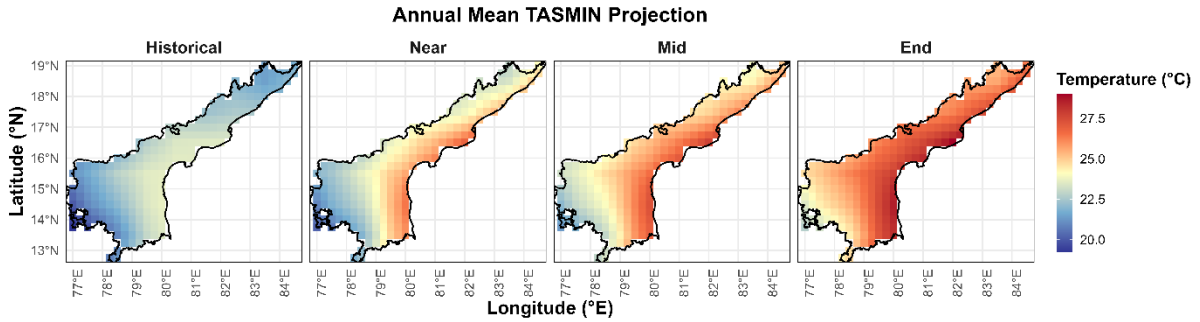

Figure 6.14. Historical and projected annual minimum temperature derived from the multi-model ensemble mean of the top five IGSS-selected CMIP6 models for near future (2021–2040), mid-century (2041–2070), and end-century (2071–2100) periods under the SSP3–7.0 scenario.

Future projections indicate a steady and spatially coherent rise in minimum temperature throughout the twenty-first century. During the near-future period (2021–2040), T_{min} increases appear across most regions, although the magnitude of warming remains modest. Interior regions show slightly stronger nighttime warming compared with coastal zones, indicating an early weakening of the historical land–sea thermal contrast. These initial changes remain subtle but signal the onset of persistent warming conditions. By mid-century (2041–2070), the warming intensifies and spreads uniformly across Andhra Pradesh. The ensemble shows a noticeable increase in T_{min} across central and southern regions, while coastal areas also experience substantial warming relative to historical conditions. The spatial temperature gradient begins to smooth, suggesting reduced nocturnal cooling efficiency across both inland and coastal environments.

End-century projections (2071–2100) display the strongest and most spatially uniform T_{min} increase. Large parts of the state experience nighttime temperatures exceeding historical averages by approximately 2–3°C. Inland regions of the Pennar River Basin emerge as zones of sustained elevated T_{min}, while coastal regions also undergo significant warming. Unlike precipitation projections that show gradual and spatially variable changes, T_{min} increases occur consistently across the entire domain, indicating a robust and high-confidence warming signal. Rising minimum temperature reduces nighttime heat dissipation and maintains higher surface energy storage, which prolongs evapotranspiration activity and limits soil moisture recovery during nocturnal periods. Even subtle early-century increases in T_{min} can influence crop water demand,

groundwater recharge efficiency, and baseflow generation. When combined with projected increases in maximum temperature, the ensemble T_{min} projection confirms sustained warming conditions that may intensify hydrological stress within the Pennar River Basin despite moderate increases in projected precipitation.

6.5. VIC Hydrological Model

This section presents the hydrological simulations derived from the calibrated Variable Infiltration Capacity (VIC) model and evaluates the response of streamflow in the Pennar River Basin under projected climate change conditions. The analysis uses bias-corrected precipitation and temperature projections obtained from the selected high-skill CMIP6 models to quantify changes in basin-scale water balance components. The VIC model translates projected climatic shifts into variations in runoff generation, evapotranspiration, and streamflow dynamics across historical and future time periods. By comparing simulated hydrological conditions for the near future, mid-century, and end-century periods against the historical baseline, this assessment examines how evolving temperature and precipitation regimes influence surface water availability and flow variability within the basin. The results provide critical insight into the sensitivity of Pennar River hydrology to climate forcing and establish the basis for evaluating sustainable water resource for the future under changing climatic conditions.

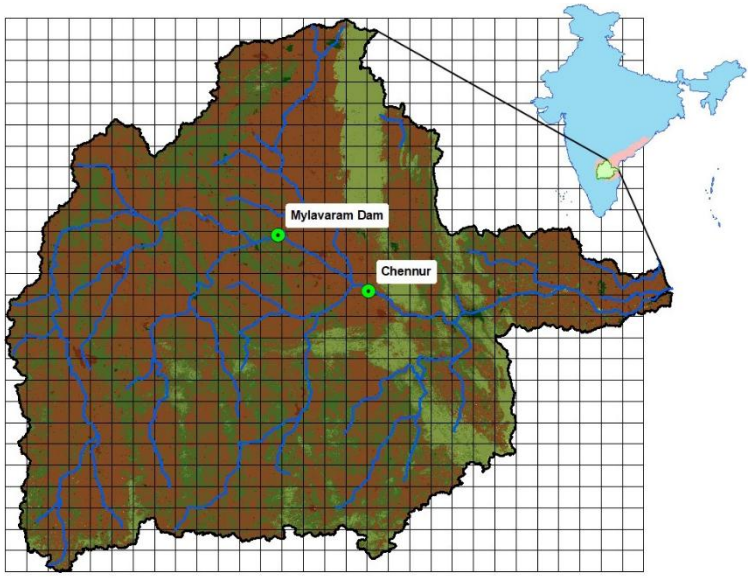

Figure 6.15. Schematic of the VIC hydrological model grid (0.1° spatial resolution) covering the Pennar River Basin along with the stream network in the basin, LULC

map and locations of streamflow gauging sites, Chennur and Mylavaram Dam used for calibration and validation of the model.

6.5.1. Sensitivity Analysis of VIC Model Parameters: Figure 6.16. presents the sensitivity of key hydrological outputs to variations in the four principal parameters of the VIC Model**:** *infilt***,** *Dsmax***,** *Ds***,** and *Ws*. The analysis evaluates how these parameters influence runoff generation, baseflow contribution, evapotranspiration, and soil moisture dynamics.

Table 6.2. Summary of sensitivity analysis of key parameters of the VIC Model showing their influence on hydrological responses, relative sensitivity levels, calibration importance, and recommended parameter ranges for model calibration.

Parameter	**Model response observed**	**Sensitivity Level**	**Calibration importance**	**Recommended range**
Infilt	Increasing *infilt* increases runoff ratio and surface runoff while decreasing evapotranspiration and soil moisture	High	Primary parameter to calibrate	0.15 – 0.25
Dsmax	Increasing *Dsmax* increases the baseflow fraction and groundwater contribution	Moderate	Important for low-flow simulation	6 – 14 mm/day
Ws	Changes in *Ws* show minimal influence on runoff ratio and soil moisture	Low	For low-flow simulation	0.65 – 0.80
Ds	Only slight changes in baseflow fraction with varying *Ds*	Very low	To fine-tune recession curves	0.01 – 0.03

Influence of the Infiltration Parameter (*infilt*): Panels (a), (b), (g), and (h) in Figure 6.16 illustrate the strong influence of the *infilt* parameter on the hydrological response of the basin. As *infilt* increases, the runoff ratio and surface runoff increase substantially, Figures 6.16(a) and 6.16(b). The infiltration parameter controls the spatial variability of infiltration capacity within each grid cell. Higher values increase the fraction of the grid area that reaches saturation quickly and therefore produce greater surface runoff. At the same time, increasing *infilt* reduces evapotranspiration (*ET*) and mean soil moisture, Figures 6.16(g) and 6.16(h). Larger runoff losses leave

less water available for soil storage and atmospheric exchange. Consequently, soil moisture storage declines and evapotranspiration decreases. The clear and consistent trends in these plots indicate that *infilt* strongly controls runoff generation and soil water balance.

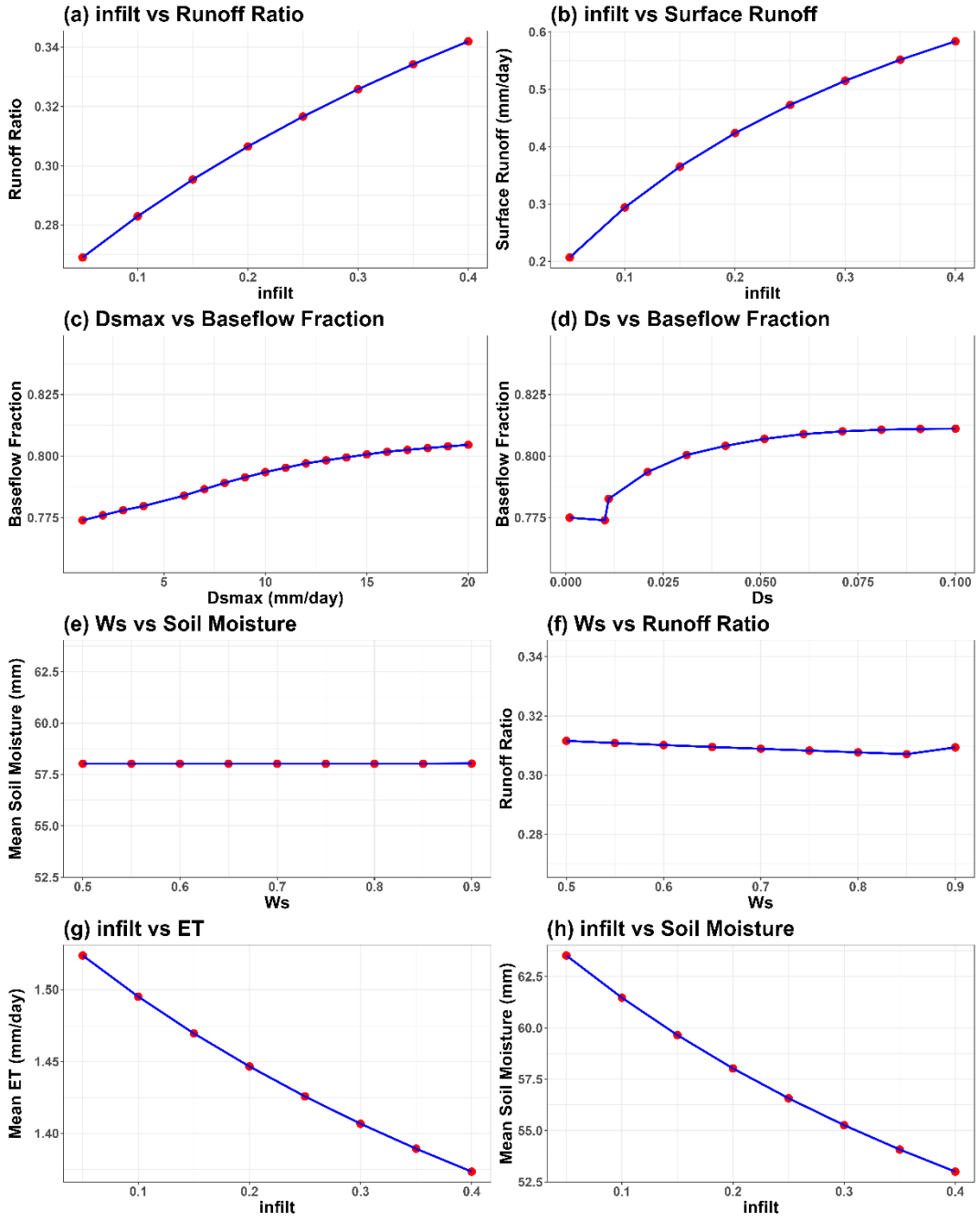

Figure 6.16. Sensitivity of key hydrological responses simulated by the VIC Model to variations in four model parameters (*infilt*, *Dsmax*, *Ds*, and *Ws*). The panels illustrate the influence of parameter changes on runoff ratio, surface runoff, baseflow fraction, mean soil moisture, and evapotranspiration

Influence of Baseflow Parameters (*Dsmax* and *Ds*): Panels (c) and (d) in Figure 6.16 show how the baseflow parameters *Dsmax* and *Ds* affect the baseflow fraction. Increasing *Dsmax* increases the baseflow fraction, Figure 6.16(c). Higher values allow more water to leave the lower soil layer as groundwater discharge. The curve gradually flattens at higher values, which indicates weaker sensitivity beyond approximately 15 mm/day. The parameter *Ds* controls the soil moisture level at which nonlinear baseflow begins. Increasing *Ds* produces only a small increase in the baseflow fraction, Figure 6.16(d). Compared with *Dsmax*, this parameter exerts a much weaker influence on the magnitude of groundwater contribution.

Influence of the Soil Moisture Threshold Parameter (*Ws*): Panels (e) and (f) in Figure 6.16 show the influence of *Ws*, the fraction of maximum soil moisture at which nonlinear baseflow begins. Changes in *Ws* produce almost no change in mean soil moisture or runoff ratio. Both variables remain nearly constant across the tested parameter range. This behavior indicates that *Ws* mainly affects the timing of baseflow generation rather than the total amount of runoff or soil water storage.

The sensitivity analysis highlights clear differences in parameter influence. The *infilt* parameter exerts the strongest control over runoff generation, evapotranspiration, and soil moisture storage. The *Dsmax* parameter moderately influences groundwater discharge and baseflow contribution. In contrast, *Ds* and *Ws* show relatively weak effects on basin-scale hydrological responses. Table 6.2 summarizes the sensitivity analysis of key parameters of the VIC model showing their influence on hydrological responses, relative sensitivity levels, calibration importance, and recommended parameter ranges for model calibration.

6.5.2. Calibration Strategy and Parameter Adjustment: The study calibrated the VIC hydrological model at a gauging station near Chennur in the Pennar River Basin to obtain reliable simulations of basin-scale streamflow. The sensitivity analysis identified the infiltration parameter (*infilt*) and the maximum baseflow velocity (*Dsmax*) as the most influential parameters, soil moisture threshold parameter (*Ws*) and *Ds* as secondary sensitive parameters controlling runoff generation and groundwater contribution. Therefore, the calibration step focused primarily on adjusting these highly sensitive parameters. The study used a manual calibration approach and conducted approximately thirty iterative simulations in which parameter values were

systematically modified to improve agreement between simulated discharge and observed inflow. The calibration procedure adjusted the parameters that exhibited the highest sensitivity in the preceding analysis, including the infiltration parameter (*infilt*), the maximum baseflow parameter (*Dsmax*), and the soil moisture threshold for nonlinear baseflow generation (*Ws*). These parameters directly control infiltration capacity, runoff partitioning, and subsurface flow response within the basin. Each iteration tested a different parameter combination to evaluate improvements in hydrograph shape, peak flow representation, recession characteristics, and seasonal flow variability. Table S1 lists the parameter sets explored during calibration of the VIC model for the Pennar River Basin.

Initial calibration runs used parameter values derived from the sensitivity analysis to establish a baseline model response. Early iterations with relatively low infiltration values produced very high surface runoff and overestimated peak discharge. Subsequent adjustments moderated the infiltration parameter and modified the baseflow parameters, which brought down the peak discharge and improved the representation of low-flow events. The final parameter combination produced a balanced simulation of peak flows, baseflow contribution, and seasonal discharge variability, indicating that the calibrated parameters effectively captured the dominant hydrological processes of the basin.

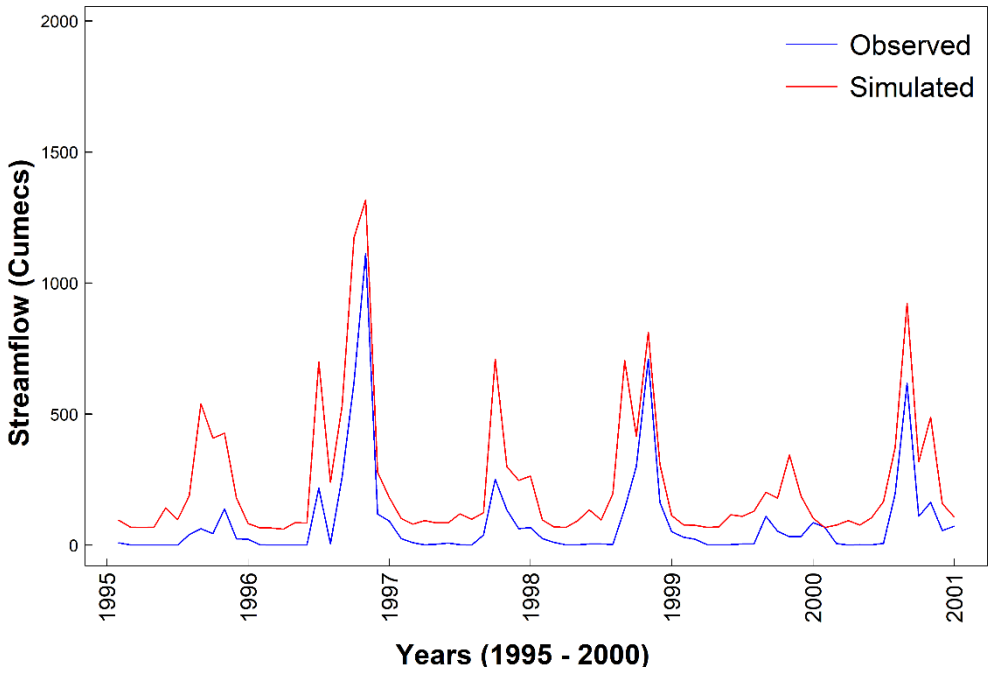

Figure 6.17. Observed versus simulated streamflow obtained from VIC model calibration at the Chennur gauging station, Pennar River Basin

6.5.2. Calibration and Validation: Figure 6.17 compares observed and VIC-simulated monthly streamflow at the Chennur gauging station during the calibration period, 1995 - 2000. The simulated hydrograph captures the overall temporal variability of streamflow, including the timing of monsoon-driven peak flows and recession behaviour during low-flow periods. The model reproduces seasonal flow patterns reasonably well, indicating that the selected parameter set adequately represents dominant hydrological processes within the basin. The simulation shows improved alignment with observed discharge after successive parameter adjustments, particularly in representing monsoon peak magnitude and post-monsoon recession trends. Minor deviations remain during extreme flow events, where the model slightly smooths peak discharge, which commonly occurs in grid-based hydrological models due to spatial averaging of rainfall and basin storage processes. Despite these differences, the calibrated model successfully represents basin response dynamics required for climate impact simulations.

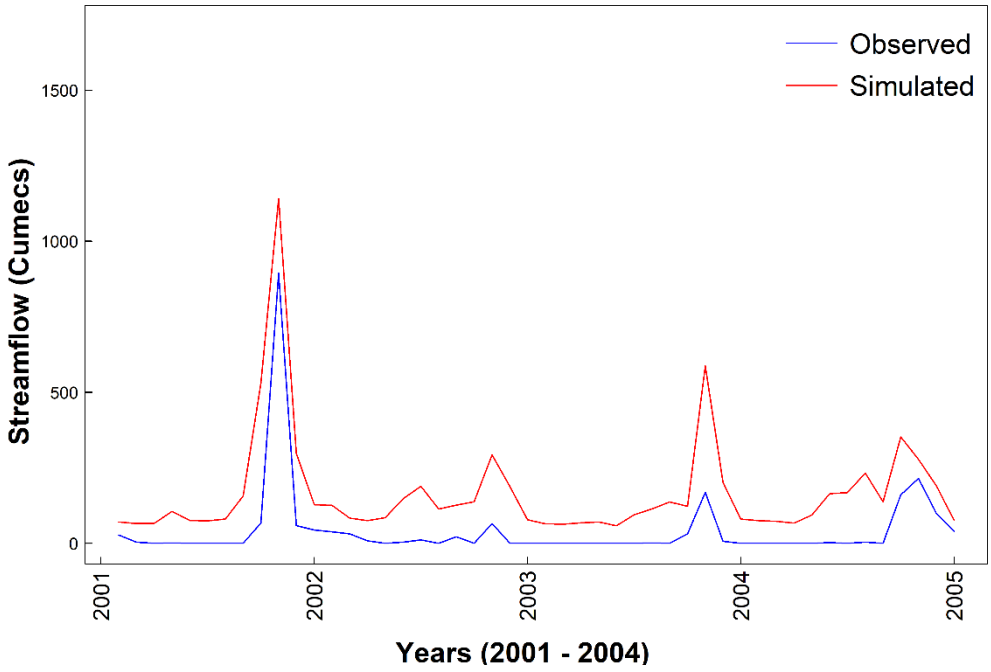

Figure 6.18. Validation of VIC-Simulated Streamflow at Chennur Gauging Station in the Pennar River Basin

Figure 6.18 evaluates model performance using an independent period without further parameter modification. The simulated streamflow maintains strong agreement with observed discharge, demonstrating that the calibrated parameter set remains stable under different hydro-climatic conditions. The model preserves seasonal flow timing and captures inter-annual variability, confirming its transferability beyond the calibration period. The validation results indicate consistent reproduction of both moderate and low-flow conditions, although slight underestimation appears during isolated high-flow events. This behaviour suggests conservative runoff estimation, which reduces the risk of over-prediction in future climate-driven simulations. Overall, the validation performance confirms that the VIC model reliably represents hydrological processes governing runoff generation and baseflow contribution in the Pennar River Basin.

Table 6.3. Performance statistics of the hydrological model during the calibration period (1995–2000) and validation period (2001–2004), evaluated using the Nash–Sutcliffe Efficiency (NSE) and the coefficient of determination (R^2) between observed and simulated streamflow

Calibration Period (1995 – 2000)		**Validation Period (2001 – 2004)**	
NSE	**R^2**	**NSE**	**R^2**
0.582	0.913	0.34	0.877

The performance of the hydrological model was evaluated using the Nash–Sutcliffe Efficiency (NSE) and the coefficient of determination (R^2) during both the calibration (1995–2000) and validation (2001–2004) periods (Table 6.3). During the calibration period, the model produced an NSE of 0.582 and an R^2 of 0.913, indicating a satisfactory representation of observed streamflow and a strong correspondence between simulated and observed variability. For the validation period, the NSE and R^2 values were 0.34 and 0.877, respectively, showing that the model continues to capture the general variability and correlation in streamflow during the independent evaluation period. The final set of calibrated parameters includes *infilt* = 0.05, *Ds* = 0.01, and *Ws* = 0.8, which together regulate the infiltration capacity and baseflow response in the model. These parameter values enable the model to reproduce the observed streamflow characteristics reasonably during the calibration period. The calibration process did not include direct calibration of the parameter *Dsmax*; instead, we

computed it using the natural slope and the saturated hydraulic conductivity of the top soil layer following the model's parameterization scheme.

The Pennar River Basin contains several dams, reservoirs, irrigation withdrawals, diversion structures, and other upstream abstractions that regulate and redistribute river flows. Such human interventions within the basin considerably influence streamflow behavior at the Chennur station. However, these anthropogenic controls are not explicitly represented in the present VIC model configuration, which primarily simulates natural hydrological processes driven by climate and land surface conditions. As a result, differences arise between simulated and observed discharge, particularly during regulated periods when reservoir releases and irrigation withdrawals significantly modify natural flow patterns. Incorporating reservoir operations and other human water management practices would therefore be an important improvement for future studies to better represent the basin's hydrological dynamics. Uncertainty in soil and land surface parameterization also affects model performance. A single parameter set cannot fully represent the spatial variability in soil depth, infiltration characteristics, and land-use conditions across the basin. Small inconsistencies in infiltration or baseflow parameters can accumulate over time and appear as systematic deviations in simulated hydrographs. Together, these factors explain why the VIC model is able to capture the seasonal variability and general flow dynamics of the basin while still exhibiting some bias in the magnitude of simulated discharge. Recognizing these limitations is important when interpreting climate change impact simulations, as projected relative changes in streamflow provide more reliable insight than absolute discharge estimates.

6.5.3. Climate Change Impact Assessment: Calibrated VIC hydrological model at the Chennur gauging station provide a strong basis for applying the model for Hydrological Impact assessment for the Pennar River Basin. Hydrological impact assessment relies on the assumption that a model calibrated under historical conditions can reliably translate projected climatic forcing into future streamflow response. We derived future climate forcing from bias-corrected GCM projections under SSP245 and SSP370 scenarios. Projected climate change over Andhra Pradesh indicates concurrent changes in precipitation patterns and rising temperature conditions. Variations in precipitation alter runoff generation and flow seasonality,

while increasing temperature modifies evapotranspiration demand, soil moisture availability, and groundwater recharge processes. The VIC model integrates these interacting processes through physically based land–atmosphere and soil moisture representations, allowing assessment of how combined climatic changes propagate through the hydrological system. Consequently, the calibrated model enables quantitative evaluation of future changes in streamflow magnitude, timing, and variability across near-future, mid-century, and end-century periods.

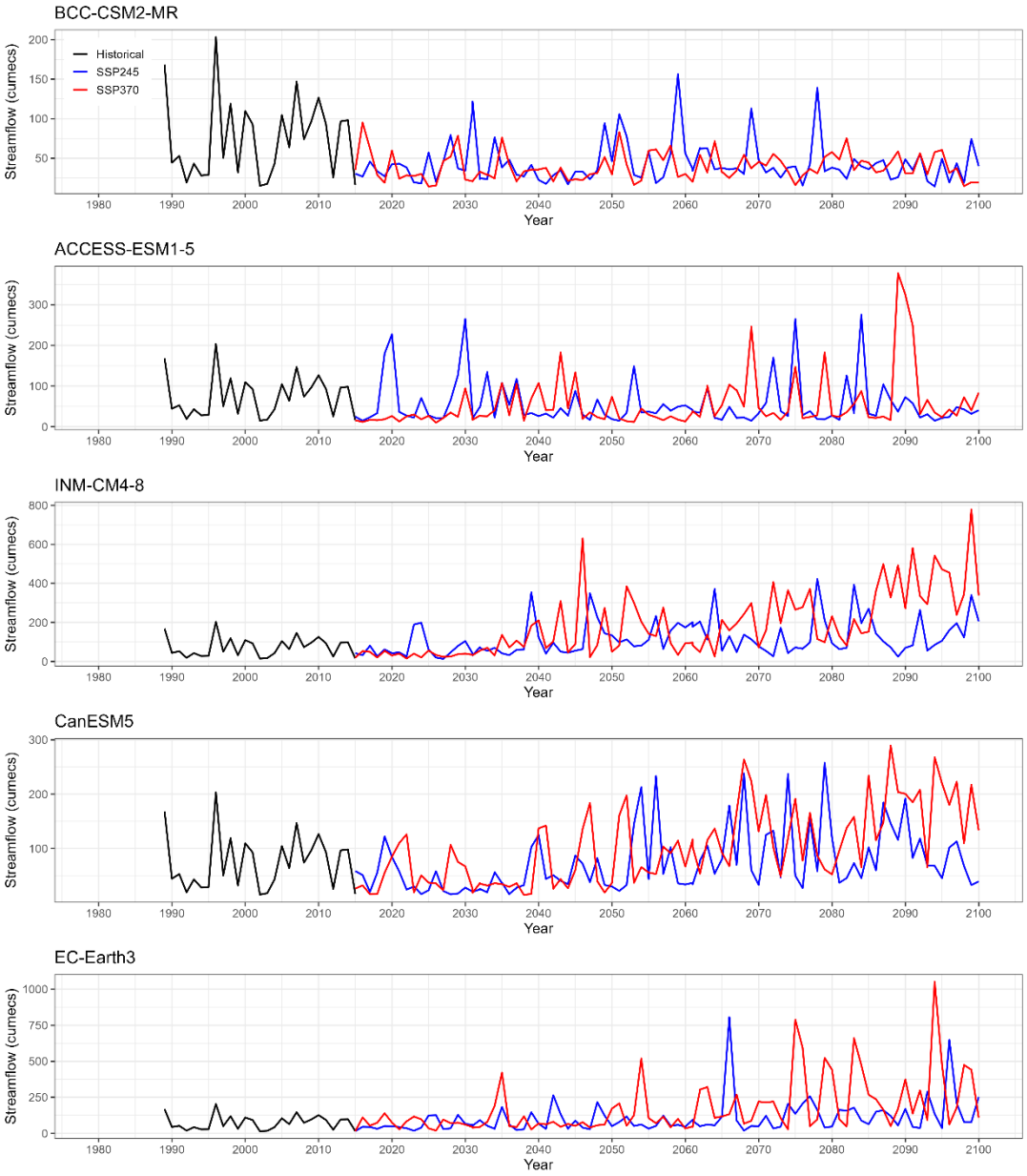

Figure 6.19. Historically recorded (1989–2014) and projected (2015–2100) annual streamflow simulated using the VIC hydrological model for the Pennar River Basin at Chennur, driven by five CMIP6 GCMs (BCC-CSM2-MR, ACCESS-ESM1-5, INM-

CM4-8, CanESM5, and EC-Earth3). Black lines represent the historical period, while blue and red lines denote projections under the SSP245 and SSP370 scenarios, respectively.

Figure 6.19 presents the historically recorded and projected annual streamflow simulated by the VIC model for the Pennar River Basin at the Chennur gauge using climate projections from five CMIP6 GCMs under SSP245 and SSP370 scenarios. The observed streamflow (1989–2014) shows a considerable inter-annual variability in streamflow, with annual flows generally ranging between approximately 20 and 200 m^3/sec. Several peak flow years occur during the late 1990s and early 2000s, indicating strong variability in basin hydrology during the historical period. These variations reflect the rainfall-driven nature of the Pennar basin, where streamflow responds rapidly to fluctuations in monsoon precipitation. Future projections (2015–2100) indicate substantial changes in the magnitude and variability of annual streamflow across the different climate models and scenarios. Under both SSP245 and SSP370, the majority of GCMs suggest an increase in the frequency and magnitude of high-flow years, particularly during the mid- and late-21st century. However, the magnitude of these changes varies significantly among the models. For example, the INM-CM4-8 and EC-Earth3 models show very large increases in projected peak flows, with several extreme years exceeding 400 - 800 m^3/sec toward the end of the century. In contrast, BCC-CSM2-MR exhibits relatively moderate increases, with flows mostly remaining below approximately 150 m^3/sec.

The ACCESS-ESM1-5 and CanESM5 projections indicate increasing variability in streamflow, with intermittent extreme flow years interspersed with relatively low-flow periods. Under SSP370, these models show larger and more frequent high-flow events, especially after 2070. This pattern indicates that hydrological variability in the basin is likely to increase under higher emission scenarios. The projections highlight a strong inter-model spread in future streamflow estimates, reflecting uncertainties in climate projections and hydrological responses. Nevertheless, a consistent feature across most models is the increase in the variability and intensity of annual streamflow, particularly under the high-emission SSP370 scenario. This suggests that climate change may amplify hydrological extremes in the basin, increasing the likelihood of both flood-prone years and water availability fluctuations. The substantial increases in

projected peak flows in some GCMs (e.g., INM-CM4-8 and EC-Earth3) indicate the potential for more intense precipitation events, which may translate into higher runoff and extreme streamflow conditions. Such changes could pose significant challenges for water infrastructure, flood management, and reservoir operation in the basin. At the same time, the large inter-annual variability in the projections implies that water availability may become more uncertain, with periods of low flows occurring alongside extreme high-flow years. These changes have significant implications for water resource management in the Pennar River Basin, which already experiences semi-arid climatic conditions and limited surface water availability.

Figure 6.20 shows the average annual hydrographs derived from VIC-simulated monthly streamflow for the Pennar River Basin at the Chennur gauging station. The historical hydrograph (1990–2014) indicates a strong seasonal flow regime, with very low flows during the dry months (January–May), followed by a sharp increase during the southwest and northeast monsoon months, peaking typically between September and October. This seasonal pattern reflects the rainfall-driven hydrology of the basin, as monsoon precipitation generates most of the annual runoff. Under future climate scenarios, the projected hydrographs suggest that the overall seasonal pattern remains similar, with peak flows continuing to occur during the late monsoon months. However, noticeable changes in the magnitude of peak flows are evident across the future time-periods and emission scenarios. During the near-future period (2021–2040), the projected hydrographs from most GCMs remain relatively close to the historical hydrograph, indicating modest changes in monthly flows. Some models show slightly higher flows during the monsoon months, suggesting an early indication of increased runoff in response to projected precipitation changes.

More pronounced changes emerge during the mid-century period (2041–2070). Several GCMs project substantial increases in peak flows during September and October, with peak discharge values considerably exceeding those observed in the historical period. This increase is evident in both emission scenarios but is generally stronger under the SSP370 scenario, indicating the influence of higher greenhouse gas forcing on basin hydrology. The widening spread among GCM projections during this period also reflects increasing uncertainty in future streamflow responses. The projections show the most significant changes during the late-century period (2071–

2100). Under both SSP245 and SSP370 scenarios, many GCMs indicate substantial amplification of peak flows, particularly during the monsoon months. Some projections show peak flows reaching several times the magnitude of the historical peak, especially under SSP370. This suggests a potential intensification of extreme runoff events, which may be associated with increases in the intensity and variability of monsoon precipitation under future climate conditions. In addition, the hydrographs indicate a sharper rise and fall of flows during the monsoon season, implying a more concentrated runoff response.

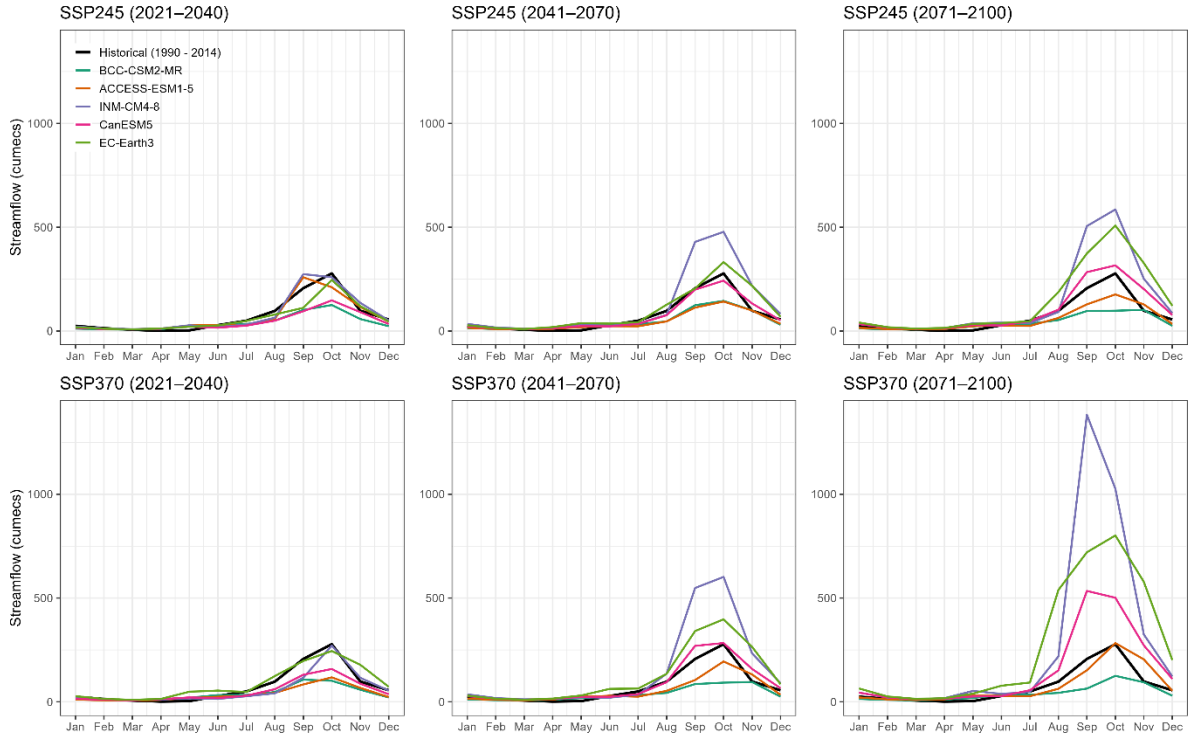

Figure 6.20. Average annual hydrographs for the Pennar River Basin at the Chennur gauge derived from VIC-simulated monthly streamflow under two emission scenarios. The top row shows projections under SSP245 and the bottom row under SSP370 for three future periods: 2021–2040, 2041–2070, and 2071–2100. Colored lines represent projections from five CMIP6 GCMs (BCC-CSM2-MR, ACCESS-ESM1-5, INM-CM4-8, CanESM5, and EC-Earth3), while the black line indicates the historically observed average hydrograph (1990–2014).

Overall, the results highlight the need for climate-resilient water management strategies in the Pennar River Basin. The projected increase in monsoon peak flows indicates a higher likelihood of flood events and greater runoff variability, particularly

under the high-emission SSP370 scenario. At the same time, the persistence of very low flows during the dry months suggests that seasonal water scarcity may continue to pose significant challenges for water availability and irrigation supply. These contrasting hydrological conditions point to an increasing variability in streamflow throughout the year. Therefore, future water management in the basin should strengthen flood preparedness, improve reservoir operation, and expand water storage and recharge systems to effectively capture excess monsoon runoff and ensure water availability during dry periods.

6.6. Random Forest Model

The Random Forest (RF) model simulates groundwater levels at 60 selected wells across the Pennar River Basin using climatic variables, hydrological fluxes, and antecedent groundwater conditions. The performance of the RF model was evaluated using independent testing data, representing 30% of the 33-year dataset. We assessed the model performance using four statistical metrics: Root Mean Square Error (RMSE), Mean Absolute Error (MAE), Coefficient of Determination (R^2), and Kling–Gupta Efficiency (KGE). Among these, we considered the NSE as the primary evaluation metric because it evaluates the overall agreement between observed and simulated values by accounting for the magnitude and timing of errors relative to the observed variability. The results indicate substantial spatial heterogeneity in predictive performance, reflecting the complex hydrogeological conditions and anthropogenic influences across the basin.

6.6.1. Model Performance: The results showed good predictive capability in around 10 out of 60 wells evaluated and overall show moderate predictive capability, although performance varies considerably across wells, Table S2. NSE values range from negative values to about 0.71, with an average close to 0.2, which indicates that the model captures groundwater variability reasonably well at certain locations but performs poorly at others. R^2 values follow a similar trend and range from near zero to values exceeding 0.9, which demonstrates strong explanatory power at some wells and weak relationships at others. MAE values also vary substantially and reflect differences in prediction accuracy that likely arise from local hydrogeological and anthropogenic influences. The results highlight strong spatial variability in model performance and reflect the heterogeneous nature of groundwater systems within the Pennar River Basin. Wells with relatively high NSE and R^2 values indicate that the

selected predictors strongly influence groundwater levels at these locations. Rainfall, temperature, soil moisture, and baseflow play a dominant role at these wells. These variables, derived from IMD gridded datasets and VIC model simulations, represent recharge processes and subsurface dynamics effectively in regions where groundwater responds primarily to climatic forcing. In contrast, wells with low or negative NSE values show that the model fails to outperform a simple mean-based prediction, which implies that other factors control groundwater variability at these sites. Localized pumping, aquifer heterogeneity, irrigation practices, and other human interventions likely influence groundwater behavior in these areas, but the model does not explicitly include these factors. In addition, missing or undefined performance metrics at some wells indicate issues related to data quality, limited variability in observed groundwater levels, or gaps in the time series.

Table 6.4. Geographic locations (latitude and longitude) of the ten selected wells in the Pennar River Basin used for detailed analysis based on satisfactory Random Forest model performance.

#	Name of the Well	Latitude	Longitude	NSE	KGE	R^2
1	Chikkapalanahalli	13.407	77.211	0.52	0.42	0.68
2	Madivala	13.507	77.911	0.58	0.49	0.67
3	Nulivedu	14.107	78.511	0.56	0.47	0.66
4	Maddimadugu	14.307	78.811	0.54	0.55	0.61
5	Simhadripuram	14.607	78.211	0.59	0.55	0.63
6	Kondapuram(rs)	14.707	78.211	0.59	0.52	0.75
7	Alludupally	14.707	78.711	0.58	0.51	0.68
8	Bata	14.707	79.211	0.71	0.58	0.79
9	Talamanchi patnam-2	14.907	78.311	0.60	0.66	0.60
10	Mallepalle	14.907	78.911	0.53	0.43	0.70

The model combines climatic inputs with hydrological variables derived from the VIC model and improves its ability to represent groundwater dynamics by capturing key processes such as infiltration, evapotranspiration, and subsurface flow. Rainfall and temperature control recharge and evaporative demand, while soil moisture and soil moisture flux indicate infiltration and percolation. Baseflow reflects groundwater–surface water interactions, and the previous season’s groundwater level introduces a memory effect that represents the persistence of groundwater systems. The model captures nonlinear relationships among these variables at several wells, which leads to relatively strong performance. However, inconsistent performance across the basin

indicates that the model does not represent all relevant processes, particularly those related to human influence and fine-scale hydrogeological variability. Based on the error statistics, we selected ten wells to assess the impacts of climate change and focuses on locations where the model shows relatively robust performance, Table 6.4. These wells exhibit higher NSE and R^2 values along with lower prediction errors, which indicate that the simulated groundwater levels remain reliable for detailed interpretation. This selection reduces uncertainty and allows a more confident assessment of groundwater dynamics. These wells likely represent regions where climatic and hydrological processes primarily control groundwater variability rather than anthropogenic disturbances.

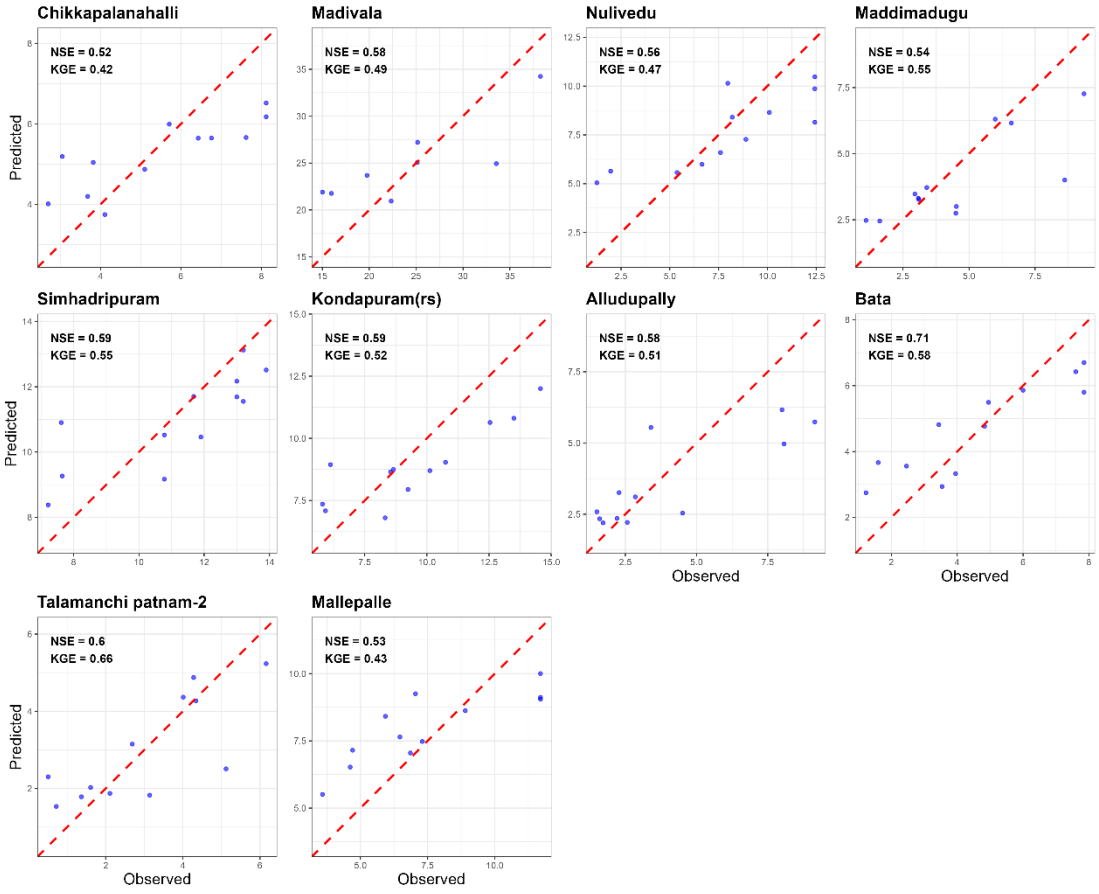

Figure 6.21. Observed vs. predicted groundwater levels across selected wells using the Random Forest model. Each panel represents an individual well, with the red dashed line indicating the 1:1 agreement line. Each subplot shows the model performance metrics (NSE and KGE).

Figure 6.21 show a generally good agreement between observed and predicted groundwater levels across the selected wells, with most points clustering around the 1:1 line, indicating reasonable model accuracy. NSE values range from moderate to high (~0.52 to 0.71), suggesting acceptable predictive skill, while KGE values (~0.42 to 0.66) indicate balanced performance in terms of correlation, variability, and bias. Some wells (e.g., Bata and Talamanchi patnam-2) exhibit stronger alignment with the 1:1 line, reflecting better model performance, whereas others show slight dispersion and systematic under- or over-prediction at higher values. Overall, the Random Forest model captures the seasonal groundwater variability reasonably well, though performance varies across wells, likely due to local hydrogeological differences.

6.6.2. Climate Change Impact Assessment: The assessment of climate change impacts on groundwater levels provides critical insight into how shifting hydro-climatic conditions may alter subsurface water availability across the Pennar River Basin. Using bias-corrected climate projections from multiple GCMs under different emission scenarios (SSP245 and SSP370), groundwater levels were simulated for near-, mid-, and far-future periods relative to the historical baseline (1985–2014). The analysis focuses on seasonal variability, particularly during the monsoon period, which governs recharge dynamics in the basin. By comparing projected groundwater responses across wells and scenarios, this section evaluates the extent to which changes in precipitation, temperature, and evapotranspiration may influence groundwater storage, highlighting spatial heterogeneity, emerging trends, and potential risks to long-term water sustainability.

Figure 6.22 presents the projected groundwater levels at the Alludupally observation well during the monsoon season, which primarily controls the groundwater recharge in the basin. During the historical period (1985–2014), the monsoon-season groundwater levels show strong year-to-year fluctuations, with several sharp declines and peaks, indicating high sensitivity to variability in seasonal rainfall and recharge processes. These fluctuations highlight the dominant role of monsoon dynamics in governing groundwater storage at the well. Periods of lower groundwater depth (shallower water table) correspond to effective recharge years, whereas higher depths indicate weaker recharge and relative groundwater stress. This variability highlights the sensitivity of the aquifer system to seasonal climatic conditions. Under future

climate scenarios (SSP245 and SSP370), the monsoon season groundwater depths show a clear shift toward higher values across all GCMs, indicating a reduction in effective recharge during the monsoon itself. This shift becomes evident in the near-future period (2015–2040), where groundwater depths frequently exceed historical levels, suggesting that even during the main recharge season; the aquifer does not recover to earlier conditions. This behaviour points to possible changes in monsoon intensity, distribution, or increased evapotranspiration limiting net recharge.

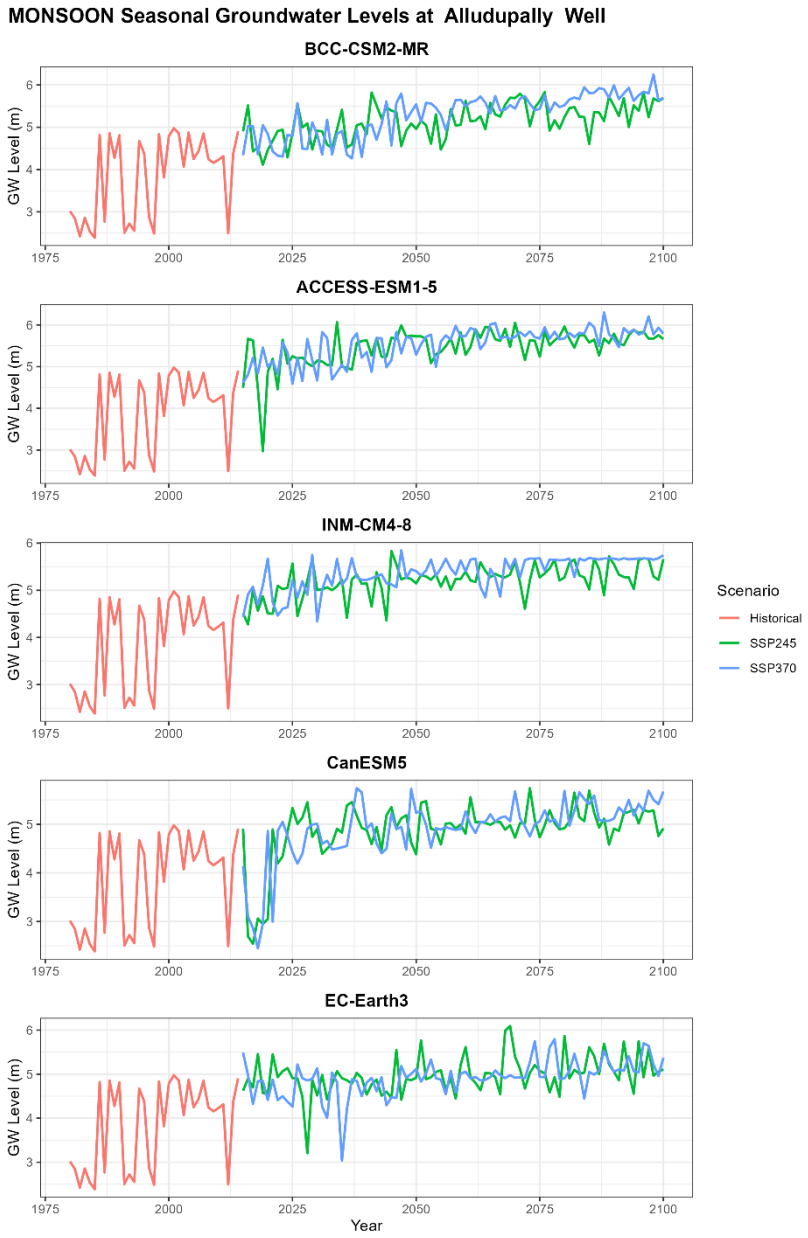

Figure 6.22. Historical and Projected monsoon-seasonal groundwater level variability at the Alludupally well under historical (1985-2014) and future (2015-2100) climate

scenarios (SSP245 and SSP 370) across multiple GCMs, showing inter-annual fluctuations and long-term trends in groundwater response.

In the mid- (2041–2070) and far-future (2071–2100) periods, the increase in monsoon-season groundwater depth persists and becomes more pronounced in several models, particularly BCC-CSM2-MR and ACCESS-ESM1-5, where depths often approach or exceed 5.5–6.0 m. This trend indicates sustained groundwater stress even during the monsoon, which is critical because this season typically governs annual recharge. Models such as INM-CM4-8 and CanESM5 show relatively moderate increases, but still maintain groundwater depths higher than historical levels, confirming an overall decline in recharge effectiveness. Despite this increasing trend, the projections retain significant inter-annual variability, especially in models like CanESM5 and EC-Earth3, where occasional years show reduced groundwater depth, indicating episodic strong monsoon recharge events. However, these events remain inconsistent and do not offset the long-term trend toward deeper groundwater levels. Differences between SSP245 and SSP370 remain relatively modest, although SSP370 tends to produce slightly higher groundwater depths, suggesting marginally greater stress under higher emission conditions.

Figures S2 - S10 in the Annexure section present the projected groundwater levels for the remaining nine (9) wells. The projected monsoon-season groundwater levels across all the wells reveal a consistent but spatially heterogeneous response to changing climatic conditions. Since the monsoon season represents the primary recharge period, these results directly reflect the effectiveness of seasonal recharge under future climate scenarios. Across the study region, most wells show a tendency toward increasing groundwater depth in future periods, indicating reduced recharge efficiency and growing groundwater stress, although the magnitude and variability of this response differ significantly between locations. At the Alludupally and Talamanchi patnam-2 wells, the projections show a clear shift from relatively shallow historical groundwater depths (~2.5 - 4 m) to consistently deeper levels (~4 - 6 m) under both SSP245 and SSP370 scenarios. This pattern indicates a substantial decline in monsoon recharge effectiveness. Although occasional years show reduced depths (indicating strong recharge events), these do not persist, and the long-term trajectory points toward groundwater depletion. A similar but more pronounced behaviour

appears at Nulivedu, where groundwater depths remain high (~9 - 11 m) and exhibit strong inter-annual variability, suggesting that recharge processes remain highly unstable under future climates.

In contrast, wells such as Bata, Chikkapalanahalli, and Simhadripuram show relatively stable groundwater depths with moderate increases. At Bata, groundwater depths remain within a narrow range (~5.5 - 6.5 m), indicating that although recharge efficiency may decline slightly, and the system maintains relative stability. Chikkapalanahalli shows a gradual increase in groundwater depth from ~5.6 to ~6.2 m, suggesting a slow but consistent decline. Simhadripuram exhibits episodic sharp reductions in depth, indicating intermittent strong recharge events; however, these events become less frequent over time, and groundwater levels stabilize at deeper levels in the long term. The Maddimadugu, Mallepalle, and Madivala wells show more complex and variable responses. Maddimadugu exhibits a clear increase in groundwater depth from ~5 - 6 m to ~6 - 7 m, indicating progressive groundwater stress despite continued variability. Mallepalle shows a noticeable increase from ~6 - 7 m to ~7 - 8 m, suggesting declining recharge during the monsoon season. Madivala, which represents a deeper groundwater system (~25 - 31 m), shows a contrasting behaviour, where groundwater depths slightly decrease or stabilize under future scenarios, particularly in some GCMs. This pattern may reflect localized hydrogeological controls, such as confined aquifer conditions or reduced abstraction relative to recharge.

The Kondapuram (rs) well presents a unique case, where only historical data is available, showing relatively stable groundwater depths (~9.5–10 m) with limited variability. The absence of future projections prevents direct comparison; however, the stability in historical conditions suggests that any future changes could significantly alter the existing equilibrium if recharge patterns shift. Across all wells, the projections retain strong inter-annual variability, reflecting the continued influence of monsoon dynamics on groundwater recharge. However, the key emerging pattern is that even during the monsoon season, which governs annual recharge, groundwater depths tend to increase in most wells, indicating reduced recharge efficiency under climate change. Differences between SSP245 and SSP370 remain relatively modest across

most locations, although SSP370 occasionally shows slightly higher groundwater depths, suggesting marginally greater stress under higher emission scenarios.

7.0. SUMMARY AND CONCLUSIONS

In this study, we evaluated climate change scenarios for Andhra Pradesh and quantified their hydrological implications for the Pennar River Basin (PRB), a semi-arid and hydrologically stressed region. We analysed CMIP6-based climate projections derived from the NEX-GDDP-CMIP6 archive and generated multi-model ensembles of temperature and precipitation change. We assessed model performance prior to ensemble construction to ensure robust regional representation. The results indicate a consistent warming trend across Andhra Pradesh, accompanied by increasing rainfall variability and intensification of monsoon-driven precipitation. These changes reflect a shift toward greater hydro-climatic variability rather than uniform changes in mean conditions.

We developed and calibrated the VIC hydrological model for the Pennar Basin using IMD gridded observations and ERA5 wind speed data to ensure physically consistent evapotranspiration estimation. The model reasonably reproduces observed streamflow patterns and captures key aspects of seasonal variability, providing a reliable framework for translating climate signals into hydrological responses. Multi-model hydrological simulations indicate a redistribution of water availability rather than a uniform decline. The projections show increases in peak flows and inter-annual variability alongside the persistence of low-flow conditions during dry periods. The basin exhibits high sensitivity to precipitation variability due to its strong monsoon dependence, limited baseflow contribution, and high evapotranspiration demand. Rising temperatures further intensify evaporative losses and reduce effective soil moisture, which may offset projected increases in precipitation. These results demonstrate that even moderate climatic shifts can produce amplified hydrological responses in semi-arid basins such as the PRB.

The groundwater analysis highlights growing risks to subsurface water sustainability under future climate conditions. Projected groundwater levels indicate a general tendency toward increasing groundwater depth across most wells, suggesting reduced recharge efficiency even during the monsoon season. However, the response remains spatially heterogeneous, with some wells showing relatively stable conditions due to local hydrogeological controls. Increased temperature, altered rainfall distribution, and variability in recharge processes collectively contribute to declining

groundwater resilience. When considered alongside existing groundwater abstraction pressures (not explicitly represented in the model), these changes may further intensify groundwater stress in the basin. The findings emphasize the need to treat surface water and groundwater as an interconnected system rather than as independent resources.

This study demonstrates the value of an integrated modelling framework that combines climate projections, process-based hydrological modelling, and data-driven groundwater analysis. The coupled VIC–Random Forest approach captures both surface and subsurface responses to climate forcing and enables a more comprehensive assessment of basin-scale water dynamics. The framework facilitates systematic evaluation of uncertainty, inter-model variability, and spatial heterogeneity, thereby improving the robustness of climate impact assessment.

The results carry important implications for water resource planning in Andhra Pradesh. The projected increase in hydrological variability, including higher peak flows and persistent seasonal water scarcity, necessitates adaptive and climate-resilient water management strategies. Future efforts should focus on strengthening flood preparedness, improving reservoir operation and regulation strategies, and expanding water storage and groundwater recharge infrastructure to effectively capture excess monsoon runoff while ensuring water availability during dry periods. Conjunctive use of surface water and groundwater, along with improved irrigation efficiency and climate-resilient agricultural practices, will be essential to reduce pressure on limited water resources. Enhancing hydro-meteorological monitoring networks and integrating climate-informed early warning systems can further support proactive water management.

Future research should extend this framework by incorporating socio-economic drivers, land use change, and water management interventions to evaluate compound impacts on basin-scale sustainability. Integrating physically based groundwater flow models with VIC simulations would improve representation of recharge–abstraction dynamics. Higher-resolution regional climate simulations and ensemble-based uncertainty quantification can further refine projections. Expanding the use of machine learning and remote sensing datasets may also enhance spatial prediction of groundwater variability and recharge processes.

In conclusion, this study provides a comprehensive and integrated assessment of climate change impacts on streamflow and groundwater in the Pennar River Basin. The findings demonstrate that rising temperatures, increasing rainfall variability, and intensified hydrological extremes will enhance hydro-climatic variability and place additional stress on water resources in this semi-arid region. Sustainable water management in the PRB will depend on effectively integrating climate-informed hydrological projections into planning, policy, and infrastructure design to address future uncertainty and ensure long-term water security.

8.0. WAY FORWARD

This study establishes a strong foundation for assessing climate change impacts in Andhra Pradesh, with detailed hydrological analysis for the Pennar River Basin. Future work should extend this framework by incorporating higher-resolution climate projections and convection-permitting regional climate models to better capture localized rainfall variability, intra-seasonal intermittency, and extreme precipitation events. The use of sub-daily climate data will further improve the representation of short-duration floods, extreme rainfall intensity, and evolving hydrological variability under future climate conditions. Updating VIC parameterization using recent land use, irrigation, and land management data will enhance the realism of basin-scale simulations under changing anthropogenic pressures.

Future research should strengthen the integration of surface and subsurface processes within a unified modelling framework. Extending the current VIC–Random Forest system by coupling VIC-simulated recharge and soil moisture dynamics with a physically based groundwater flow model will improve the representation of groundwater levels, baseflow contributions, and seasonal water availability. Incorporating irrigation withdrawals, canal diversions, and groundwater pumping data will enable explicit representation of human–water interactions and support the development of socio-hydrological modelling approaches. Such integration is essential to evaluate long-term water sustainability under combined climate variability and anthropogenic stress.

Given the strong spatial heterogeneity observed in groundwater and hydrological responses across the basin, future studies should focus on improving spatial representation through high-resolution datasets, distributed modelling approaches, and region-specific parameterization. This will enhance the ability to capture localized responses to climate forcing and improve the reliability of projections at the sub-basin and watershed scales. Future work should also prioritize uncertainty quantification and decision relevance. Large ensemble approaches, multi-scenario comparisons, and probabilistic risk assessment frameworks can help quantify uncertainty in climate and hydrological projections. Systematic evaluation of bias correction methods and hydrological parameter uncertainty will further clarify the robustness of projected streamflow and groundwater responses. Translating these

projections into actionable indicators—such as flood risk, irrigation reliability, drought frequency, reservoir performance, and groundwater stress indices—will directly support climate-resilient water resource planning.

Overall, advancing this integrated modelling framework will enable a more comprehensive understanding of how increasing hydro-climatic variability, rising temperatures, and changing rainfall patterns interact with human interventions to shape future water availability in the Pennar River Basin. Such efforts will support the development of adaptive, data-driven, and climate-informed water management strategies to ensure long-term sustainability in semi-arid regions.

REFERRED LETTER FROM END-USER AGENCY

Email **Sunil Gurrapu**

Fwd: study of "Projected rainfall and temperatures data analysis under varying climatic conditions in A.P and its impact on stream flow and groundwater levels in selected river basins -Reg

From : Dr.Y.R.Satyaji Rao <yrsrao.nihr@gov.in> Mon, Apr 04, 2022 02:47 PM

Subject : Fwd: study of "Projected rainfall and temperatures data analysis under varying climatic conditions in A.P and its impact on stream flow and groundwater levels in selected river basins -Reg

To : Sunil Gurrapu <gurrapus.nihr@gov.in>

Dear Dr Sunil,

I have discussed with CE about our study and received this trailing email.
Hope this email may be usefull for us.

With best wishes
YRS Rao

From: "T. V. N. A. R. Kumar" <andhrasw@ap.gov.in>
To: "Dr.Y.R.Satyaji Rao" <yrsrao.nihr@gov.in>
Cc: kumarthota2009@gmail.com
Sent: Monday, April 4, 2022 2:04:31 PM
Subject: study of "Projected rainfall and temperatures data analysis under varying climatic conditions in A.P and its impact on stream flow and groundwater levels in selected river basins -Reg

Sir,

It is learned that NIH, Kakinada is contemplating a study of "Projected rainfall and temperatures data analysis under varying climatic conditions in A.P and its impact on streamflow and groundwater levels in selected river basins".

In the wake of drastic changes in the climate in recent years, the study may be useful for Andhra Pradesh state. We are willing to extend our support and provide the necessary available information related to this study.

With Regards,
T. V. N. A. R. Kumar,
Chief Engineer, Hydrology (APSW)
Water Resources Department
H.No.76-16-16, 2nd floor
Bhavanipuram, By Pass Road,
Vijayawada - 520012

REFERENCES

1. Acharjee T K, et al. 2017. Impacts of Climate Change on Groundwater Resources in Peninsular India. *Environmental Earth Sciences*, 76 (15), 532.
2. Bera M, Das S, Mandal S, Choudhury M R. 2025. Chapter 23 - Assessing the impacts of climate change on groundwater resources in India: Challenges and adaptive strategies. *In Jayanta Das, Biswajeet Pradhan, Rajib Mitra, Pradip Chouhan, Changwook Lee, Uday Chatterjee (eds.), Developments in Environmental Science*. Elsevier. Volume 19: 491-516. DOI: 10.1016/B978-0-443-33787-1.00020-4.
3. Bhanja S N, Mukherjee A, Rodell M. 2020. Groundwater storage change detection from in situ and GRACE-based estimates in major river basins across India. *Hydrological Sciences Journal 65* (4): 650–659. DOI: 10.1080/02626667.2020.1716238
4. Buchhorn M, Lesiv M, Tsendbazar N-E, Herold M, Bertels L, Smets B. 2020. Copernicus Global Land Cover Layers-Collection 2. Remote Sensing 12 (108), 1044. DOI: 10.3390/rs12061044.
5. CGWB. 2022. *Dynamic Groundwater Resources of Andhra Pradesh (2020-21)*. Central Ground Water Board, India.
6. Chandra N A, Sahoo S N. 2023. Groundwater levels and resiliency mapping under land cover and climate change scenarios: a case study of Chitravathi basin in Southern India. *Environmental Monitoring and Assessment* 195 (11): 1394. DOI: 10.1007/s10661-023-11995-z.
7. Christensen J H, Boberg F, Christensen O B, Lucas-Picher P. 2008. On the need for bias correction of regional climate change projections of temperature and precipitation. *Geophysical Research Letters* 35 (20). DOI: 10.1029/2008GL035694
8. Chuphal D S, Mishra V. 2023. Increased hydropower but with an elevated risk of reservoir operations in India under the warming climate. *iScience*, *26* (2): 105986. DOI: 10.1016/j.isci.2023.105986
9. Dhara C, Deshpande A, Roxy M K, Dalpadado P, Shreshta M S. 2025. A post-AR6 update on observed and projected climate change in India. *PLOS Climate* 4 (11): e0000724. DOI: 10.1371/journal.pclm.0000724
10. Eyring V, Bony S, Meehl G A, Senior C A, Stevens B, Stouffer R J, Taylor K E. 2016. Overview of the Coupled Model Intercomparison Project Phase 6 (CMIP6)

experimental design and organization. *Geoscientific Model Development* **9**, 1937–1958. DOI: 10.5194/gmd-9-1937-2016

11. Ghosh S, et al. 2018. *High-Resolution Climate Projections for India under CORDEX South Asia*. *Current Science*, 114 (10), 1996–2007.
12. Gilbert J, Boateng C D, Aryee J N A, Osei M A, Wemegah D D, Gidigasu S S R, Britwum A, Afful S K, Touré H, Mensah V, Owusu-Afriyie P. 2025. A systematic review of machine learning models for groundwater level prediction. *Applied Computing and Geosciences* 28: 100303. DOI: 10.1016/j.acags.2025.100303.
13. Gosain A K, Rao S, Arora A. 2011. Climate Change Impact Assessment of Water Resources of India. *Current Science* 101 (3): 356–71. www.jstor.org/stable/24078515.
14. Gossain A K, Rao S, Basuray D. 2006. Climate change impact assessment on hydrology of Indian river basins. *Current Science* 90 (3), 346 – 353.
15. Gummadi, S., Rao, K.P.C. (2015). Addressing the Potential Impacts of Climate Change and Variability on Agricultural Crops and Water Resources in Pennar River Basin of Andhra Pradesh. *In: Leal Filho, W., Esilaba, A., Rao, K., Sridhar, G. (eds) Adapting African Agriculture to Climate Change*. Climate Change Management. Springer, Cham. DOI: 10.1007/978-3-319-13000-2_6
16. Gurrapu, S. 2025. Estimation of Groundwater Levels Using Machine Learning Techniques. In: *Applications of Machine Learning in Hydroclimatology. The Springer Series in Applied Machine Learning*. Springer, Cham. DOI: 10.1007/978-3-031-64403-0_3
17. ICHARM Report, 2009. Global trends in water related disasters: an insight for policymakers. International Centre for Water Hazard and Risk Management (UNESCO), Tsukuba, Japan. http://www.icharm.pwri.go.jp.
18. IMD. 2022. Statement on Climate for the state of Andhra Pradesh: 2021. Climate Monitoring and Prediction Group, Office of Climate Research and Services, India Meteorological Department, Pune. 14 pp. Access from: https://www.imdpune.gov.in/Reports/Statewise%20annual%20climate/2021/Climate_Statement_2021_Andhra_Pradesh_Draft.pdf
19. IPCC. 2021. *Climate Change 2021: The Physical Science Basis*. Sixth Assessment Report.
20. Jacob D, Petersen J, Eggert B, Alias A, Christensen O B, Bouwer L M, et al. 2014. EURO-CORDEX: new high-resolution climate change projections for European impact research. *Regional Environmental Change*, 14 (2), 563–578.

21. Kumar S, et al. 2013. Assessment of Climate Change Impacts on Water Resources in India. *Hydrological Processes*, 27 (27), 3872–3886.
22. Liang X, Lettenmaier D P, Wood E F, Burges S J. 1994. A simple hydrologically based model of land surface water and energy fluxes for general circulation models. *Journal of Geophysical Research* 99(14) 415-14,428. DOI: 10.1029/94jd00483
23. Litrico X, Fromion V. 2003. Infinite dimensional modelling of open-channel hydraulic systems for control purposes. DOI: 10.1109/CDC.2002.1184762
24. Liu X, Attarod P, Li Z, (eds). 2021. *Understanding Hydrological Extremes and their Impact in a Changing Climate: Observations, Modeling and Attribution*. Lausanne: Frontiers Media SA. DOI: 10.3389/978-2-88966-594-5
25. Lohmann D, Raschke E, Nijssen B, Lettenmaier D P. 1998. Regional scale hydrology: I. Formulation of the VIC-2L model coupled to a routing model. *Hydrological Sciences Journal* **43**, 131–141. DOI: 10.1080/02626669809492107
26. Manfreda S, Iacobellis V, Gioia A, Fiorentino M, and Kochanek K (eds.). 2018. Special Issue “Impact of climate on hydrological extremes”. *Water* 10.
27. Mishra V, Bhatia U, Tiwari A D. 2020. Bias-corrected climate projections for South Asia from Coupled Model Intercomparison Project-6. *Scientific Data* 7 (1): 338. DOI: 10.1038/s41597-020-00681-1.
28. Mishra V, Lilhare R. 2016. Hydrologic Sensitivity of Indian Sub-Continental River Basins to Climate Change. *Climate Dynamics*, 46 (1–2), 255–273.
29. Mondal A, Lakshmi V. 2021. Estimation of total water storage changes in India. *International Journal of Digital Earth 14* (10): 1294–1315. DOI: 10.1080/17538947.2021.1914759
30. Nageswararao M M, Sannan M C, Sahai A K, Kumar K R B, Joseph S, Reddy M A. 2023. District-Level Seasonal Rainfall Characteristics over Andhra Pradesh and its Global Teleconnections in Changing Climate. *Journal of Basic and Applied Sciences* 19: 1-19. DOI: 10.29169/1927-5129.2023.19.01.
31. O’Neill B C, Tebaldi C, van Vuuren D P, Eyring V, Friedlingstein P, Hurtt G, Knutti R, Kriegler E, Lamarque J-F, Lowe J, Meehl G A, Moss R, Riahi K, Sanderson B M. 2016. The scenario model intercomparison project (ScenarioMIP) for CMIP6. *Geoscience Model Development* **9**: 3461 – 3482. DOI: 10.5194/gmd-9-3461-2016.

32. O'Niell B C, Kriegler E, Riahi K, Ebi K L, Hallegatte S, Carter T R, Mathur R, van Vuuren D P. 2014. A new scenario framework for climate change research: the concept of shared socioeconomic pathways. *Climatic Change* 122: 387 – 400. DOI: 10.1007/s10584-013-0905-2
33. Pai D S, Rajeevan M, Sreejith O P, Mukhopodhyay B, Satbha N S. 2014. Development of a new high spatial resolution (0. 25 ° × 0. 25 °) Long Period (1901–2010) daily gridded rainfall data set over India and its comparison with existing data sets over the region. *Mausam* 65 (1): 1–18. DOI: 10.54302/mausam.v65i1.851
34. Pechlivanidis I G, Olsson J, Bosshard T, Sharma D, Sharma KC. 2016. Multi-Basin Modelling of Future Hydrological Fluxes in the Indian Subcontinent. *Water* 8 (5): 177. DOI: 10.3390/w8050177
35. Raju K S, et al. 2020. *Climate Change Impacts and Adaptation in Water Resources of Andhra Pradesh*. *Water Policy Research*, 8 (2), 145–159.
36. Rentachintala L R N P, Reddy M G M, Mohapatra P K. 2024. Climate change impacts assessment on precipitation within and around an urbanizing city under shared socioeconomic pathways. *Journal of Earth System Science 133* (4). DOI: 10.1007/s12040-024-02403-2
37. Shah M, Kulkarni H. 2019. Re-imagining Groundwater Governance in India. *Economic & Political Weekly*, 54 (24), 31–39.
38. Shuttleworth W J. 1991. Evaporation Models in Hydrology. *In* Schmugge, T.J., André, J.-C. (eds.), *Land Surface Evaporation: Measurement and Parameterization*. Springer, New York, NY, pp. 93–120. DOI: 10.1007/978-1-4612-3032-8_5
39. Srinivas V V, et al. 2019. *Future Climate Scenarios for Southern India Using RCM Projections*. *Climate Research*, 78, 39–52.
40. Tabari H. 2020. Climate change impact on flood and extreme precipitation increases with water availability. *Scientific Reports* 10 (1), 13768. DOI: 10.1038/s41598-020-70816-2.
41. Vogel R M, Yaindl C, and Walter M. 2011. Nonstationarity: flood magnification and recurrence reduction factors in the United States. *Journal of American Water Resources Association* 47(3), 464 – 474. DOI: 10.1111/j.1752-1688.2011.00541.
42. Wang J, Liang Z, Wang D, Liu T, Yang J. 2016. Impact of climate change on hydrologic extremes in the upper basin of the Yellow River Basin in China. *Advances in Meteorology*, 1404290. DOI: 10.1155/2016/1404290.

ANNEXURES

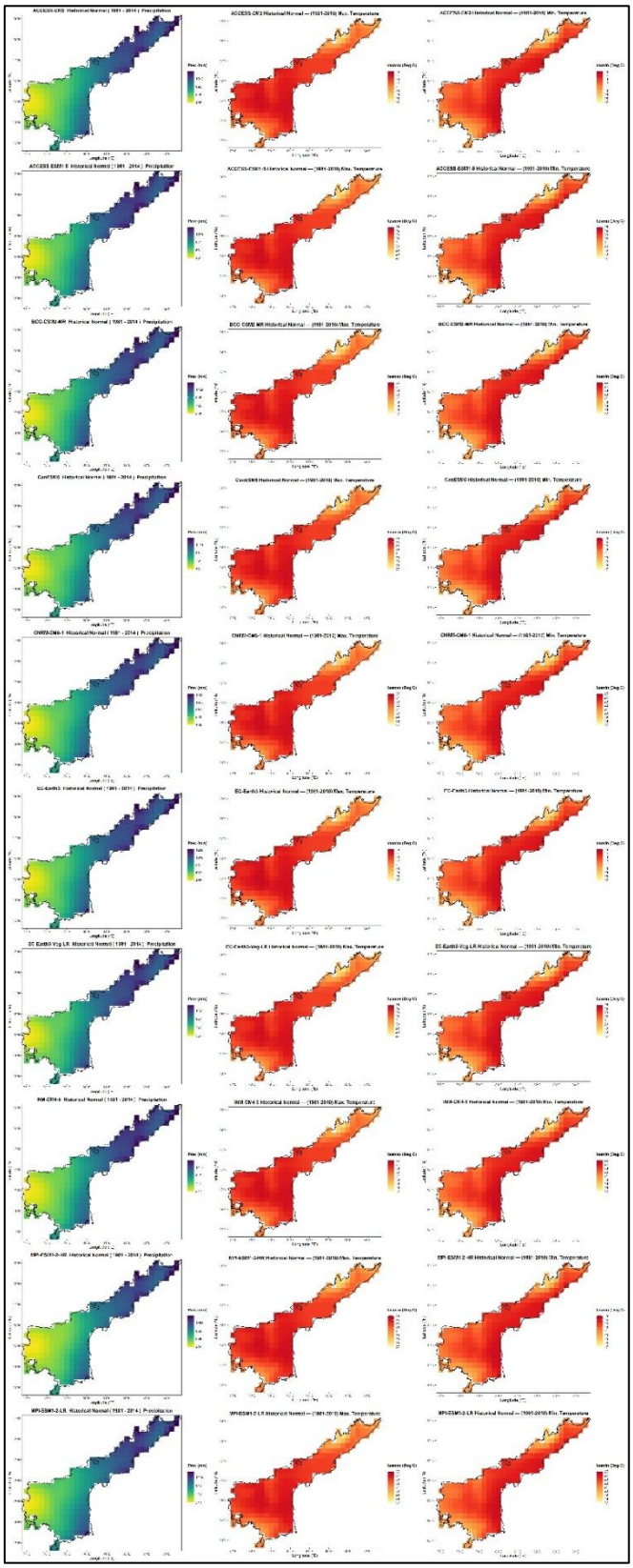

Figure S1. Spatial Distribution of Historical Climate Normals (1981–2014) Simulated by Selected GCMs over Andhra Pradesh: Precipitation, Maximum Temperature, and Minimum Temperature

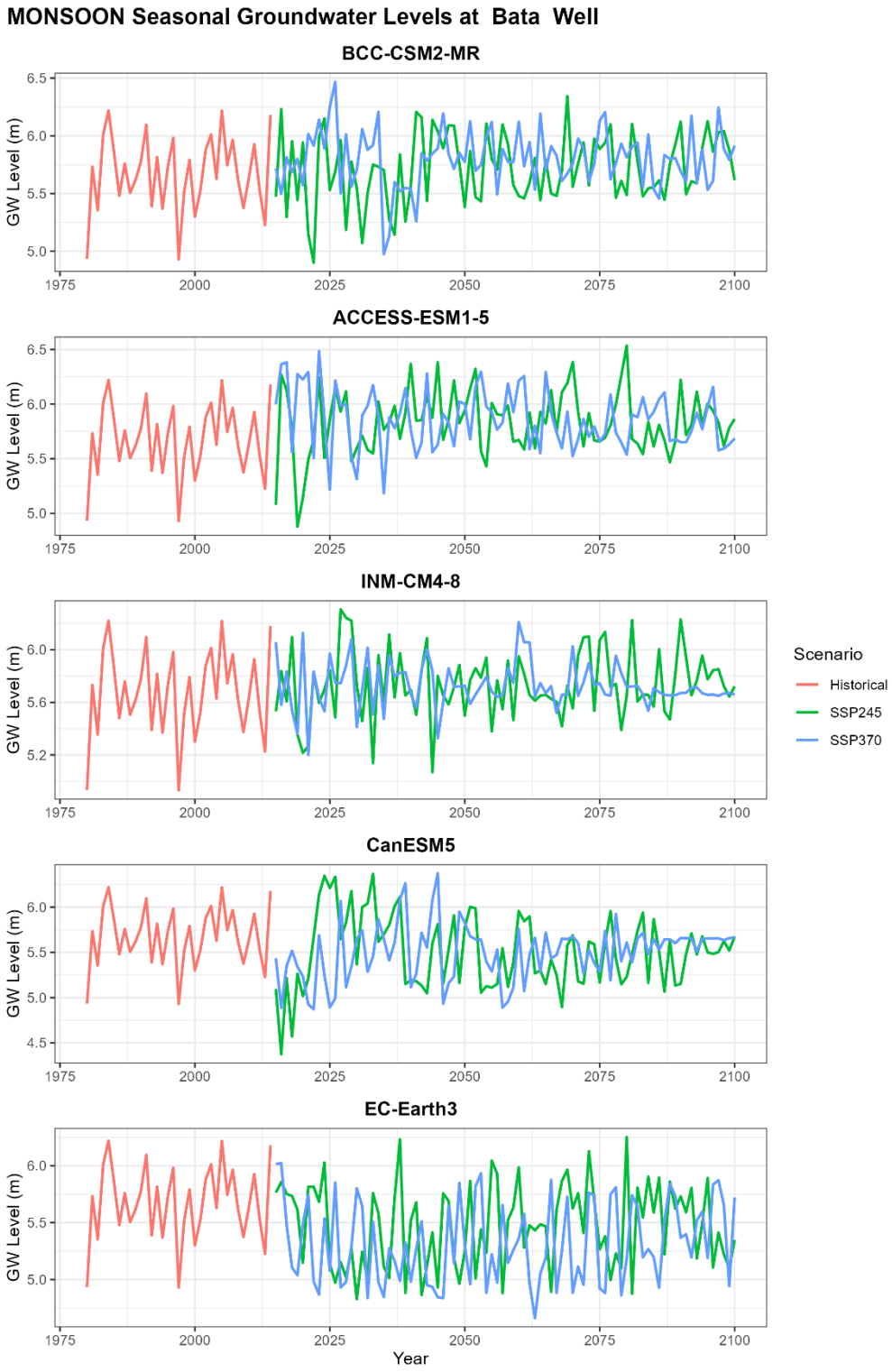

Figure S2. Historical and Projected monsoon-seasonal groundwater level variability at the Bata well under historical (1985-2014) and future (2015-2100) climate scenarios (SSP245 and SSP 370) across multiple GCMs, showing inter-annual fluctuations and long-term trends in groundwater response.

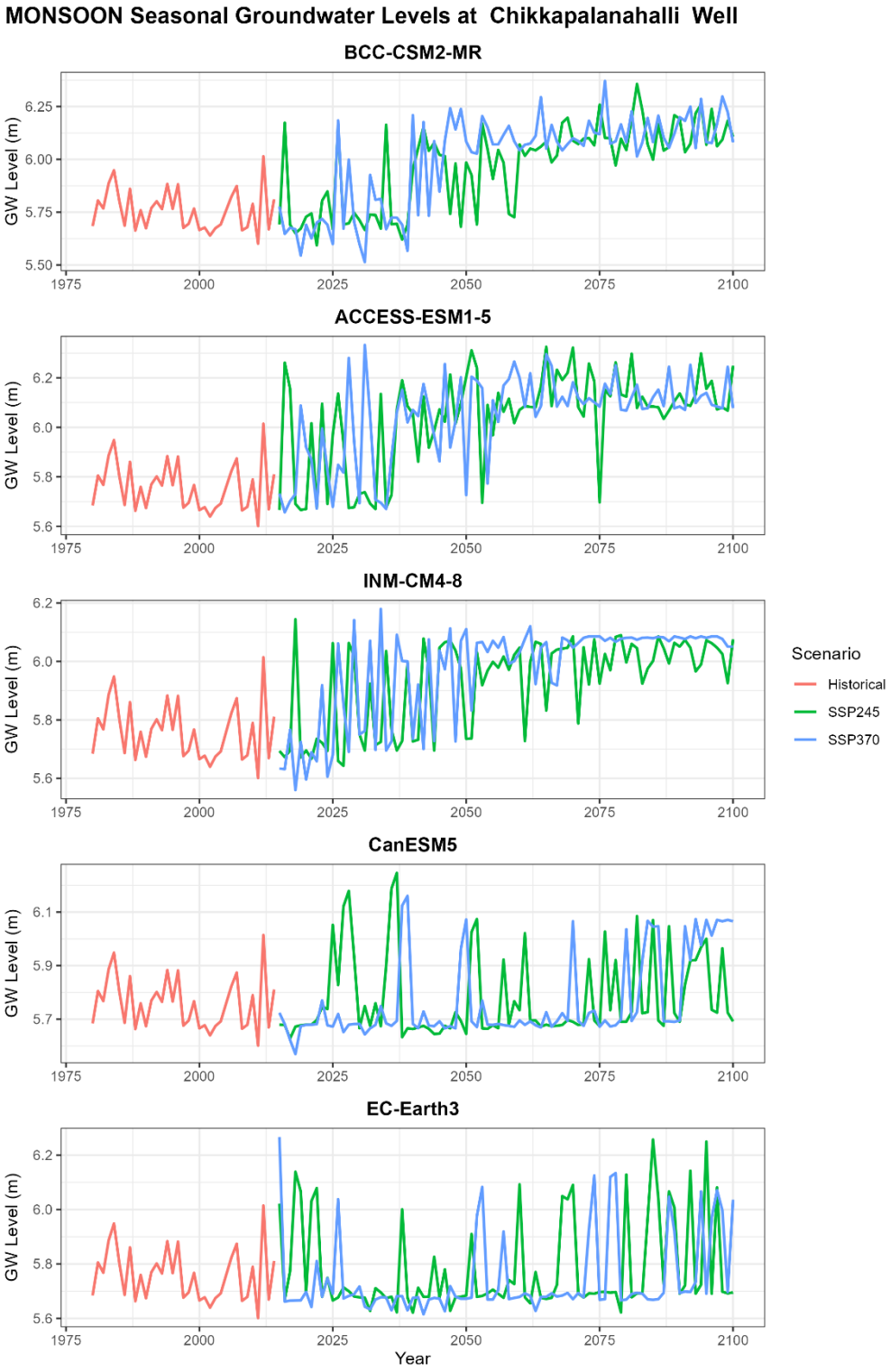

Figure S3. Historical and Projected monsoon-seasonal groundwater level variability at the Chikkapalanahalli well under historical (1985-2014) and future (2015-2100) climate scenarios (SSP245 and SSP 370) across multiple GCMs, showing inter-annual fluctuations and long-term trends in groundwater response.

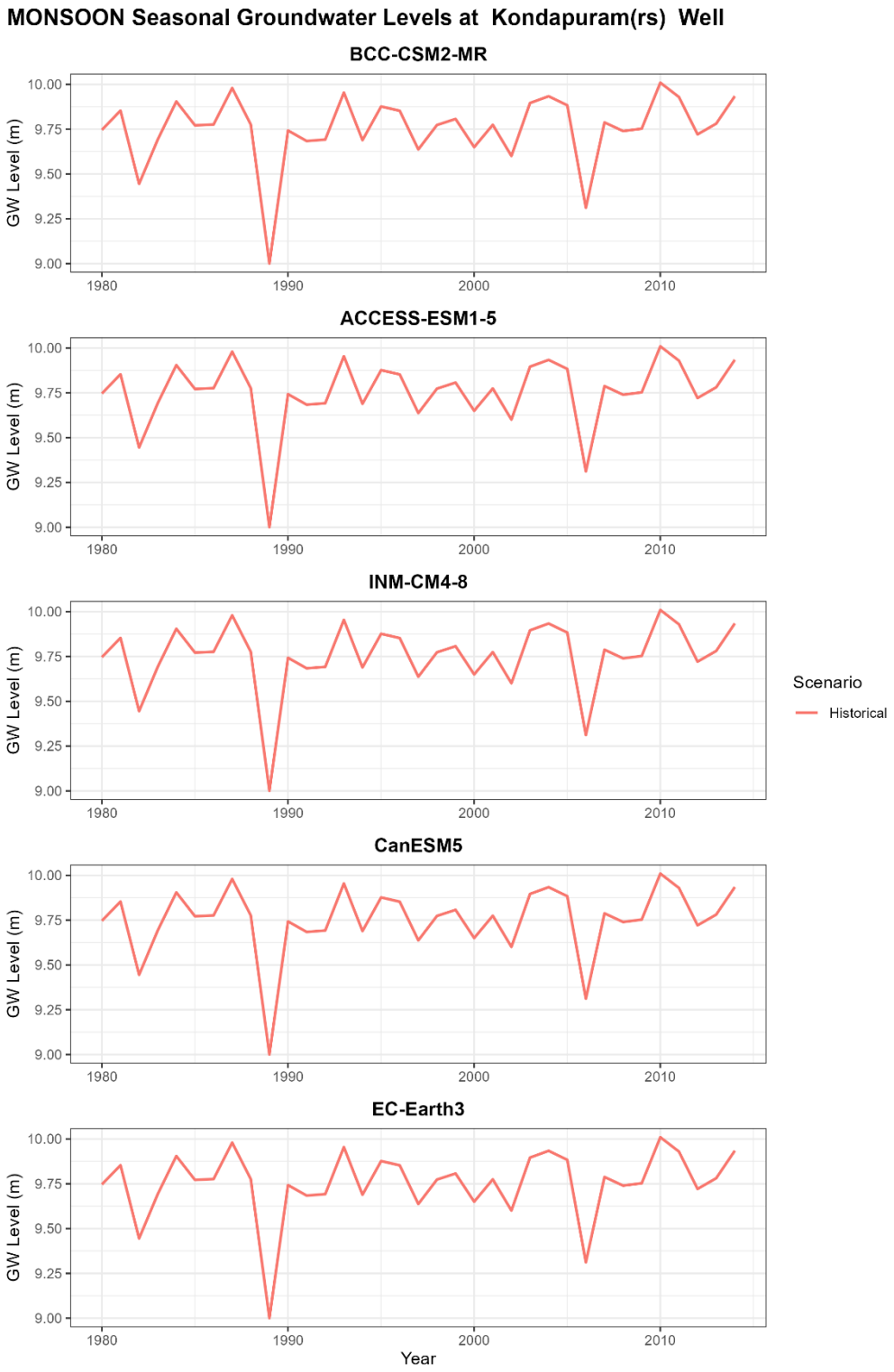

Figure S4. Historical and Projected monsoon-seasonal groundwater level variability at the Kondapuram well under historical (1985-2014) and future (2015-2100) climate scenarios (SSP245 and SSP 370) across multiple GCMs, showing inter-annual fluctuations and long-term trends in groundwater response.

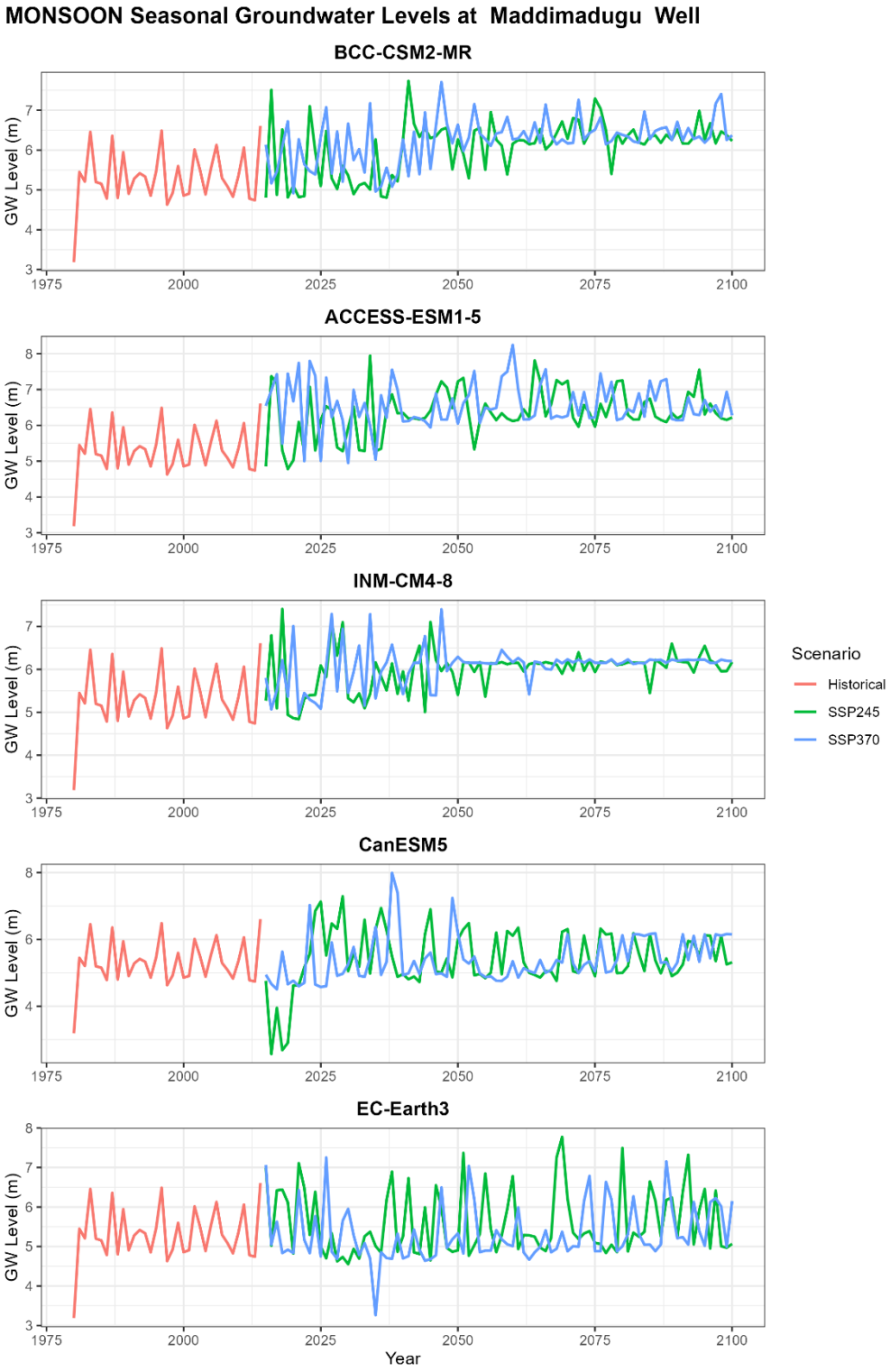

Figure S5. Historical and Projected monsoon-seasonal groundwater level variability at the Maddimadugu well under historical (1985-2014) and future (2015-2100) climate scenarios (SSP245 and SSP 370) across multiple GCMs, showing inter-annual fluctuations and long-term trends in groundwater response.

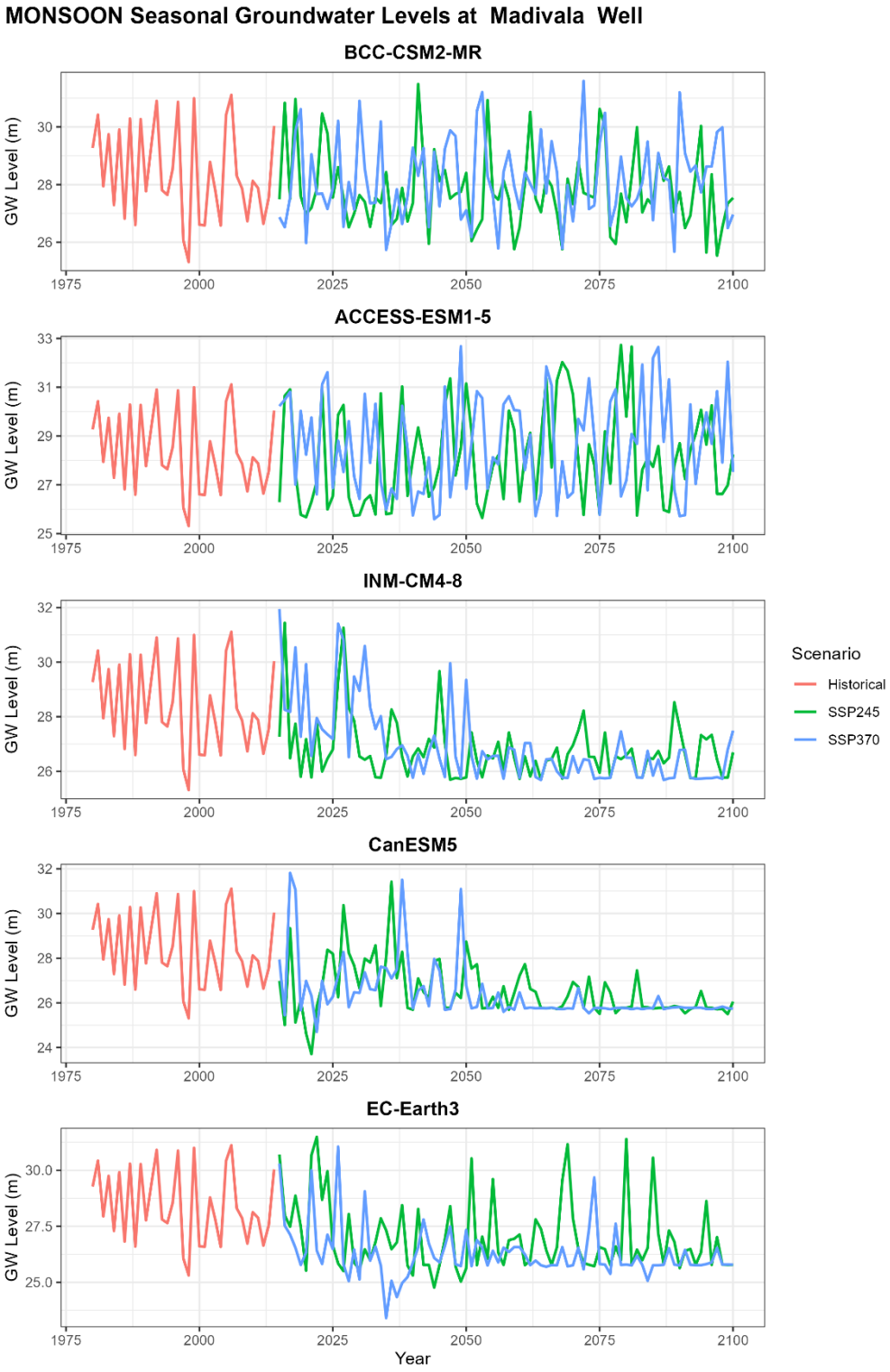

Figure S6. Historical and Projected monsoon-seasonal groundwater level variability at the Madivala well under historical (1985-2014) and future (2015-2100) climate scenarios (SSP245 and SSP 370) across multiple GCMs, showing inter-annual fluctuations and long-term trends in groundwater response.

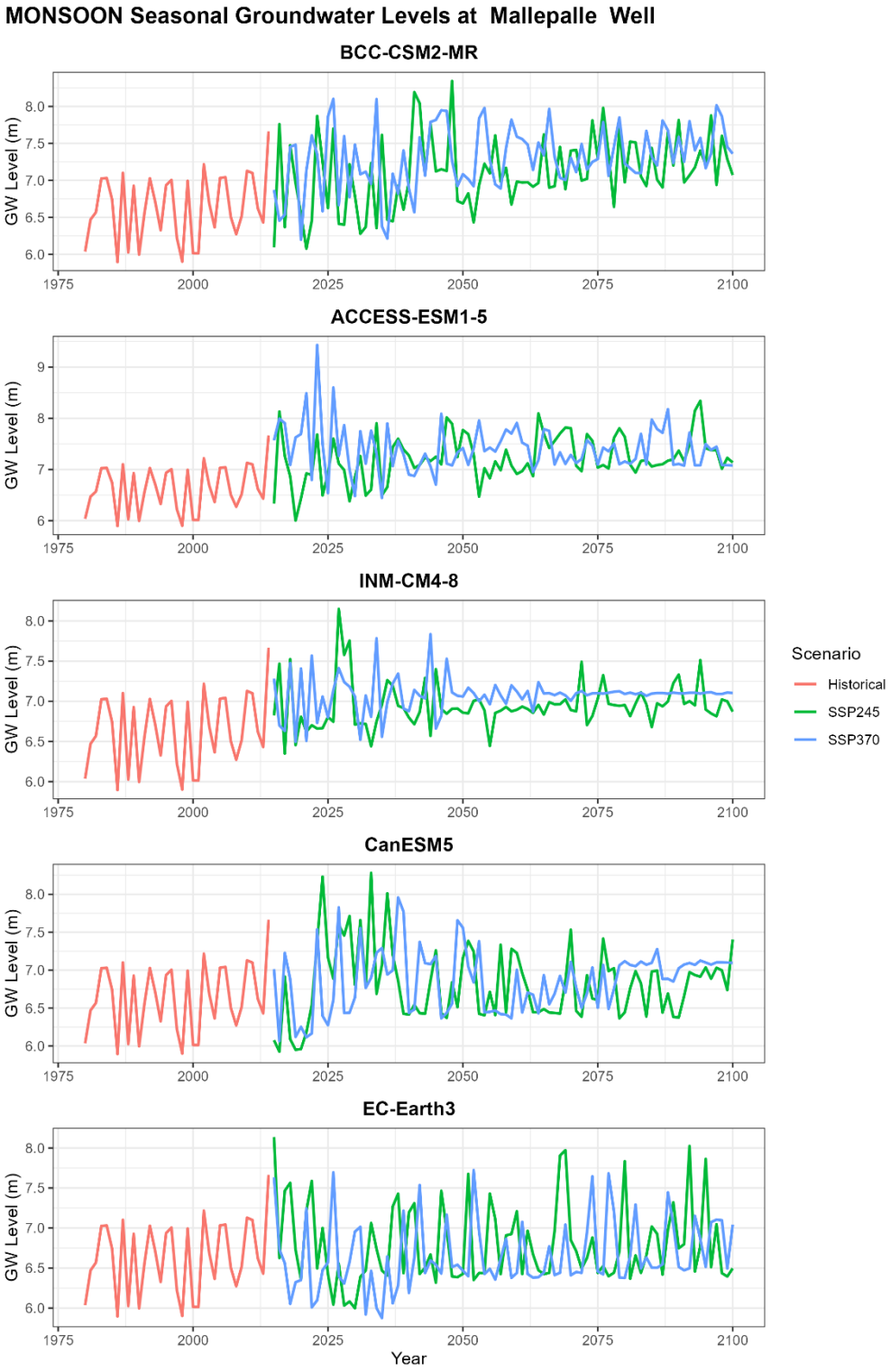

Figure S7. Historical and Projected monsoon-seasonal groundwater level variability at the Malllepalle well under historical (1985-2014) and future (2015-2100) climate scenarios (SSP245 and SSP 370) across multiple GCMs, showing inter-annual fluctuations and long-term trends in groundwater response.

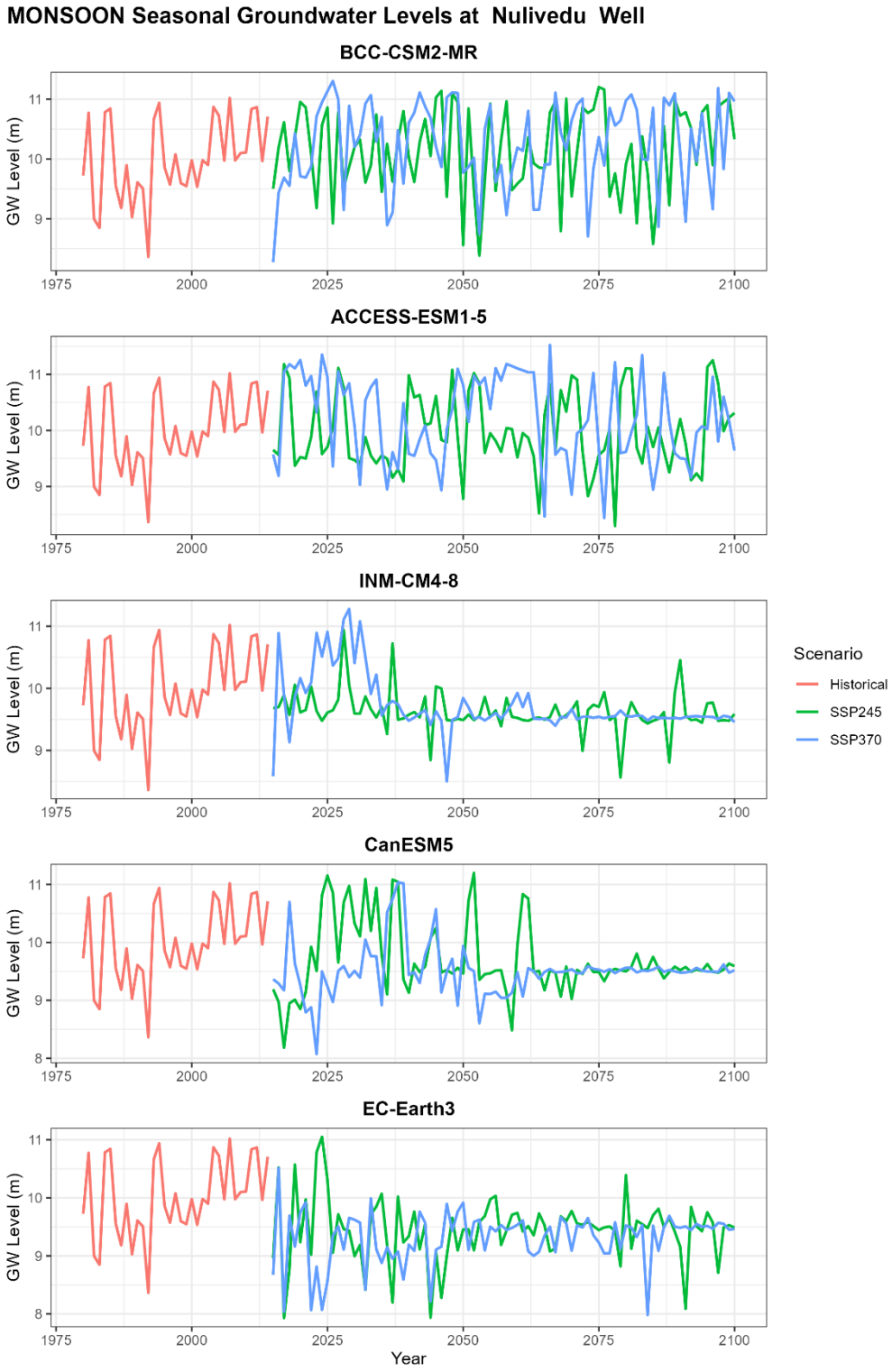

Figure S8. Historical and Projected monsoon-seasonal groundwater level variability at the Nulivedu well under historical (1985-2014) and future (2015-2100) climate scenarios (SSP245 and SSP 370) across multiple GCMs, showing inter-annual fluctuations and long-term trends in groundwater response.

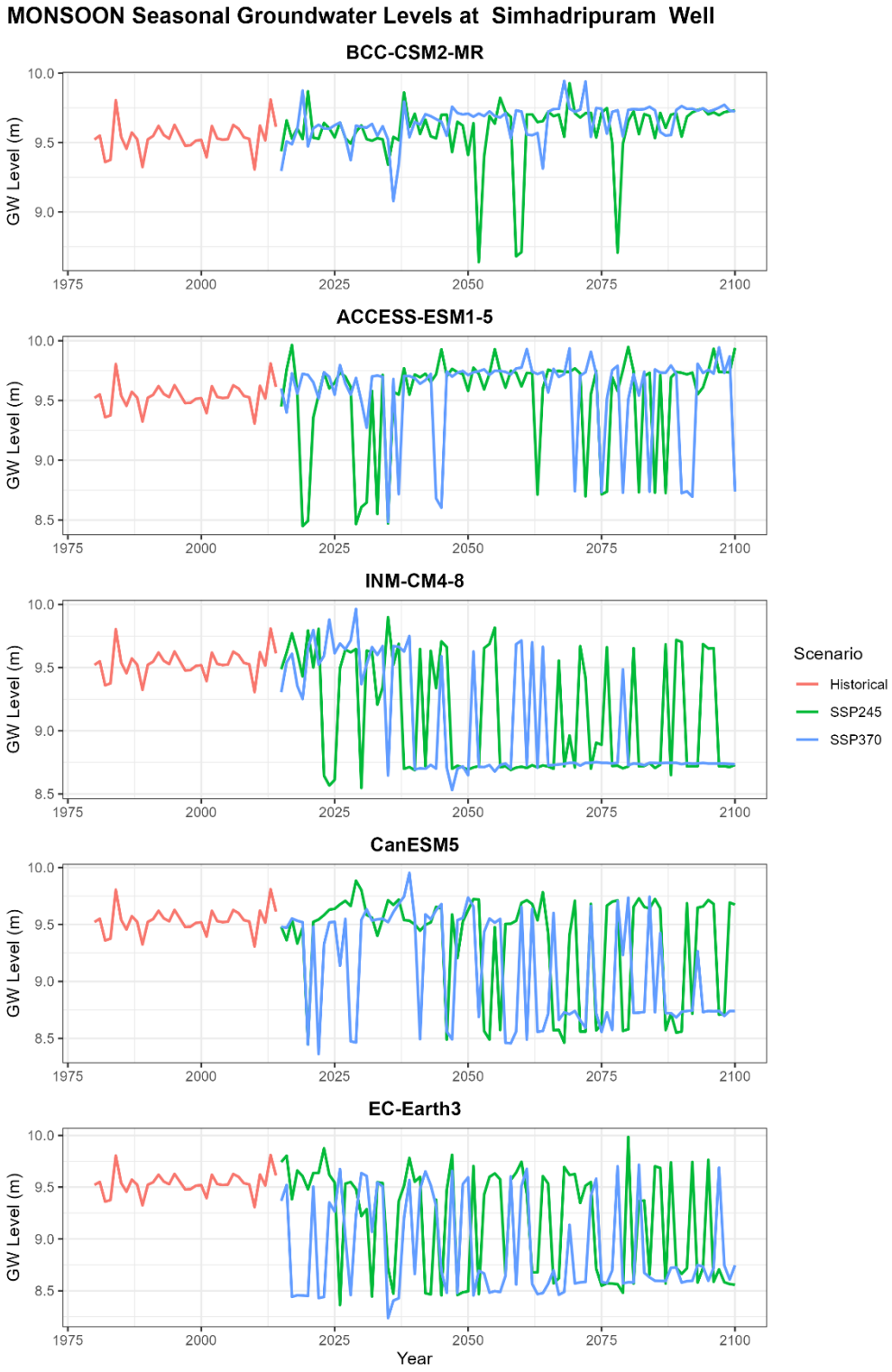

Figure S9. Historical and Projected monsoon-seasonal groundwater level variability at the Simhadripuram well under historical (1985-2014) and future (2015-2100) climate scenarios (SSP245 and SSP 370) across multiple GCMs, showing inter-annual fluctuations and long-term trends in groundwater response.

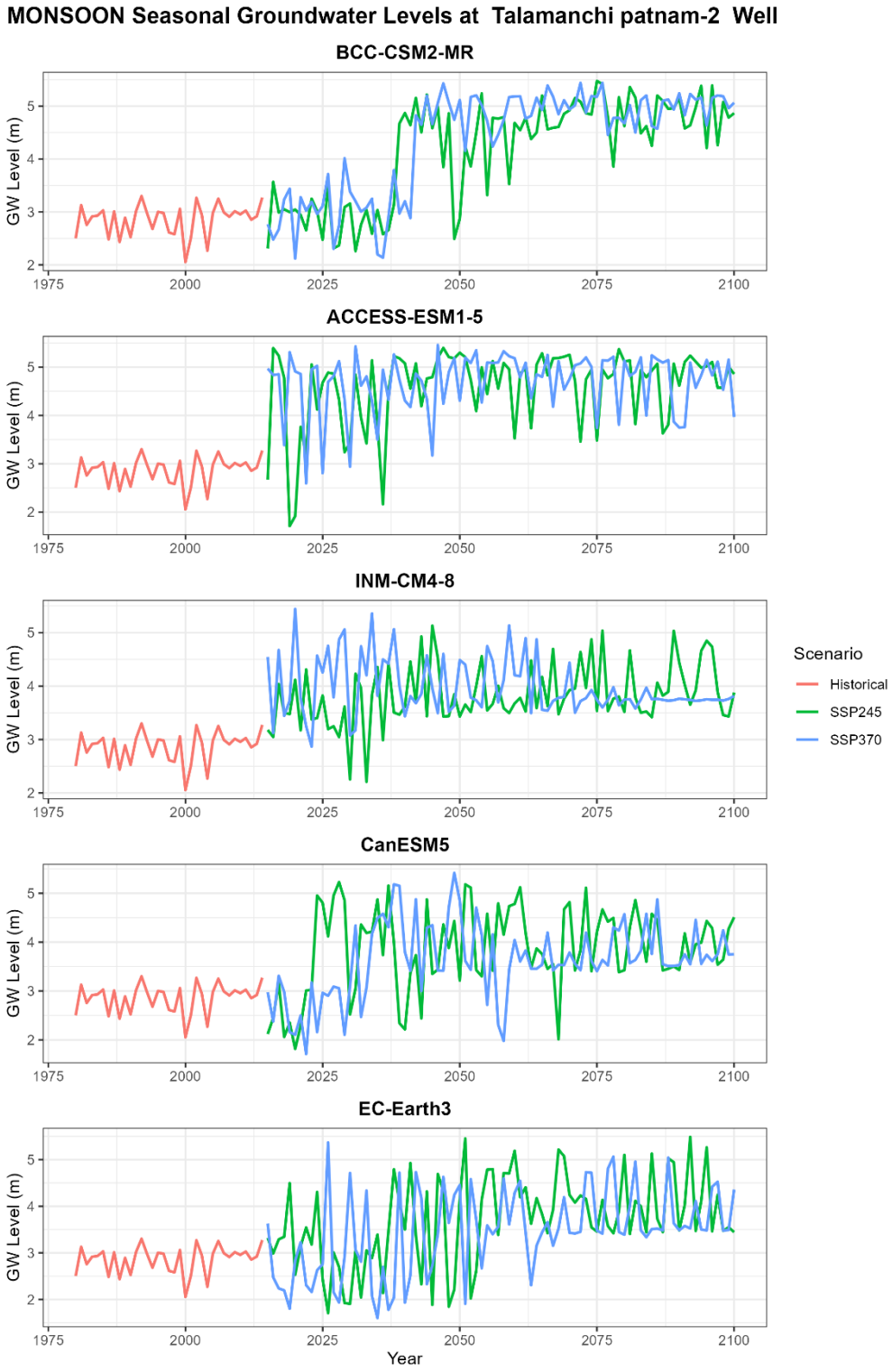

Figure S10. Historical and Projected monsoon-seasonal groundwater level variability at the Talamanchipatnam well under historical (1985-2014) and future (2015-2100) climate scenarios (SSP245 and SSP 370) across multiple GCMs, showing inter-annual fluctuations and long-term trends in groundwater response.

Table S1. Parameter combinations tested during manual calibration of the VIC Model for the Pennar River Basin. Run 78 (Highlighted in the table), represents the final parameter set used for model calibration and validation.

Run	*infilt*	*Ds*	*Dsmax*	*Ws*	Run	*infilt*	*Ds*	*Dsmax*	*Ws*
1	0.1	0.01	8	0.75	41	0.03	0.1	2	0.5
2	0.15	0.01	8	0.75	42	0.005	0.01	3	0.6
3	0.16	0.01	8	0.75	43	0.01	0.01	3	0.6
4	0.17	0.01	8	0.75	44	0.015	0.01	3	0.6
5	0.18	0.01	8	0.75	45	0.02	0.01	3	0.6
6	0.19	0.01	8	0.75	46	0.025	0.01	3	0.6
7	0.2	0.01	8	0.75	47	0.3	0.001	3	0.7
8	0.21	0.01	8	0.75	48	0.3	0.001	3	0.9
9	0.22	0.01	8	0.75	49	0.15	0.001	3	0.99
10	0.23	0.01	8	0.75	50	0.2	0.001	3	0.85
11	0.24	0.01	8	0.75	51	0.2	0.001	3	0.95
12	0.25	0.01	8	0.75	52	0.15	0.01	3	0.95
13	0.3	0.01	8	0.75	53	0.02	0.1	2	0.5
14	0.2	0.01	6	0.75	54	0.01	0.1	2	0.5
15	0.2	0.01	7	0.75	55	0.005	0.1	2	0.5
16	0.2	0.01	8	0.75	56	0.01	0.08	2	0.5
17	0.2	0.01	9	0.75	57	0.015	0.08	2	0.5
18	0.2	0.01	10	0.75	58	0.02	0.08	2	0.5
19	0.2	0.01	11	0.75	59	0.01	0.12	2	0.5
20	0.2	0.01	12	0.75	60	0.015	0.12	2	0.5
21	0.2	0.01	13	0.75	61	0.02	0.1	3	0.5
22	0.2	0.01	14	0.75	62	0.01	0.1	3	0.5
23	0.2	0.01	15	0.75	63	0.01	0.1	4	0.5
24	0.2	0.01	8	0.65	64	0.02	0.1	4	0.5
25	0.2	0.01	8	0.7	65	0.02	0.1	5	0.5
26	0.2	0.01	8	0.75	66	0.01	0.1	5	0.5
27	0.2	0.01	8	0.8	67	0.015	0.15	2	0.5
28	0.2	0.01	8	0.75	68	0.015	0.2	2	0.5
29	0.2	0.02	8	0.75	69	0.005	0.1	2	0.5
30	0.2	0.03	8	0.75	70	0.01	0.01	3	0.6
31	0.05	0.03	8	0.75	71	0.03	0.2	K_{sat} * slope	0.6
32	0.05	0.01	3	0.75	72	0.05	0.2	“	0.6
33	0.05	0.01	3	0.6	73	0.05	0.1	“	0.6
34	0.05	0.01	3	0.65	74	0.05	0.05	“	0.6
35	0.05	0.01	3	0.8	75	0.04	0.1	“	0.6
36	0.01	0.01	3	0.6	76	0.15	0.01	“	0.9
37	0.02	0.01	3	0.6	77	0.05	0.01	“	0.6
38	0.03	0.01	3	0.6	**78**	**0.05**	**0.01**	**“**	**0.8**
39	0.04	0.01	3	0.6	79	0.25	0.2	“	0.6
40	0.02	0.01	2	0.5	80	0.15	0.2	“	0.6

Table S2. Performance statistics (KGE, NSE, R^2, MAE, and RMSE) of the Random Forest model for groundwater level simulation across 60 wells in the Pennar River Basin using climatic variables (IMD gridded rainfall and temperature), VIC-derived hydrological fluxes, and antecedent groundwater conditions. *NA* represents the wells which do not fulfill the criterion of having at least 50 observations.

#	Name of the Well	KGE	NSE	R2	MAE	RMSE
1	Chikkapalanahalli	0.4190	0.5238	0.6756	1.1221	1.3023
2	Nagenahalli	0.0168	0.0398	0.0584	1.6700	2.3012
3	Machenahalli	*NA*	*NA*	*NA*	*NA*	*NA*
4	Pura	0.4465	0.4927	0.6084	1.1215	1.2245
5	Settigere	0.0544	-0.0599	0.0377	2.5173	3.2867
6	Madivala	0.4943	0.5825	0.6744	4.0917	4.9081
7	Battuvaripalli	-0.2553	-0.0782	0.0001	1.6461	2.3608
8	Tumbadi	-0.1923	-0.1322	0	1.8605	2.3488
9	Thondebhavi	0.0687	0.1033	0.3367	2.2171	3.4843
10	Madhugiri	0.2715	0.2608	0.3035	1.9654	2.3251
11	Hampasandra	*NA*	*NA*	*NA*	*NA*	*NA*
12	Chauluru-bh	*NA*	*NA*	*NA*	*NA*	*NA*
13	Mittemari	*NA*	*NA*	*NA*	*NA*	*NA*
14	Midigeshi	0.3865	-0.1502	0.2969	1.2537	1.5407
15	Kandlamadugu	0.3642	0.4173	0.4801	2.0853	2.2983
16	Kalakada-2	-0.0410	-0.0623	0.0203	1.6135	1.8132
17	Bidarakere1	0.1914	0.0763	0.1200	1.3104	1.5933
18	Madakasira-2	0.2076	0.2874	0.4093	9.3033	10.6980
19	Tanakallu	0.2177	0.3694	0.9459	3.1382	5.3806
20	Chinnamandyam	*NA*	*NA*	*NA*	*NA*	*NA*
21	Pincha	0.2465	0.1087	0.1755	1.7218	2.9815
22	Madakasira-1	0.0155	0.0626	0.0918	2.3357	3.9593
23	Palasamudram	0.3016	0.3619	0.4822	0.9280	1.5071
24	O.d.cheruvu	0.3991	0.1803	0.2345	1.8404	2.3031
25	Pavagada	-0.2258	-0.1652	0.0020	1.8400	2.2273
26	Penukonda-2	0.3086	0.2639	0.2714	1.9739	2.3644
27	Nulivedu	0.4738	0.5636	0.6638	1.9651	2.3725
28	Sanipai	0.3193	0.1729	0.1995	1.9166	2.4602
29	Palavalli	0.3750	0.3831	0.4038	1.5748	1.7157
30	Mamillakunta	*NA*	*NA*	*NA*	*NA*	*NA*
31	Alampur	0.1756	0.1856	0.1998	1.9056	2.4661
32	Talapula	0.3887	0.5243	0.7247	1.7773	2.1125
33	Anjaneya puram	0.1548	0.2054	0.2234	1.6744	2.1804
34	Lakkireddipalli	0.1458	0.1572	0.1573	2.3635	2.6945
35	Chenna Kothapalli	0.3538	0.5296	0.8644	1.9634	2.5199
36	Malakavemula-rs	0.3727	0.3968	0.4288	0.8475	1.0127
37	Maddimadugu	0.5515	0.5384	0.6124	1.1812	1.6929

38	Dharmavaram	-0.0777	0.0061	0.0280	2.3546	2.6045
39	Diguva lingala	0.0541	0.0016	0.0536	4.4101	4.9654
40	Kaluvaya	0.3843	0.4476	0.7419	2.3280	2.8093
41	Kovvuru	0.3597	0.1393	0.3239	0.7579	0.9255
42	Atmakur2	-0.2070	-0.2861	0.0058	3.0455	4.6264
43	Simhadripuram	0.5514	0.5862	0.6316	1.2202	1.4865
44	Atmakur	0.2257	0.2410	0.2490	1.2411	1.4201
45	Sangam-1	0.4126	0.1126	0.2146	0.7004	0.8955
46	Waddipalli	-0.071	-0.0421	0.0215	1.6679	1.9679
47	Rekulakunta	-0.4727	-0.4185	0.1160	3.6339	4.2290
48	Korrapadu	0.0678	-0.0504	0.0446	1.7894	2.3144
49	Kondapuram(rs)	0.5163	0.5939	0.7468	1.5713	1.7830
50	Alludupally	0.5077	0.5810	0.6767	1.3757	1.7374
51	Bata	0.5816	0.7065	0.7944	1.0335	1.2124
52	Amidala	-0.2351	-0.1081	0.0002	1.9039	2.2250
53	Pullareddypet	*NA*	*NA*	*NA*	*NA*	*NA*
54	Tadipatri-1	0.1960	0.2247	0.3653	1.0900	1.6300
55	Talamanchi patnam-2	0.6605	0.5989	0.5999	0.8339	1.0944
56	Muddireddipalle	0.2527	0.2016	0.3423	2.2070	2.723
57	Mallepalle	0.4304	0.5311	0.7019	1.6416	1.8794
58	Vajrakarur	0.1340	0.0808	0.1021	1.7674	2.5108
59	Yadikal	0.1010	-0.1826	0.0352	1.9519	2.2632
60	Gooty-alt	-0.0038	-0.1879	0.0121	1.5020	2.1168

PUBLICATIONS FROM THE STUDY

1. Gurrapu S, Rao Y R S, Ramana R V. 2026. Projected changes in temperature and precipitation over Andhra Pradesh using NEX-GDDP-CMIP6: multi-model assessment and uncertainty quantification. *In preparation*, *to be submitted to the International Journal of Climatology*.
2. Gurrapu S, Rao Y R S, Ramana R V. 2026. Impact of projected climate change on streamflow regimes in thePennar River Basin using a calibrated VIC model. *In preparation*, *to be submitted to the Journal of Water and Climate Change*

SOFTWARE / DATA USED IN THE STUDY

This study uses R as the primary computational platform for statistical analysis, data processing, visualization, and development of Artificial Intelligence / Machine Learning (AI/ML) models. We implemented bias correction, climate variability analysis, extreme value assessment, and predictive modelling entirely in R to ensure transparency and reproducibility. We developed and executed the Variable Infiltration Capacity (VIC) hydrological model using the Cygwin interface, which provides a Unix-based environment for compiling and running the VIC source code on a Windows system. We prepared meteorological forcing files, soil and vegetation parameter datasets, and other VIC input layers using a combination of R and ArcGIS. ArcGIS supported watershed delineation, raster processing, re-projection, and grid alignment, while R handled temporal aggregation and formatting of model-ready datasets.

For historical climate inputs, we used gridded precipitation and temperature datasets from the India Meteorological Department (IMD). We used these datasets for calibration, validation, and bias assessment of the hydrological model. We obtained wind speed data required for evapotranspiration calculations from the ERA5 reanalysis dataset produced by the European Centre for Medium-Range Weather Forecasts under the Copernicus Climate Change Service. ERA5 provides high-resolution, physically consistent atmospheric variables that support reliable hydrological simulations. For future climate projections, we selected ten Global Climate Models (GCMs) from the NASA Earth Exchange NEX-GDDP-CMIP6 archive. These datasets provide statistically downscaled daily projections derived from CMIP6 models under different emission scenarios. We evaluated the performance of these GCMs before

conducting impact assessment to ensure robust representation of regional climate characteristics. This integrated software and data framework enables systematic evaluation of climate change signal, hydrological impact assessment using VIC, and AI/ML-based predictive analysis within a consistent workflow.

For further information, please contact

DIRECTOR
NATIONAL INSTITUTE OF HYDROLOGY
JAL VIGYAN BHAWAN
ROORKEE – 247667 (UTTARAKHAND), INDIA
Email: dir.nihr@gov.in
Website: http://www.nihroorkee.gov.in
Phone: +91-1332-249201
Fax: +91-1332-272123

Printed by: ******** Mobile *****